

**Characterization of murine pancreatic
carcinoma models regarding
immunosuppressive mechanisms and
therapy with bifunctional siRNA targeting
galectin-1**



Tina Adunka

2014

Aus der Abteilung für Klinische Pharmakologie

Leiter: Prof. Dr. med. Stefan Endres

Medizinische Klinik und Poliklinik IV der Ludwig-Maximilians-Universität München

Direktor: Prof. Dr. med. Martin Reincke

**Characterization of murine pancreatic carcinoma models
regarding immunosuppressive mechanisms and therapy with
bifunctional siRNA targeting galectin-1**

Dissertation

zum Erwerb des Doktorgrades der Humanbiologie

an der Medizinischen Fakultät der

Ludwig-Maximilians-Universität zu München

vorgelegt von

Tina Adunka

aus

Freising

2014

**Mit Genehmigung der Medizinischen Fakultät
der Universität München**

1. Berichterstatter: Prof. Dr. med. Max Schnurr

Mitberichterstatter: Priv.Doz. Dr. med. Antje Habicht
Priv.Doz. Dr. med. Stefan Böck

Mitbetreuung durch den
promovierten Mitarbeiter: Dr. rer. biol. hum. Peter Düwell

Dekan: Prof. Dr. med. Dr. h.c. M. Reiser, FACR, FRCR

Tag der mündlichen Prüfung: 16. September 2014

CONTENTS

1	SUMMARY	1
2	INTRODUCTION	3
2.1	Biology and clinical aspects of pancreatic ductal adenocarcinoma	3
2.2	Mouse models for pancreatic ductal adenocarcinoma	4
2.2.1	Chemically induced Panc02 tumor model	5
2.2.2	Genetically engineered mouse models	5
2.3	Tumor immunology and immunotherapy	7
2.3.1	The innate and adaptive immune system	7
2.3.1.1	Dendritic cells	8
2.3.1.2	T lymphocytes	9
2.3.1.3	Co-signaling interactions in T cells	9
2.3.1.4	Interaction of T lymphocytes with dendritic cells	10
2.3.2	Role of T cells in pancreatic cancer	10
2.3.3	Immunotherapy of pancreatic cancer	11
2.4	Mechanisms of immune suppression in pancreatic cancer biology	12
2.4.1	Cellular aspects	13
2.4.1.1	Tumor-associated macrophages	13
2.4.1.2	Myeloid-derived suppressor cells	13
2.4.1.3	Dendritic cells	13
2.4.1.4	Regulatory T cells	14
2.4.1.5	Tumor microenvironment	14
2.4.2	Molecular mechanisms	15
2.4.2.1	Galectin-1	15
2.4.2.2	Transforming growth factor beta (TGF- β)	15
2.4.2.3	Indoleamine 2,3-dioxygenase (IDO)	16
2.5	Therapeutic application of RNA interference	17
2.5.1	RNA interference	17
2.5.2	5'ppp-modified siRNA	18
3	OBJECTIVES	20
4	MATERIAL	21

4.1	Technical equipment	21
4.2	Chemicals, reagents and buffers	22
4.3	Cell culture reagents and media	25
4.4	Cell lines	26
4.5	Kits	26
4.6	Antibodies	26
4.6.1	Primary conjugated antibodies and reagents for FACS	26
4.6.2	Purified antibodies for immunohistochemistry	27
4.6.3	Blocking antibodies	27
4.6.4	Antibodies for Western Blot	27
4.7	Inhibitors	28
4.8	Recombinant cytokines and proteins	28
4.9	siRNA sequences	28
4.10	DNA-template sequences for <i>in vitro</i> transcription	28
4.11	Primer sequences for qRT-PCR	29
4.12	Software	29
5	<u>METHODS</u>	30
5.1	Tumor cell culture	30
5.2	Immunological methods	30
5.2.1	Enzyme-linked immunosorbent assay (ELISA)	30
5.2.2	Western Blot	30
5.2.3	Histology	31
5.2.3.1	Fixation, paraffin embedding and microtoming of mouse tumors	31
5.2.3.2	Hematoxylin and eosin staining	31
5.2.3.3	Masson's Trichrome staining	31
5.2.3.4	Alcian Blue staining	32
5.2.3.5	Immunohistochemistry	32
5.2.3.6	Immunocytochemistry	33
5.2.4	Flow cytometry	33
5.2.4.1	Surface staining	34
5.2.4.2	Intracellular staining	35
5.2.5	T cell assays	35
5.2.5.1	T cell proliferation assay	35
5.2.5.2	T cell degranulation assay	35
5.3	Molecular biology methods	36
5.3.1	<i>In vitro</i> transcription	36

5.3.2	Transfection of siRNAs	37
5.3.3	RNA isolation	37
5.3.4	cDNA transcription	37
5.3.5	Quantitative <i>real time</i> – polymerase chain reaction	38
5.4	Animal experiments	39
5.4.1	Animals	39
5.4.2	Organ and single cell preparation	39
5.4.2.1	Preparation of serum and isolation of peripheral blood mononuclear cells	39
5.4.2.2	Isolation of T cells from mouse spleen	40
5.4.2.3	Generation of bone marrow-derived dendritic cells	40
5.4.3	<i>In vivo</i> experiments	41
5.4.3.1	Tumor models	41
5.4.3.2	Therapy with siRNAs	41
5.5	Statistical analysis	41
6	RESULTS	42
6.1	Histological characterization of murine pancreatic cancer models	42
6.1.1	H&E staining	42
6.1.2	Collagen staining of tumor stroma	44
6.1.3	Differentiation of PDAC and PanIN lesions	44
6.1.4	Tumor blood vessels	45
6.1.5	Infiltrating T cells	46
6.1.6	Galectin-1 and α -smooth muscle actin	48
6.1.7	Indoleamine 2,3-dioxygenase	50
6.1.8	Survival of mice bearing orthotopic Panc02 or T110299 tumors	50
6.2	Immunotherapy with siRNA targeting galectin-1 in the Panc02 tumor model	52
6.2.1	Murine Panc02 pancreatic carcinoma cells express functional RIG-I	52
6.2.2	<i>In vitro</i> actions of unmodified and 5'ppp-modified siRNA targeting galectin-1	54
6.2.3	<i>In vivo</i> actions of unmodified and 5'ppp-modified siRNA targeting galectin-1	56
6.3	Tumor immune escape mechanisms in pancreatic ductal adenocarcinoma	60
6.3.1	Soluble factor(s) in tumor supernatant inhibit T cell proliferation	60
6.3.2	Tumor supernatant induces T cell apoptosis	62
6.3.3	Soluble factors do not impair cytotoxic T cell degranulation	63
6.3.4	T cell inhibition is mediated by a tumor-derived soluble protein	64
6.3.5	T cell inhibition is not mediated by galectin-1	67
6.3.6	Blocking TGF- β receptor signalling partially restores T cell proliferation	69
6.3.7	Blocking IDO activity partially restores T cell proliferation	71

7	<u>DISCUSSION</u>	74
7.1	T110299 cells generated from KPC tumors represent a valuable tool for studying PDAC	74
7.2	Treatment with 5'ppp-modified siRNA targeting galectin-1 prolongs survival in the Panc02 tumor model	77
7.3	Murine pancreatic cancer cells induce potent T cell inhibition via TGF-β and IDO	80
7.4	Conclusion and perspectives	83
8	<u>REFERENCES</u>	85
9	<u>APPENDICES</u>	92
9.1	Abbreviations	92
9.2	List of figures	96
9.3	List of tables	97
9.4	Publications	98
	9.4.1 Original publications	98
	9.4.2 Oral presentations	98
9.5	Acknowledgements	99

1 Summary

Pancreatic ductal adenocarcinoma (PDAC) is a very aggressive tumor that is characterized by abundant tumor stroma and a potent immunosuppressive microenvironment. Further studies to clarify why T cells infiltrate the tumor but are not able to perform effector functions as well as to find new effective therapies to overcome immunosuppression are urgently needed.

The aims of the present study were (1) to characterize different murine PDAC tumor models in regard to their utility for studying novel immunotherapeutic approaches, (2) to assess the therapeutic efficacy of a novel bifunctional ppp-siRNA that combines silencing of the immunosuppressive molecule galectin-1 and RIG-I-mediated immune activation in murine PDAC and (3) to characterize the immunosuppressive mechanisms leading to T cell inhibition in the tumor microenvironment.

(1) This study revealed that the pancreatic cancer cell line T110299, which was developed from a primary tumor of the KPC mouse model, is a new valuable tool for studying novel treatment strategies for PDAC. The histological appearance of T110299 tumors reflects in many aspects the primary tumors in KPC mice, which harbor mutations in the Kras oncogene and p53, and the human disease with regard to tumor differentiation, extensive tumor stroma development, poor vascularization and expression of immunosuppressive molecules, like indoleamine 2,3-dioxygenase (IDO) and galectin-1 (Gal-1). In contrast, Panc02 tumors were found to have a sarcomatoid architecture with very little tumor stroma. In Panc02 cells, galectin-1 was strongly expressed by the tumor cells, which differs from the situation found in humans, KPC mice and T110299 tumors, where galectin-1 is preferentially expressed in tumor-associated pancreatic stellate cells (PSC). However, expression of the cytosolic helicase RIG-I was functional in Panc02 cells, but defective in T110299 cells. As RIG-I is expressed in all human PDAC cell lines tested, the Panc02 model appears to be better suited to study RIG-I-based immunotherapies (Ellermeier et al., 2013). Thus, the histological and functional characterization of the tumor models in this thesis will allow selecting the best-suited tumor model for addressing specific aspects of immunotherapy.

(2) Treatment studies of PDAC were performed with the 5'ppp-modified siRNA molecule ppp-Gal-1 in the orthotopic Panc02 tumor model. The dual activities of this molecule were confirmed *in vitro*, leading to (i) reduced galectin-1 expression via RNAi; and (ii) production of CXCL10 and IFN- β , MHC-I up-regulation and apoptosis of tumor cells via RIG-I activation. Treatment of mice with orthotopic pancreatic tumors with ppp-Gal-1 significantly prolonged survival, as compared to unmodified OH-Gal-1 or control RNA. In addition, 20% of the mice completely rejected their tumors leading to long-term tumor control. Thus, bifunctional 5'ppp-modified siRNA is a promising treatment strategy for PDAC deserving further pre-clinical evaluation.

(3) Pancreatic tumor cells employ multiple mechanisms for suppression of T cell responses. This study identified TGF- β and IDO as two potent mechanisms leading to inhibition of T cell proliferation. Minute amounts of PDAC supernatants effectively blocked T cell proliferation induced by CD3 and CD28 triggering. This could be partially prevented by SD-208, a small molecule inhibitor of TGF- β receptor signaling, or by blocking IDO activity with D-1-MT. Interestingly, tumor supernatants induced up-regulation of IDO mRNA expression in T cells. Furthermore, blocking IDO activity in T cells appeared to be more effective than blocking IDO in tumor cells. This leads to a new hypothesis that factors secreted by the tumor cells induce IDO expression in T cells, which in turn leads to auto-intoxication of the T cells via kynurenine production and eventually T cell apoptosis. Further studies confirming this hypothesis are warranted.

2 Introduction

2.1 Biology and clinical aspects of pancreatic ductal adenocarcinoma

Pancreatic ductal adenocarcinoma (PDCA) is one of the most lethal solid malignancies and the fourth leading cause of cancer related deaths in North America (Howlader N, 1975-2010). PDAC accounts for the majority (>90%) of pancreatic malignancies (Cubilla and Fitzgerald, 1984). The incidence rate among men accounts for 13.9 and among women 10.9 per 100.000 persons (Howlader N, 1975-2010). Most patients are between 65 and 80 years old. Risk factors are smoking, diabetes mellitus, and chronic pancreatitis, e.g. due to alcohol abuse or a genetic predisposition (Schmiegel and Budach, 2011). Pancreatic carcinoma has a high propensity for local invasion and distant metastases (Stathis and Moore, 2010). At the microscopic level, a dense and desmoplastic stroma surrounds the tumor, which is largely composed of fibrillar elements such as collagen I, fibroblastic and inflammatory cells (Chu et al., 2007, Mahadevan and Von Hoff, 2007). The interactions between the stroma and the cancer cells play critical roles in the process of tumor development and metastasis. Furthermore, the poorly vascularized stroma acts as a barrier for drug delivery in PDAC and contributes to the creation of a hypoxic microenvironment (Hidalgo and Von Hoff, 2012).

The cancer originates in the ductal epithelium and evolves from premalignant lesions to dysplastic lesions and finally to fully invasive cancer. The initial lesion called pancreatic intraepithelial neoplasia (PanIN) is the best-characterized histologic precursor of pancreatic cancer (Hruban et al., 2008). PanINs can be divided into several stages. PanIN-1A reveals elongated cells with massive mucin production and PanIN-1B demonstrates a papillary architecture. PanINs of stage 2 depicts nuclear abnormalities, e.g. enlargement, some loss of polarity and crowding. Further, stage 3 shows budding into the lumen, severe nuclear atypia and abnormal mitosis events. These stages lead to adenocarcinoma with invasive growth and marked stromal reaction (desmoplasia) (Bardeesy and DePinho, 2002). Almost all patients with fully established pancreatic cancer carry one or more of four genetic defects (Maitra and Hruban, 2008). 90% of tumors have activating mutations in the Kirsten RAS (KRAS) oncogene. Transcription of the mutant KRAS gene produces an abnormal Ras protein that is “locked” in its activated form, resulting in aberrant activation of proliferative and survival signaling pathways. Likewise, 95% of tumors exhibit an inactivation of the CDKN2A gene, leading to the loss of the p16 protein and a corresponding increase in cell proliferation. Furthermore, the expression of TP53 is abnormal in 50 to 75% of tumors, permitting cells to bypass DNA damage control checkpoints and apoptotic signals and contributing to genomic instability. DPC4, also known as SMAD4, is lost in approximately 50% of pancreatic cancers, resulting in aberrant signaling by the transforming growth factor β (TGF- β) cell surface receptor (Hidalgo, 2010, Hidalgo and Von Hoff, 2012, Iovanna et al., 2012).

The majorities of tumors develop in the head of the pancreas and cause obstructive cholestasis and jaundice (Hidalgo, 2010, Stathis and Moore, 2010). Many patients develop nonspecific nausea and abdominal or back pain. Other unspecific clinical signs are disglycemia or pancreatitis (Maitra and Hruban, 2008). Anorexia, weight loss, gastric outlet obstruction and ascites are usually manifestations of an advanced disease (Stathis and Moore, 2010).

Therapy and prognosis of patients with PDAC depend on the extent of the disease at diagnosis. Surgical resection followed by an adjuvant therapy is the standard of care for patients diagnosed with early-stage disease. In most cases however, patients present with an advanced stage disease precluding surgical resection. In this situation the impact of standard chemotherapy is minimal (Stathis and Moore, 2010). Today's standard first-line therapy for advanced stage disease is chemotherapy with the cytotoxic agent gemcitabine (Burris et al., 1997). Gemcitabine is a chemically analogue to the nucleoside cytidin. Upon uptake of gemcitabine during DNA replication the process is stopped and followed by apoptosis of the cell. Combination therapy of gemcitabine with erlotinib, which blocks EGF receptor signaling, showed some improvement in median survival of patients with metastatic disease, but only in patients with KRAS wild-type (Moore et al., 2007). In the last few years FOLFIRINOX (oxaliplatin, irinotecan, fluorouracil and leucovorin) has emerged as the combination of choice for patients with excellent performance status. However, this aggressive therapy is accompanied by high toxicity (Conroy et al., 2011). FOLFIRINOX provided a median survival of 11.1 months compared to 6.8 months in gemcitabine treated patients in a pivotal phase II/III trial (Conroy et al., 2011). Recently von Hoff et al. published a phase III trial evaluating weekly nab-paclitaxel (albumin-bound paclitaxel) plus gemcitabine versus gemcitabine alone (Von Hoff et al., 2013). Here they reported that the combination of nab-paclitaxel and gemcitabine prolongs the overall survival to 8.5 months compared to 6.8 months for exclusively gemcitabine treated patients. This treatment appears to be less toxic than FOLFIRINOX and therefore patients with an excellent or average performance status can be treated (Von Hoff et al., 2013, Jarboe and Saif, 2013).

2.2 Mouse models for pancreatic ductal adenocarcinoma

In order to study the pathogenesis and novel therapies for PDAC mouse models mimicking the disease have been developed. These include subcutaneous or orthotopic implantation of murine pancreatic carcinoma cell lines in syngeneic, immunocompetent mice, xenografts of human cell lines in immune compromised mice and genetically engineered mouse models (GEMM), in which mutations that are commonly found in human cancers are introduced under the control of pancreas specific promoters (Herreros-Villanueva et al., 2012, Zhang et al., 2013). In this study two different murine cancer models for PDAC were employed: the chemically induced, widely used Panc02 model in which tumor cells are implanted in syngeneic C57BL/6 mice and GEMM, in which tumors express mutant p53 and Kras under the control of a pancreas-specific promoter, the so called KPC tumor model.

2.2.1 Chemically induced Panc02 tumor model

Corbett et al. described in 1984 the establishment of the murine Panc02 tumor cell line (Corbett et al., 1984). Briefly, cotton threads saturated with 3-methylcholantren (3-MCA) were implanted in the pancreas of C57BL/6 mice. Tumors arising after 220 days post implantation displayed pancreatic ductal adenocarcinomas, whereas tumors with shorter latency (>220 days) usually represented fibrosarcomas. Panc02 were established in a serial passage in the host of origin (latency: 528 days) and originated as a grade II tumor, producing copious amounts of fluid and ulcerating through the skin after trocar implant at a very small size (< 400 mg). The tumor was characterized by a benign connective tissue component and was unsuitable for chemotherapy trials. With passage 26, a stable murine tumor cell line was established and transplantation back into mice showed that the tumor retained a well-differentiated histological appearance but produced very little fluid, did not ulcerate to the surface and contained no connective tissue elements. Panc02 tumors metastasized into the lung, lymph nodes and kidneys. Numerous groups have studied the Panc02 model since its first description in 1984 due to its easy handling, aggressive tumor growth characteristics and low sensitivity towards chemotherapy, which are typical features of the human disease.

2.2.2 Genetically engineered mouse models

In the last years numerous research groups have established GEMM by introducing specific mutations that had turned out to play a role in human disease to study PDAC carcinogenesis. These models reproduce genetic alterations implicated in the progression of pancreatic cancer, which includes activating Kras mutations and inactivation of tumor suppressor genes, such as p53, p16/INK4a, BRCA2 and Smad4 (Herreros-Villanueva et al., 2012). Since an activating mutation of Kras oncogene can be identified in up to 90% of all human pancreatic carcinomas, thus representing the most frequent genetic alteration, most of the GEMM are based on mutant Kras (Herreros-Villanueva et al., 2012).

A mouse model targeting oncogenic Kras is the LSL-Kras^{G12D} model. This model is generated by a conditionally expressed allele, using a vector containing genetic elements flanked by functional LoxP sites that inhibit transcription and translation. This Lox-Stop-Lox (LSL) construct was inserted into the mouse genomic Kras locus upstream of locus 1 comprising a G-A transition in codon 12 (G12D). This transition mutation results in a glycine to aspartic acid substitution in the expressed protein that activates constitutive downstream signaling of Ras effector pathways. Using the Cre-loxP-system, Cre-expression can be restricted to pancreatic cells by placing Cre under the PDX1 or Ptf1a (P48) promoter. The transcription factors PDX-1 and P48 play important roles in the embryonic development of the pancreas. For the generation of Ptf1a(P48)-Cre, LSL-Kras^{G12D} mice, a mouse model, which expresses a Cre-activated Kras^{G12D} allele inserted into the endogenous Kras locus, was crossed with mice expressing Cre recombinase under the tissue specific promoter Ptf1a(P48)

(Hingorani et al., 2003). These mice express numerous PanIN lesions, but showed low frequency of progression to invasive and metastatic adenocarcinoma (Herrerros-Villanueva et al., 2012).

Another transgenic mouse model, PDX-1-Cre, LSL-Kras^{G12D}, LSL-Trp53^{R172H/-}, was generated by Hingorani et al. (Hingorani et al., 2005). They generated a conditionally expressed point mutant allele of the Li-Fraumeni human ortholog, TRP53^{R172H}. Activation of both the Kras^{G12D} and the Trp53^{R172H} alleles occurs in tissue progenitor cells of the developing mouse pancreas through interbreeding with PDX-1-Cre transgenic animals (KPC mice) (Hingorani et al., 2005). KPC mice develop early PanIN lesions and later invasive lesions whereby histological analysis showed a well-differentiated morphology as in human PDAC. Cytokeratin 19 (CK 19) expression shows ductal phenotype and the carcinomas contain frequently mucin as revealed by Alcian blue staining (Hingorani et al., 2005). KPC mice develop liver and lung metastasis and the median survival decreased from 12 month of PDX-1-Cre, LSL-Kras^{G12D} mice to 5 month. Clinical features of the triple mutant mice are cachexia, abdominal distension and hemorrhagic ascites (Hingorani et al., 2005).

Besides the described GEMM, there are further models resulting in PDAC, which are summarized in Table 2-1. The cell line T110299, which was used in this study, was developed from a primary tumor of a KPC mouse in the Jens Siveke lab (TU Munich).

Table 2-1: GEMMs of pancreatic ductal adenocarcinoma (modified from Mazur et al.(Mazur and Siveke, 2011))

genotype	Preneoplastic lesion	Onset (months)	Median survival (months)	comments
Pdx1-Cre;Kras ^{G12D}	+	>12	>12	Long latency, PanINs
Ptf1a ^{+Cre} ;Kras ^{G12D}	+	>12	>12	Long latency, PanINs
Ela-Tgfa	+	---	>12	Development of ADM and fibrosis
Ptf1a ^{+Cre} ;Kras ^{G12D} ; Ela-Tfga	+	5	7	PanIN and IPMN-derived PDAC
Pdx1-Cre;Kras ^{G12D} ; INK4a/ARF ^{lox/lox}	+	2	2	Short latency, high penetrance
Pdx1-Cre;Kras ^{G12D} ; INK4a/ARF ^{+/-}	+	8	10	Gross metastasis
Pdx1-Cre;Kras ^{G12D} ; INK4a ^{-/-}	+		5	PDAC with short latency
Pdx1-Cre;Kras ^{G12D} ; p53 ^{lox/lox}	+	1.5	3	Well-differentiated PDAC, with short latency
Pdx1-Cre;Kras ^{G12D} ; p53 ^{R172H/+}	+	2.5	5	Accelerated development of metastatic well-diff. PDAC
Ptf1a ^{+Cre} ;Kras ^{G12D} ; Notch1 ^{lox/lox}	+	>6	12	Similar to Ptf1a ^{+Cre} ;Kras ^{G12D}
Ptf1a ^{+Cre} ;Kras ^{G12D} ; Notch2 ^{lox/lox}	+	>9	>15	MCNs, only PanIN1, sarcomatoid PDAC with long latency
Pdx1-Cre;Kras ^{G12D} ; Smad4 ^{lox/lox}	+	4	9	Model of IPMN-to-PDAC progression
Ptf1a ^{+Cre} ;Kras ^{G12D}	+	3.5	8	MCNs resembling human disease

Smad4 ^{lox/lox}				
Ptf1a ^{+Cre} ;Kras ^{G12D} ; p53 ^{R270H/+} ;Brca2 ^{Tr/D11}	+	2	2.5	Model of familial PDAC
Ela-tTA TRE-Cre; Kras ^{G12V}	+	12	18	PDAC after chronic pancreatitis
Ptf1a ^{+Cre} ;Kras ^{G12D} ; TFGβIIR ^{lox/lox}	+		2	Aggressive, undifferentiated PDAC
Ela-CreERT; Kras ^{G12D}	+		>18	Acinar-derived PanINs

ADM=acinar-ductal metaplasia; IPMN=intraductal papillary mucinous neoplasm; MCN=mucinous cystic neoplasm; PanIN=pancreatic intraepithelial neoplasia; PDAC=pancreatic ductal adenocarcinoma; + = yes

2.3 Tumor immunology and immunotherapy

Tumor immunology studies the interactions of cancer cells with immune cells. Immunotherapy aims at exploiting immune effector mechanisms to specifically target and to eradicate tumor cells. The concept of immune surveillance by Burnet et al. states that a physiologic function of the immune system is to recognize and destroy clones of transformed cells before they grow into tumors and to kill these cells after they are formed (Burnet, 1970, Abbas et al., 2007). However, some clones may survive the immune attack and after an equilibrium period, in which tumors are usually small, tumor cells evolve mechanisms to escape immunosurveillance leading to clinical apparent tumor outgrowth (Hanahan and Weinberg, 2000, Zitvogel et al., 2006). A major challenge for future immunotherapies will be to identify and overcome these immunosuppressive mechanisms (Clark et al., 2009). In the following paragraphs important components of the immune system in regard to tumor immunotherapy will be discussed.

2.3.1 The innate and adaptive immune system

The immune system is divided in two major divisions, the innate or non-specific immune system and the adaptive or specific immune system. The innate immune system represents the first line of defense against invading pathogens whereas the adaptive immune system acts as a second line of defense and enables protection against re-exposure to the same pathogen (Abbas et al., 2007).

The mechanisms of innate immunity provide the initial defense against infections, which are triggered by phagocytes (macrophages, neutrophils), dendritic cells (DCs), mast cells and natural killer (NK) cells. These cells use non-clonal recognition receptors, including membrane-bound Toll-like receptors (TLRs), NOD-like receptors (NLRs) and cytosolic helicases (Palucka and Banchereau, 2012). The innate immune system can also be considered to be a property of the skin and epithelia that line our internal organs, such as the gut and lungs, providing a first line defense against invading pathogens (Janeway and Medzhitov, 2002). Innate immunity is antigen-nonspecific (Palucka and Banchereau, 2012).

The adaptive immune system can specifically recognize proteins, carbohydrates, lipids and nucleic acids (antigen-specific). The adaptive immune response develops later as the innate response and consists mainly of the activation of T and B cells. T and B cells have clonal receptors allowing enormous variability in immune recognition (Palucka and Banchereau, 2012). The adaptive immune system is separated into humoral and cell-mediated immune responses. In humoral immunity, B cells secrete antibodies that prevent infections and eliminate extracellular microbes. In cell-mediated immunity, T helper cells activate macrophages to kill phagocytosed microbes or cytotoxic T cells directly destroy infected cells (Abbas et al., 2007, Janeway and Medzhitov, 2002, Palucka and Banchereau, 2012).

Dendritic cells of the innate immune system express co-stimulatory molecules, such as CD80 and CD86 on the cell surface, to instruct the adaptive immune system about the nature of the pathogenic challenge. The virtue of having both innate and adaptive systems of recognition is that the interplay of these two distinct systems allows the discrimination of an infectious attack on the host from noninfectious self (Janeway and Medzhitov, 2002).

In the following sections DCs and T cells are explained in more detail.

2.3.1.1 Dendritic cells

DCs are rare cell types and key cellular sensors of microbes. They provide an essential link between innate and adaptive immune responses and the generation of protective anti-tumor immunity depends on the presentation of tumor antigens by DCs (Diamond et al., 2011, Fuentes et al., 2011, Palucka and Banchereau, 2012). DCs are specialized for the capture, processing and presentation of antigens to T cells. There are differences in the maturity and the function of DCs during their life cycle. DCs located in peripheral tissues are immature and induce T cell tolerance by presenting self-antigens to T cells, which leads to T cell deletion or expansion of regulatory T cells (Tregs) (Palucka and Banchereau, 2012). By contrast, mature, antigen-loaded DCs can mediate the differentiation of antigen-specific T cells into effector cells.

DCs can be divided into different subtypes. The subtypes differ in location, migratory pathways, immunological function and dependence on infections or inflammatory stimuli for their activation (Palucka and Banchereau, 2012). There are conventional DCs (cDCs) and plasmacytoid DCs (pDCs), also known for their function to secrete high levels of type I interferons. Subtypes of cDCs are migratory DCs and lymphoid-tissue-resident DCs (Palucka and Banchereau, 2012, Shortman and Naik, 2007). Migratory DCs act as sentinels in the peripheral tissue. They are activated by pathogen-associated molecular patterns (PAMPS), e.g. via Toll-like receptors (TLRs), migrate to the draining lymph nodes, and present endocytosed antigen as processed peptides on major histocompatibility complex (MHC) class I or II molecules to T cells (Shortman and Naik, 2007, Palucka and Banchereau,

2012). Lymphoid-tissue-resident DCs collect and present foreign and self-antigens and can be further subdivided into CD4⁺ and CD8⁺ and double-negative cDCs (Shortman and Naik, 2007).

Mouse bone marrow cells cultured with granulocyte-macrophage colony stimulating factor (GM-CSF) and other cytokines (like IL-4) produce mixtures of granulocytes, macrophages, and monocyte-derived DCs, expressing high levels of CD11c and MHC class II and thereby acting as potent antigen-presenting cells (APC) (Liu and Nussenzweig, 2010, Sallusto and Lanzavecchia, 1994). These “model” DCs are frequently used for *in vitro* studies of antigen presenting cell (APC) functions.

2.3.1.2 T lymphocytes

T cells are the mediators of cellular immunity and consist of three major subsets, CD4⁺ helper T lymphocytes (T_H), CD8⁺ cytotoxic T lymphocytes (CTL) and regulatory T lymphocytes (Tregs) which all express the αβ-antigen receptor (Andersen et al., 2006).

CD4⁺ T cells recognize peptides presented onto MHC class II on APCs and can only be activated with appropriate co-stimulatory molecules on the surface of professional APCs, such as DCs (Andersen et al., 2006, Stockwin et al., 2000). The effector functions of CD4⁺ T cells are triggering the humoral and cell-mediated immune response by activation of macrophages and B cells.

CD8⁺ T cells recognize specific peptide epitopes presented on MHC class I molecules, which are expressed by virtually all cells and present endogenous peptides generated by the proteasome (Andersen et al., 2006). In addition CD8⁺ T cells can be activated by DCs via cross-presentation of extracellular peptides which were phagocytosed and processed by DCs and finally presented on MHC class I molecules (Zhang and Bevan, 2011, Andersen et al., 2006). CD8⁺ T cells have three possible ways of killing a target cell. Firstly, the release of lytic molecules, such as perforin and granzymes, into the intercellular space. Secondly, CTLs express Fas ligand (CD95L) on their surface which binds to Fas receptor (CD95) on the target cell, triggering apoptosis through the classical caspase cascade (Nagata, 1996). The third possibility does not require cell-cell contact but can reach target cells distal to T effector cells by secreting cytokines, such as IFN-γ and TNF-α. TNF-α induces its receptor on the target cell and mediates the caspase cascade leading to apoptosis of the target cell. IFN-γ induces up-regulation of MHC class I molecules and increases Fas mediated cell lysis (Andersen et al., 2006). CTLs can provide protection against malignant cells by their ability to detect antigenic differences in transformed cells due to their altered protein repertoire (Andersen et al., 2006).

2.3.1.3 Co-signaling interactions in T cells

For full activation of T cells, co-stimulatory molecules are required, which deliver positive signals to T cells following their engagement by ligands and counter-receptors on APCs. Binding of CD28 on T

cells to B7-1 (CD80) and B7-2 (CD86) on APCs or CD40 on T cells to CD40L on APCs stimulate proliferation, cytokine production, differentiation, cytotoxic function, memory formation and survival (Chen and Flies, 2013).

In contrast, co-inhibitory molecules deliver negative signals to T cells. For example, CTLA-4 on T cells is induced after T cell activation and binds to B7-1 and B7-2 in competition to CD28. This binding induces expression of Indoleamine 2,3-dioxygenase (IDO) in APCs, which acts *in trans* to suppress activation of conventional T cells and promote the function of Tregs. In addition, B7-H1, also known as programmed death-ligand 1 (PD-L1), is expressed on APCs and binds to the PD-1 receptor on T cells, thereby inducing cell cycle inhibition, inhibition of effector functions, T cell anergy and apoptosis (Chen and Flies, 2013).

2.3.1.4 Interaction of T lymphocytes with dendritic cells

DCs are the most effective APCs for initiating primary T cell response. DCs are strategically located at common entry sites of microbes and they are enabled to capture and respond to them via specific receptors. DCs migrate preferentially to the T cell zone of lymph nodes and mature DCs up-regulate co-stimulatory molecules (CD80 and CD86) and secrete IL-12 to activate T cells (Abbas et al., 2007). The T cell receptors of CD4⁺ or CD8⁺ T cells recognize peptides loaded onto MHC class I or II molecules on DCs, leading to the formation of the immunological synapse or supramolecular activation cluster (SMAC). While naïve CD4⁺ T cells can differentiate into T helper cells (T_H1, 2 and 17) as well as Tregs, naïve CD8⁺ T cells can give rise to effector cytotoxic T lymphocytes (CTLs) (Palucka and Banchereau, 2012). Both T cell types produce IL-2 after their activation to stimulate T cell proliferation in an autocrine and paracrine manner.

2.3.2 Role of T cells in pancreatic cancer

Tumors with reduced immunogenicity or those that have acquired mechanisms to suppress immune effector functions can emerge from cancer immunosurveillance and grow progressively. This is an important issue in pancreatic cancer (Clark et al., 2009). Studies in mouse models of PDAC give rise to the assumption that immune cells with suppressive properties infiltrate the pancreas early during tumorigenesis, preceding and undermining any lymphocytes with potential antitumor function (Clark et al., 2007). Therefore, the failure of cancer immunosurveillance is likely to be an early event in PDAC.

In the development from PanINs to invasive cancer, a massive infiltration with CD45⁺ leukocytes can be observed. In early stages immunosuppressive leukocytes, such as tumor-associated macrophages (TAM), myeloid-derived suppressor cells (MDSC) and Tregs enter the tumor stroma accompanied by progressive tumor growth (Clark et al., 2009, Clark et al., 2007, Vonderheide and Bayne, 2013).

Effector T cells are rare in preinvasive and invasive lesions and most T cells show a naïve phenotype without evidence of activation. Some tumor-specific T cells have been noted but these were typically dysfunctional (Garbe et al., 2006, Mukherjee et al., 2001). Vonderheide et al. proposed a hypothesis for T cell evasion in PDAC (Vonderheide and Bayne, 2013, Clark et al., 2009). They propose a dynamic model of the “four I” hypothesis: induction, inflammation, immune suppression and immune privilege. Induction – through alterations in oncogenes and tumor-suppressor genes like Kras and p53. Inflammation – through soluble factors secreted by PanIN lesions that facilitate a local inflammatory reaction composed of stromal and immune cells. Immune suppression – via infiltrating suppressive immune cells (TAMs, MDSCs, Tregs) inhibiting the development of an adaptive immune response through both the secretion of immunosuppressive cytokines, such as TGF- β , IL-10 and GM-CSF (Bayne et al., 2012, Pylayeva-Gupta et al., 2012), and direct cell-cell contact. And last but not least, immune privilege – with progression to PDAC, as neoplastic lesions maintain the capacity for immune evasion through both tumor- and immune-mediated mechanisms of suppression thereby establishing a site of immune privilege (Clark et al., 2009).

2.3.3 Immunotherapy of pancreatic cancer

Pancreatic cancer is mostly diagnosed in an advanced stage. Therefore, surgical resection can be performed in only a small number of patients and even after resection, recurrence occurs in the majority of the patients. Although adjuvant treatment with both chemotherapy and radiation therapy was demonstrated to induce some improvements in disease-free and overall survival rates, new therapeutic approaches are still urgently needed (Koido et al., 2011).

The aim of cancer immunotherapy is to activate the immune system for therapeutic benefit. Therefore, the cancer-immunity cycle has to be initiated or reinitiated (Chen and Mellman, 2013, Mellman et al., 2011). This cycle includes seven steps: (1) the release of tumor antigens through immunogenic cancer cell death. (2) the presentation of tumor antigens by DCs on MHC class I or II molecules to T cells in the lymph node, leading to (3) the priming and activation of these T cells. Afterwards, effector T cells traffic to the tumor site (4) and infiltrate the tumor (5). CTLs specifically recognize and bind to cancer cells (6) to kill their targets (7), leading to the release of new tumor antigens (back to step 1) (Chen and Mellman, 2013). Though, in most cancer patients this cancer-immunity cycle does not perform faultless.

For immunotherapy of PDAC different strategies have been developed to activate the immune system, including therapeutic vaccines using tumor associated antigens (TAAs) and adoptive T cell transfer.

For the traditional therapeutic vaccination whole cancer vaccines or established cell lines as crude vaccines have been used (Gaudernack, 2006). The advantages that accrued from this approach are that (1) no specific tumor antigen needs to be identified, (2) immune responses to multiple tumor antigens

can be generated, and (3) such vaccines are not limited by patient HLA haplotype (Dodson et al., 2011). A further refinement of this approach is to increase the immunogenicity of such vaccines by genetically introducing immune stimulating genes, such as GM-CSF gene (Jaffee et al., 1998).

Another approach has been the characterization of TAAs. The idea is based on the assumption that molecules associated with pancreatic cancer and that have been used for diagnostic purposes could also be utilized for therapeutic vaccines (Gaudernack, 2006). To date there are several TAAs that have been identified in pancreatic cancer, such as Wilms' tumor gene 1 (WT1), mucin 1 (MUC1), mutated Kras, carcinoembryonic antigen (CEA), human telomerase reverse transcriptase (hTERT), survivin, HER2/neu, and p53 or mesothelin (Koido et al., 2011, Dodson et al., 2011). However, there has been the problem that the immune system has already generated tolerance towards them. Furthermore, most of the TAAs are not exclusively restricted to malignant tissue (Gaudernack, 2006).

Another promising alternative with respect to a vaccination therapy is the design of DC-based cancer vaccines (Koido et al., 2011). DCs can be pulsed with synthetic peptides derived from known tumor antigens, tumor cell lysates or apoptotic tumor cells (Koido et al., 2011). Besides, DCs can be transfected with whole tumor cell DNA or RNA, or fused to tumor cells to induce antigen-specific polyclonal CTL responses (Koido et al., 2011). An alternative strategy is to target DC directly *in vivo* using tumor antigens formulated with adjuvants, such as DEC205 mAb (Bonifaz et al., 2004) or ISCOMATRIX adjuvant (Jacobs et al., 2011, Davis et al., 2004).

The adoptive T cell transfer technology includes the selective expansion of the patient's own T cells directed against a specific antigen followed by reinfusion into the patient (Dodson et al., 2011). Moreover, much effort is spent on the development of chimeric antigen receptors (CARs), these are engineered receptors grafting the specificity of a monoclonal antibody onto a T cell. For this purpose, the T cells of patients are transfected with a construct encoding an antibody against a tumor surface antigen fused to T cell signaling domains (Chen and Mellman, 2013). The resulting T cells recognize the tumor antigen in its native form and do not rely on presentation of antigens by MHC molecules (Dodson et al., 2011).

2.4 Mechanisms of immune suppression in pancreatic cancer biology

The microenvironment in PDAC as well as the cancer cells themselves contribute to the immunosuppressive milieu found in the tumors. A multitude of cellular and molecular aspects have to be considered.

2.4.1 Cellular aspects

Different cell types are responsible for tumor immune evasion, including tumor-associated macrophages (TAMs), myeloid derived suppressor cells (MDSCs), regulatory T cells (Tregs), and tolerogenic dendritic cells (DCs). Another important aspect with regard to immune suppression is the tumor microenvironment including stromal cells.

2.4.1.1 Tumor-associated macrophages

The most abundant leukocyte subset in PDAC is represented by TAMs, that can be identified by CD11b⁺ expression, which cluster around neoplastic ducts starting in very early stages (Clark et al., 2009). TAMs can be divided into two different populations, the classical/M1-activated macrophages (CD68⁺) and the alternative/M2-activated macrophages (CD163⁺). The M1-activated macrophages act against intracellular pathogens as well as tumor cells, providing an anti-tumorigenic response by secreting IFN- γ (Ruffell et al., 2012, Wormann et al., 2013). The M2-activated macrophages initiate a pro-tumorigenic response by promoting angiogenesis and invasion (Wormann et al., 2013, Ruffell et al., 2012). Furthermore, TAMs can inhibit anti-tumor T cell responses by production of Indoleamine 2,3-dioxygenase metabolites and reactive oxygen species (Pollard, 2004, Bronte et al., 2003).

2.4.1.2 Myeloid-derived suppressor cells

Other immunosuppressive myeloid cell types are MDSCs, representing prominent populations in tumors as well as in spleens of tumor-bearing hosts. MDSCs are characterized by CD11b and Gr-1 expression on their surface and are recruited to tumors by GM-CSF, which is secreted by tumor cells (Bayne et al., 2012). Two major subtypes can be discriminated in mice, Ly6G⁺ granulocytic MDSCs and Ly6C⁺ monocytic MDSCs (Gabrilovich et al., 2012). MDSCs are able to impair T effector T cell functions in a number of ways. They can inhibit antigen-specific responses (proliferation, cytokine production and cytotoxicity) mediated by T cells (Clark et al., 2009, Gabrilovich et al., 2001). Furthermore, they can cause down-regulation of the T cell ζ chain, a key component in TCR signaling. Last but not least, they can induce the development of Tregs and have the capacity to induce T cell apoptosis (Clark et al., 2009). Within the tumor microenvironment the predominance of MDSCs inversely correlates with that of CTLs in the leukocytic infiltrate of pancreatic tumors, raising the possibility that MDSCs may negatively affect T cell trafficking or T cell survival within PDAC (Clark et al., 2009, Clark et al., 2007).

2.4.1.3 Dendritic cells

Tumor cells have the capability to establish an immunosuppressive environment by inhibiting maturation and function of DCs (Wormann et al., 2013, Pinzon-Charry et al., 2005). Differentiation and antigen presentation of DCs can be suppressed by PDAC conditioned medium *in vitro* (Wormann et al., 2013, Bharadwaj et al., 2007). But additionally DCs and macrophages produce

immunosuppressive enzymes, such as IDO and COX2, and secrete immune modulatory and chemotactic factors, such as IL-6, TGF- β , CCL2 and CCL20 (Wormann et al., 2013). Therefore, DCs may also exhibit tumor-promoting functions including active suppression of cytotoxic T cell functions by TGF- β -dependent Treg proliferation and l-arginine metabolism (Wormann et al., 2013). Besides, DCs may have impaired antigen presenting function and diminished capacity to induce tumor-specific T cell activation (Wormann et al., 2013).

2.4.1.4 Regulatory T cells

Infiltration of Tregs in preinvasive lesions is an early event during PDAC development (Liyanage et al., 2002), possibly mediated by tumor-derived TGF- β and CCL5, which converts CD4⁺ T cells into Tregs (Moo-Young et al., 2009). Their presence within tumors has been linked with decreased survival (Curiel et al., 2004). Tumor-associated Tregs can inhibit T cell production of IFN- γ and IL-2 in response to tumor-associated antigens, as well as their cytotoxic functions. In PDAC, Tregs control the anti-tumor response from PanINs to invasive cancer and are markers of poor prognosis (Hiraoka et al., 2006).

2.4.1.5 Tumor microenvironment

A prominent feature of pancreatic cancer is the presence of an abundant tumor stroma accounting for up to 90% of the tumor mass (Neesse et al., 2011). Tumor stroma as a physical barrier can be one factor contributing to the failure of systemic therapies (Feig et al., 2012). Pancreatic tumor stroma is very heterogeneous, comprising fibroblasts, myofibroblasts, pancreatic stellate cells (PSCs), immune cells, blood vessels, extracellular matrix (ECM) and soluble proteins, such as cytokines and growth factors. The tumor microenvironment is not a static entity but dynamic in its composition, especially in the progression from preinvasive to invasive lesions (Feig et al., 2012).

ECM components include collagen, fibronectin, proteoglycans and hyaluronic acid and the composition is regulated by matrix metalloproteinases (MMPs). MMP-2 and MMP-9 are overexpressed in PDAC and play an important role in tumor cell migration and invasion by degrading the surrounding ECM (Neesse et al., 2011, Ellenrieder et al., 2000). The immunosuppressive actions of MMPs are cleaving growth factors and cytokine receptors, e.g. the IL-2 receptor (IL-2 α), thereby inhibiting proliferation and activation of T cells (Becker et al., 2013). MMPs also increase the bioavailability of TGF- β by regulating the release from an inactive extracellular complex (Becker et al., 2013).

PSCs are an important regulator of desmoplasia in PDAC and are normally located in the space between acini and endothelial cells. Stellate cells can be found in two stages, a quiescent form under physiological conditions and an activated form under acute and chronic inflammatory conditions.

Pancreatic cancer cells induce PSC activation *in vitro* by growth factors such as TGF- β_1 , PDGF and VEGF. In the activated stage PSCs undergo morphological changes and express α -smooth muscle actin (α -SMA). They secrete high amounts of collagen I and III, fibronectin and MMPs, leading to the deposition of ECM (Neesse et al., 2011, Omary et al., 2007, Apte et al., 1998). Xue et al. identified PSCs as the primary source of galectin-1 in PDAC stroma where it promotes proliferation and invasion of pancreatic cancer cells (Xue et al., 2011). At the same time, Tang et al. demonstrated that galectin-1 secreted by PSCs plays a role in the development and maintenance of an immunosuppressive microenvironment in PDAC by inducing apoptosis of CD4⁺ and CD8⁺ T cells (Tang et al., 2011).

2.4.2 Molecular mechanisms

2.4.2.1 Galectin-1

It is known that pancreatic carcinoma cells produce a variety of immunosuppressive proteins. One of these is galectin-1. Dimeric galectin-1 secreted by tumor cells contributes to tumor immune escape by inducing apoptosis in effector T cells, especially T helper cells 1 (T_H1) and T_H17 cells, but not in naïve, T_H2 or regulatory FoxP3⁺ T cells (Treg). This is caused by the glycosylation on these cells that prevents binding to galectin-1. Galectin-1 secretion leads to the expansion of regulatory T cells, promotes angiogenesis and inhibits transendothelial migration of effector T cells into the tumor (Yang et al., 2008, Cedeno-Laurent and Dimitroff, 2011, Toscano et al., 2007). In addition, galectin-1 changes the cytokine balance towards a T_H2 type, characterized by increased IL-4 and IL-5 levels, whereas the levels of IFN- γ , IL-2 and IL-17 decreases. Cedeno-Laurent et al. showed that both uncommitted and polarized T_H cells exposed to galectin-1 express an immune regulatory signature defined by IL-10 production (Cedeno-Laurent et al., 2012). Tumor cells secreting galectin-1 use this strategy to promote tumor growth and to escape from the immune system. It is of importance, that killing of T cells by Galectin-1 secreting tumor cells depends on the expression and cell surface presentation of galectin-1 by the tumor cells and requires intimate cell-cell contact between the target and effector cells (Kovacs-Solyom et al., 2010).

2.4.2.2 Transforming growth factor beta (TGF- β)

TGF- β is a member of a superfamily of growth factors and consists of five isoforms of which type 1 to 3 are found in mammals (de Visser and Kast, 1999). TGF- β_1 circulates in the blood and is the most rapidly induced factor. TGF- β mediates protection against immune attack in the tumor (Rubtsov and Rudensky, 2007). In the presence of TGF- β_1 and IL-2 naïve CD4⁺ T cells differentiate into FoxP3⁺ Treg cells, which themselves secrete TGF- β in an auto- and paracrine manner, thereby suppressing effector T cells (Rubtsov and Rudensky, 2007). TGF- β is produced by a variety of cells, including platelets and osteoblasts but also lymphocytes, macrophages and neutrophils secrete TGF- β under

certain conditions (de Visser and Kast, 1999). Furthermore, tumor cells are also known to express TGF- β (de Visser and Kast, 1999). The production of TGF- β can be advantageous for tumor growth due to the suppression of immunosurveillance. Other mechanisms include the promotion of angiogenesis, metastasis and connective tissue formation (de Visser and Kast, 1999). In addition, TGF- β has inhibitory effects on CTLs, i.e. it suppresses the expression of pore-forming protein (PFP), a crucial molecule in the cytolytic pathway. Inhibition of cytokine production in CTLs, like IFN- γ and TNF- α , as well as down-regulation of IL-2R inhibits T cell proliferation (de Visser and Kast, 1999). Another mechanism of TGF- β -induced suppression of T cell expansion in response to antigen and IL-2 is the induction of apoptosis (Weller et al., 1994). We have shown *in vitro* and *in vivo* that TGF- β is highly abundant in tumor-conditioned medium of Panc02 tumor cells and in serum of Panc02-tumor-bearing mice, respectively (Ellermeier et al., 2013).

2.4.2.3 Indoleamine 2,3-dioxygenase (IDO)

IDO catalyzes the first and rate limiting step of the oxidative catabolism of tryptophan to kynurenine, the first step in the biosynthesis of the central metabolic regulator nicotinamide adenine dinucleotide (NAD) (Prendergast, 2008, Johnson et al., 2009). Functional IDO activity depends on the binding of IDO to heme, on a substrate supply, redox potentials and the absence of heme toxins, such as nitric oxide (Johnson et al., 2009). There are two closely linked, homologous genes (IDO1 and IDO2) located in syntenic regions of chromosome 8 in humans and mice encoding IDO proteins (Ball et al., 2007, Johnson et al., 2009). The genes possess one or more IFN response elements in their promoter regions, thus IFNs are potent inducers of IDO in several cell types, including DCs, macrophages, eosinophils, epithelial and endothelial cells (Johnson et al., 2009).

In DCs, IDO expression can be induced by binding of CTLA-4 to B7 molecules (Fallarino et al., 2003, Muller and Prendergast, 2007). In tumors, IDO⁺ pDCs are present protecting the tumor from immunosurveillance by regulating local T cell responses that could otherwise eliminate premalignant cells (Johnson et al., 2009). The tryptophan metabolites cause cell cycle arrest, apoptosis and anergy in T cells, meaning that IDO activity blocks both clonal expansion of CD8⁺ and CD4⁺ T cells and generation of CTLs and T_H cells while having less impact on T_H2 cells (Fallarino et al., 2002). In contrast, IDO activity in pDCs promotes *de novo* Treg differentiation from naïve CD4⁺ precursors (Fallarino et al., 2003). But how does IDO block T cell responses? Activated T cells secrete INF- γ , which results in the up-regulation of IDO in APCs, suggesting a negative feedback loop to regulate T cell activation (Grohmann et al., 2003, Katz et al., 2008). Moreover, the secretion of IFN- γ induces T cells to undergo IDO-mediated apoptosis by activation of the caspase pathway and tryptophan deprivation causes enhanced Fas-dependent apoptosis and growth arrest of activated T cells (Lee et al., 2002, Johnson et al., 2009, Katz et al., 2008). Additionally, T cells respond to tryptophan starvation by inducing the stress-signaling pathway via GCN2 that alters eIF2 α phosphorylation and translational

initiation at the ribosome leading to cell growth arrest (Munn et al., 2005). The combined effects of tryptophan starvation and tryptophan catabolites act via the aryl hydrocarbon receptor (AHR) of T cells (Fallarino et al., 2012). Indirectly, IDO induced Tregs mediate suppression of effector T cells via a unique and distinctive mechanism dependent on intact PD-1/PD-L1 signaling (Johnson et al., 2009, Sharma et al., 2007). Witkiewicz et al. found that IDO is expressed in the cytoplasm of well-differentiated pancreatic adenocarcinomas, in lymph node metastasis and in human pancreatic cancer cell lines but it is not expressed in healthy pancreatic tissue (Witkiewicz et al., 2008). They could also show that Tregs were increased in IDO expressing tumors. In addition, IDO2 is overexpressed in PDAC and may represent an attractive target in pancreatic cancer (Witkiewicz et al., 2009). Recently, it has been reported that the aggressiveness of intraductal papillary mucinous neoplasms (IPMN), another kind of precursor lesion of pancreatic cancer, significantly correlated with the number of Tregs and IDO-expressing cells in pancreatic tissue (Ikemoto et al., 2013). In Figure 2-1 the effects of IDO-expressing tumors are summarized.

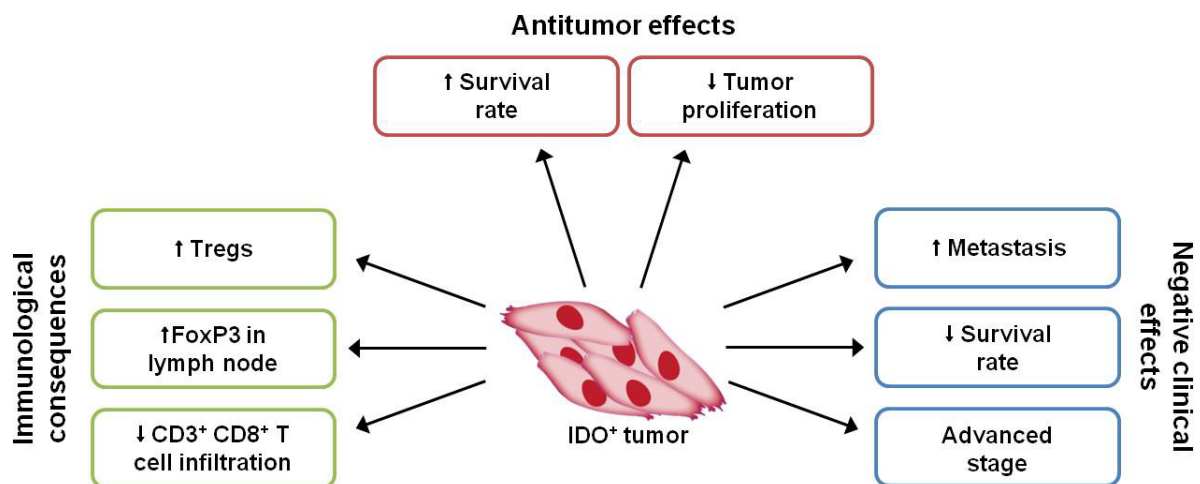


Figure 2-1: Effects of IDO-positive tumors (modified from Godin-Ethier et al.)

The different aspects are divided based on their impact on the immune system, tumor progression or tumor regression (Godin-Ethier et al., 2011).

2.5 Therapeutic application of RNA interference

In this study, a novel therapeutic strategy involving RNA interference (RNAi) was used to counteract immunosuppressive mechanisms mediated by galectin-1 in tumor-bearing mice. In addition, the immune activating properties of 5'ppp-modified siRNA were assessed for the treatment of murine PDAC by generating a bifunctional siRNA that combines galectin-1 gene silencing with RIG-I-mediated immune activation in one molecule.

2.5.1 RNA interference

The RNAi machinery, which is found in all cells, can be harnessed to silence gene expression with a high degree of specificity. When synthetic, short double-stranded RNAs, called small interfering RNAs (siRNA) that resemble sequences of the mRNA are introduced to the cytoplasm of cells, the

double strand is split up into the passenger (sense) and the guide (antisense) strand. While the passenger strand is degraded, the guide strand is incorporated into the RNA-induced silencing complex (RISC) and can guide the cleavage of mRNAs bearing an exactly complementary sequence (Elbashir et al., 2001, Petrocca and Lieberman, 2011). This cleavage is performed by argonaute or Ago protein which is a RISC ribonuclease enzyme (Ambros, 2004). In case of a partial complementarity between the mRNA and the siRNA, the mRNA is not degraded, however the translation is interrupted (Petrocca and Lieberman, 2011). siRNAs can be designed to silence any gene of interest. In cancer, RNAi can be used to suppress for example oncogenic transcription factors or other regulating proteins (Petrocca and Lieberman, 2011). It is relatively simple to develop a new candidate siRNA once a target has been identified. Another advantage of siRNAs is that they are active at low concentrations (Petrocca and Lieberman, 2011). However, a negative aspect of this gene silencing technique is that the effect is temporally limited as the RISC with the incorporated siRNA gets divided between daughter cells. Therefore, in fast proliferating tumor cells, gene silencing lasts for less than a week (Petrocca and Lieberman, 2011). Furthermore, there are off-target effects of RNAi, including that the siRNA is recognized by immune sensors of viral infection, such as TLRs in the endosomes or RIG-I like helicases in the cytoplasm (Hornung et al., 2005). These off-target effects can be deliberately exploited using the 5' ppp-modified siRNA technology.

2.5.2 5'ppp-modified siRNA

A distinct and independent biological property of RNA oligonucleotides is their ability to activate immunoreceptors specialized for the detection of viral nucleic acids (Poeck et al., 2008). One cytoplasmic sensor for viral RNA is the RIG-I helicase retinoic-acid inducible gene-I (RIG-I) (Yoneyama et al., 2004). RIG-I detects RNA with a triphosphate (ppp) group at the 5' end (Hornung et al., 2006, Pichlmair et al., 2006). Detection of ppp-siRNA by RIG-I leads to the induction of type I interferons (IFN) as well as the secretion of pro-inflammatory cytokines and chemokines via recruitment of the adapter molecule Interferon- β promoter stimulator 1 (IPS-1) and phosphorylation of the transcription factor IFN regulatory factor 3 (IRF-3) and IRF-7 (Cao, 2009). Both biological activities, gene silencing via RNAi and stimulation of the immune system via RIG-I, can be combined in one molecule, the ppp-siRNA (Poeck et al., 2008). Such ppp-siRNA can be generated by *in vitro* transcription (IVT), in which a double-stranded DNA template is produced by annealing a T7 promoter primer at the TATA-box of DNA templates of the desired genes. Templates are then transcribed *in vitro* by a T7 RNA polymerase into single-stranded ppp-siRNAs. These ppp-siRNAs can be applied as ligand for RIG-I to trigger pro-apoptotic signaling via the intrinsic mitochondrial pathway (Besch et al., 2009, Poeck et al., 2008, Ellermeier et al., 2013, Meng et al., 2013). Apoptosis induction affects predominantly tumor cells as non-malignant cells are protected from pro-apoptotic signaling via Bcl-xL (Besch et al., 2009, Meng et al., 2013). Therapeutic strategies exploiting the ppp-siRNA technology were recently described by Ellermeier et al. and Meng et al.. Ellermeier et al.

could show that ppp-siRNA targeting the immunosuppressive cytokine TGF- β reduced systemic and tumor-associated TGF- β levels, induced type I IFNs, CXCL10 and apoptosis of tumor cells and activated immune cells systemically. Treatment of Panc02 tumor-bearing mice with ppp-TGF- β prolonged survival and led to an increase of CD8⁺ T cells in pancreatic tumors (Ellermeier et al., 2013). Meng et al. generated a bifunctional ppp-siRNA targeting glutaminase (ppp-GLS). Silencing of glutaminase sensitized tumor cells to RIG-I, mediated apoptosis, and enhanced cytotoxicity through disturbed glutaminolysis (Meng et al., 2013).

3 Objectives

PDAC is a very aggressive tumor with abundant tumor stroma and a strong immunosuppressive microenvironment. Further studies to clarify why T cells infiltrate the tumor but are not able to perform killing function as well as to find new effective therapies are urgently needed. The present study addressed three main goals:

1. To characterize murine PDAC models in regards to their utility for studying immunotherapeutic approaches.
2. To assess the therapeutic efficacy of a novel bifunctional ppp-siRNA that combines silencing the immunosuppressive molecule galectin-1 with activation of RIG-I in murine PDAC.
3. To characterize the immunosuppressive actions on T cells in the microenvironment of PDAC.

Along with advances in the generation of GEMM, new tumor models for studying PDAC have become available in the last years. These models have several advantages regarding phenocopying of the human disease. Traditionally, syngeneic tumor models have been used to study PDAC, such as subcutaneous or orthotopic implantation of Panc02 cells in C57BL/6 mice. With GEMM new cell lines have been generated for transplantation in syngeneic mice. In this study, two different GEMM for PDAC (KPC models) were compared with two syngeneic models (Panc02 cells and T110299 cells, a cell line derived from KPC mice) regarding histological appearance, expression of immunosuppressive molecules and growth characteristics. These studies were performed to gain insight into specific aspects of tumor biology for further therapeutic studies. The questions addressed were: How abundant is the stromal component in the tumors? Can preinvasive lesions resembling PanINs be detected? How are patterns of T cell infiltrations? Do the tumors express immunosuppressive molecules, such as galectin-1 and IDO, which can be targeted by immunotherapy?

As mentioned above, PDAC express the immunosuppressive molecule galectin-1. This led to the idea to study siRNA molecules targeting Galectin-1 either as unmodified OH-siRNA or as modified ppp-siRNA. Both molecules (OH-Gal-1 and ppp-Gal-1) were tested *in vitro* and *in vivo* to assess whether the application of siRNA and especially ppp-siRNA has therapeutic efficacy against PDAC.

Pancreatic cancer is characterized by its ability to suppress T cells leading to inefficient tumor control by the immune system. The present study addresses several potential mechanisms for T cell inhibition, such as the PD-1/PD-L1 axis, galectin-1, TGF- β and IDO. Functional aspects of T cell suppression, such as T cell proliferation, apoptosis induction and T cell degranulation, were investigated.

4 Material

4.1 Technical equipment

Blotting system	Bio-Rad, Germany
Cell culture CO ₂ incubator (BD 6220)	Heraeus, Germany
Cell culture Laminar Flow	Thermo Scientific, Germany
Centrifuge (Multifuge 3L-R)	Thermo Scientific, Germany
Centrifuge (5424 and 5415R)	Eppendorf, Germany
ELSIA reader (Mithras LB940)	Berthold Technologies, Germany
FACSCanto II	BD Bioscience, Germany
Gel electrophoresis system	peqlab, Germany
Lightcycler [®] 480 II	Roche, Germany
Microscope Axiovert25 and Axiovert200M	Zeiss, Germany
Microscope TCS SP5 II	Leica, Germany
NanoDrop [®] 2000c	Thermo Scientific, Germany
pH meter	WTW, Germany
Power Pac Basic	Bio-Rad, Germany
Rotator RM5	Karl Hecht AG, Germany
Scale SBC21	Scale Tec, USA
Thermocycler T3	Biometra, Germany
Thermomixer	Eppendorf, Germany
Vortex Genie 2	Scientific Industries, Germany
Water bath	Köttermann, Germany
Western Blot analyzer (LAS4000 mini)	FujiFilm, Germany
Cover glass	VWR, Germany
Glass capillary pipette	Hirschmann Laborgeräte, Germany
Gel blotting paper	Whatman Paper GmbH, UK
Insulin U-100 0.3 ml	BD Microfine, Germany
Lab-Tek [®] Chamber slide	Thermo Scientific, Germany
Microscope slides (Superfrost [®] Plus Menzel-Gläser)	Thermo Scientific, Germany
Nitrocellulose membrane (Amersham [™] -Hybond [™] -ECL)	GE Healthcare, Germany
Scalpel (No. 22)	Feather, Japan
Sutures (Prolene 5-0)	Ethicon, USA

4.2 Chemicals, reagents and buffers

Alcian Blue solution (pH 2.5)	Sigma-Aldrich, Germany
Ammonium acetate	life technologies, Germany
Antisedan	Pfizer, USA
Bovine serum albumin	Roth, Germany
Catalase	Sigma-Aldrich, Germany
Cell lysis buffer (10x)	Cell Signaling Technology, USA
Chloroform	Roth, Germany
Collagen (rat tail tendon)	Roche, Germany
Collagenase	Sigma-Aldrich, Germany
CountBright™ absolute Counting Beads	life technologies, Germany
3,3-diaminobenzidine (DAB)	Dako, USA
4-dimethylamino-benzaldehyde (Ehrlich's reagent)	Sigma-Aldrich, Germany
DC Protein Assay (Bradford)	Bio-Rad, Germany
Dimethyl sulfoxide	Roth, Germany
DNase I	Roche, Germany
Dorbene	Pfizer, USA
DPX	Merck, Germany
Dulbecco's PBS (1x)	Lonza, Belgium
Easy Coll solution (d=1.124g/l)	Biochrome, Germany
ECL	Thermo Scientific, Germany
Eosin Y	Merck, Germany
Ethanol	Sigma-Aldrich, Germany
Ethylenediaminetetraacetic acid (EDTA)	Sigma-Aldrich, Germany
FACSFlow, FACSClean	BD Biosciences
Flumazenil	Inresa, Germany
Formal-FIXX	Thermo Shandon, UK
Glacial acetic acid	Merck, Germany
Heparin-Natrium Braun 25000 I.E./5 ml	Rathiofarm, Germany
Hydrogen peroxide (H ₂ O ₂ , 30%)	Merck, Germany
<i>In vivo</i> -JetPEI™	Polyplus transfection, USA
Isoflurane-CP®	CP-Pharma, Germany
Isopropanol	Applichem, Germany
KAPA PROBE FAST Universal qPCR Master Mix	peqlab, Germany
Lipofectamine RNAiMax	life technologies, Germany
Lipopolysaccheride-EK, ultrapure (LPS)	InvivoGen, USA
L-Tryptophan	Sigma-Aldrich, Germany

Mayer's Hemalum	Roth, Germany
Methanol	Merck, Germany
Midazolam	Ratiopharm, Germany
Naloxone	Inresa, Germany
Nuclear fast red solution (0.1%)	Sigma-Aldrich, Germany
PageRuler™ Plus Prestained Protein Ladder	Thermo Scientific, USA
Paraformaldehyde (PFA)	Merck, Germany
Pharmlyse	BD Bioscience, Germany
Phenol-chloroform isoamyl alcohol	Sigma-Aldrich, Germany
Potassium hydrogenphosphate	Merck, Germany
Primer-probe mix, 10x conc.	Roche, Germany
Propidium iodide	Sigma-Aldrich, Germany
Proteinase K beads	Sigma-Aldrich, Germany
Saponine	Sigma-Aldrich, Germany
Sodium ascorbate	Sigma-Aldrich, Germany
Sodium azide (NaN ₃ , 10%)	Sigma-Aldrich, Germany
Sodium chloride (NaCl 0.9%)	Baxter, UK
Sulfuric acid (H ₂ SO ₄ , 2N)	Apotheke Uni Munich, Germany
Target antigen retrieval solution (10 x, pH 6.0)	Dako, USA
Temgesic (Buprenorphin)	RB Pharmaceuticals, UK
TMB Substrate Reagent Set	BD Bioscience, Germany
Trichloroacetic acid	Roth, Germany
Trypan blue	Sigma-Aldrich, Germany
Trypsin-EDTA(10x)	PAA, Austria
Turbo-DNase	life technologies, Germany
Tween® 20	Roth, Germany
Vectashield mounting medium	Vector Laboratories, USA
Xylene	J.T. Baker, Netherlands

Western Blot:

<u>Laemmli buffer (6x)</u>	<u>Stacking buffer (4x, pH 6.8)</u>
347 mM SDS	248 mM Tris
299 µM Bromphenol blue	14 mM SDS
4.7 ml Glycerol	15 µM Bromphenol blue
0.5 M Tris, pH 6.0	in ultrapure water
649 mM DTT	
4.1 ml ultrapure water	

Separating buffer (4x, pH 8.8)

1.5 M Tris
14 mM SDS
in ultrapure water

Running buffer (10x)

248 mM Tris
1.92 M Glycine
35 mM SDS
in ultrapure water

Transfer buffer (20x)

198 mM Tris
2 M Glycine
in ultrapure water

Transfer buffer (1x)

20x stock
10% MeOH
in ultrapure water

Blocking buffer

5% BSA
in TBST

Washing buffer (TBST)

165.9 mM Tris-HCl
44.5 mM Tris
1.5 M NaCl
0.5% Tween 20

Immunocytochemistry:Fixation buffer

4% PFA
in PBS

Permeabilization buffer

0.2% TritonX-100
in PBS

Blocking buffer

2% BSA
in PBS

Flow cytometry:FACS acid buffer

2 mM EDTA
2% FBS
0.1% NaN₃
in PBS

Permeabilization buffer

0.5% saponine
in PBS

Fixation buffer

1% PFA
in PBS

T cell assay:MACS-buffer

0.2% FBS

2mM EDTA

in PBS

4.3 Cell culture reagents and media

β-mercaptoethanol	Roth, Germany
Dulbecco's modified Eagle's medium (DMEM), high glucose	Roth, Germany
Dynabeads [®] Mouse T activator CD3/CD28	life technologies, Germany
Fetal bovine serum (FBS)	life technologies, Germany
L-glutamine (200 mM)	PAA, Austria
MEM-NEAA (non-essential amino acids)	life technologies, Germany
Penicilline/Streptomycin (100 x)	PAA, Austria
Opti-MEM	life technologies, Germany
OVA ₂₅₇₋₂₆₄ peptide (SIINFEKL)	InvivoGen, USA
Roswell Parl memorial Institute (RPMI) 1640 medium	Biochrome, Germany
Sodium pyruvat	Biochrome, Germany
VLE RPMI 1640 (very low endotoxin)	Biochrome, Germany

Plastic material for cell culture experiments were purchased from BD Bioscience (Germany), Corning (USA), Eppendorf (Germany), Greiner bio-one (Germany) or Sarstedt (Germany).

Tumor cell medium

10% FBS

2 mM L-glutamine

100 IU/ml penicillin

100 µg/ml streptomycin

in DMEM

Transfection medium

10% FBS

2 mM L-glutamine

in DMEM

T cell medium

10% FBS

2 mM L-glutamine

100 IU/ml penicillin

100 µg/ml streptomycin

1 mM sodium pyruvat

1% MEM-NEAA

DC medium

10% FBS

2 mM L-glutamine

100 IU/ml penicillin

100 µg/ml streptomycin

1 mM sodium pyruvat

1% MEM-NEAA

50 μ M β -mercaptoethanol
in RPMI 1640

50 μ M β -mercaptoethanol
in VLE RPMI 1640

4.4 Cell lines

Panc02
T110299
PANC-1
IMIM-PC1

kindly provided by Peter Nelson lab
kindly provided by Jens Siveke lab
Cell Lines Service (CLS), Germany
kindly provided by Patrick Michl lab

4.5 Kits

Cell Trace™ CFSE Cell Proliferation kit
CXCL10 murine (ELSIA)
Galectin-1, murine (ELISA)
IFN- α , murine (ELISA)
HiScribe™ T7 *In Vitro* Transcription kit

LS columns
MACS Pan T cell isolation kit II
MACS CD8a T cell isolation kit II
Masson's Trichrome Stain kit
peqGOLD Total RNA isolation kit
RevertAid™ First strand cDNA Synthesis kit
TGF- β , murine (ELISA)
TNF- α , murine (ELISA)
Vectastain ABC Elite rabbit-IgG/rat-IgG kit

life technologies, Germany
R&D Systems, Germany
R&D Systems, Germany
R&D Systems, Germany
New England Biolabs GmbH,
Germany
Miltenyi Biotech, Germany
Miltenyi Biotech, Germany
Miltenyi Biotech, Germany
Polyscience Inc., USA
peqlab, Germany
Thermo Scientific, USA
eBioscience, Germany
R&D Systems, Germany
Vector Laboratories, USA

4.6 Antibodies

4.6.1 Primary conjugated antibodies and reagents for FACS

Table 4-1: Primary conjugated antibodies and reagents for flow cytometry

Specificity	Fluorochrome	Species/isotype	Clone	Concentration	Company
Annexin V	APC	chicken recombinant		1:33	Immunotools
CD3	APC	hamster/IgG ₁	145-2C11	1:100	BD Bioscience
CD3	PB	rat/IgG _{2b}	17A2	1:200	BioLegend
CD4	FITC	rat/IgG _{2a}	RM4-5	1:200	BD Bioscience
CD4	PE-Cy7	rat/IgG _{2a}	RM4-5	1:200	BioLegend
CD4	PerCP	rat/IgG _{2a}	RM4-5	1:200	BioLegend

CD8a	APC-Cy7	rat/IgG _{2a}	53-6.7	1:200	BioLegend
CD8a	PB	rat/IgG _{2a}	53-6.7	1:200	BioLegend
CD8a	PerCP	rat/IgG _{2a}	53-6.7	1:200	BioLegend
CD11c	APC	hamster/IgG	N418	1:200	BioLegend
CD19	PE	rat/IgG _{2a}	6D5	1:200	BioLegend
CD45R/B220	PE-Cy7	rat/IgG _{2a}	RA3-6B2	1:200	BioLegend
CD69	FITC	hamster/IgG ₁	H1.2F3	1:100	BD Pharmingen
CD69	PE	hamster/IgG ₁	H1.2F3	1:100	BD Pharmingen
CD86	FITC	rat/IgG _{2a}	GL-1	1:100	BD Pharmingen
CD95	PE-Cy7	hamster/IgG ₂	Jo2	1:200	BD Pharmingen
CD107a	FITC	rat/IgG _{2a}	1D4B	1:5000	BD Pharmingen
CD107b	FITC	rat/IgG _{2a}	ABL-93	1:200	BD Pharmingen
CD274	Purified	rat/IgG _{2a}	MIH5	1:200	eBioscience
Anti-rat	AF488	goat/IgG	---	1:200	life technologies
NK1.1	PerCP	mouse/IgG _{2a}	PK136	1:200	BioLegend
MHC-I	FITC	mouse/IgG _{2a}	AF6-88.5	1:200	BioLegend
MHC-II	FITC	mouse/IgG _{2a}	AF6-120.1	1:200	BD Pharmingen

APC: Allophycocyanine; FITC: Fluorescein-5-isocyanate; PB: Pacific blue; PE: Phycoerythrine; PerCP: Peridinin-chlorophyll-protein complex;

4.6.2 Purified antibodies for immunohistochemistry

Table 4-2: Purified antibodies for IHC

Specificity	Species/isotype	Clone	Concentration	Company
α -SMA	rabbit-IgG	polyconal	1:400	abcam
CD3	rabbit/IgG	SP7	1:250	abcam
CD31	rabbit/IgG	polyconal	1:1.000	abcam
Galectin-1	rat/IgG _{2B}	201002	1:20.000	R&D Systems
IDO	rabbit/IgG	polyclonal	1:50	abcam
Isotype	rabbit/IgG	polyclonal	depending on primary antibody	abcam
Isotype	rat/IgG _{2B}	RTK4530		Biolegend

4.6.3 Blocking antibodies

Table 4-3: Blocking antibodies for *in vitro* assays

Specificity	Fluorochrome	Species/isotype	Clone	Concentration	Company
CD279	Func. grade purified	hamster IgG	J43	5 μ g/ml	eBioscience
CD80	Func. grade purified	hamster IgG	16-10A1	5 μ g/ml	eBioscience
Isotype	Func. grade purified	hamster IgG	eBio299Arm	5 μ g/ml	eBioscience

4.6.4 Antibodies for Western Blot

Table 4-4: Western Blot antibodies

Specificity	Fluorochrome	Species/isotype	Clone	Concentration	Company
pIRF3 (S396)	purified	rabbit/IgG	4D4G	1:1000	Cell signaling
CD274	purified	rat/IgG _{2a}	MIH5	1:1000	eBioscience
Anti-rabbit	HRP	goat/IgG	---	1:2000	Santa Cruz

Anti-rat	HRP	goat/IgG	---	1:2000	Santa Cruz
β -actin-HRP	HRP	mouse/IgG ₁	C4	1:2000	Santa Cruz

4.7 Inhibitors

β -lactose (Gal-1)	Sigma-Aldrich, Germany
Celecoxibe (COX2)	Sigma-Aldrich, Germany
D-1-Methyltryptophan (D-1-MT) (IDO)	Sigma-Aldrich, Germany
SC-560 (COX1)	Sigma-Aldrich, Germany
SD-208 (TGF- β RI)	TOCRIS bioscience, USA
Thiodigalactoside (Gal-1)	Carbosynth, UK

4.8 Recombinant cytokines and proteins

Interleukin-2 (IL-2), mouse	Peptotech, Germany
Interleukin-4 (IL-4), mouse	Peptotech, Germany
Interferon α (IFN- α), mouse	Miltenyi Biotech, Germany
Interferon β (IFN- β), mouse	
Interferon γ (IFN- γ), mouse	Immunotools, Germany
GM-CSF, mouse	Peptotech, Germany
Galectin-1, mouse	R&D Systems, Germany
TGF- β , human/mouse	R&D Systems, Germany

4.9 siRNA sequences

Table 4-5: siRNA sequences for RNAi

gene	sequence (5'->3')
OH-RNA (control)	GCGCTATCCAGCTTACGTATT
Galectin-1	GAUGGAGACUUCAAGAUUAAU
TGF- β ₁	GAACUCUACCAGAAAUAUAAU
RIG-I	GAAGCGUCUUCUAAUAAU

4.10 DNA-template sequences for *in vitro* transcription

Table 4-6: DNA-template sequences for IVT

gene	sequence (5'->3')
OH-RNA (control)	GCGCTATCCAGCTTACGTAGAGCTCTACGTAAGCTGGATAGCGCTAT AGTGAGTCGTA
Galectin-1	GATGGAGACTTCAAGATTACTCGAGTAATCTTGAAGTCTCCATCTAT AGTGAGTCGTA

4.11 Primer sequences for qRT-PCR

Table 4-7: Primer sequences for qRT-PCR

gene	5'→3'	
Galectin-1	left	CTCTCGGGTGGAGTCTTCTG
	right	GGTTTGAGATTCAGGTTGCTG
Interferon β	left	ACTGCCTTTGCCATCCAA
	right	CCCAGTGCTGGAGAAATTGT
TGF- β_1	left	TGGAGCAACATGTGGAAGTC
	right	CAGCAGCCGGTTACCAAG
IDO	left	GCACTCAGTAAAATATCTCC
	right	CTAAGGCCAACTCAGAAGA
HPRT	left	GGAGCGGTAGCACCTCCT
	right	CTGGTTCATCATCGCTAATCAC

4.12 Software

Adobe Photoshop CS4

Adobe Systems, USA

Adobe Illustrator CS4

Adobe Systems, USA

Axiovision Rel.4.4

Zeiss, Germany

EndNote X4

Thomson Reuters, USA

FACSDiva

BD Bioscience, Germany

FlowJo 7.6.5

Tree Star, USA

Graphpad Prism 5.0

Graphpad Software, USA

Image J

Image J Software, USA

LAS AF V2.2.1

Leica, Germany

Lightcycler 480 SW 1.5

Roche, Germany

5 Methods

5.1 Tumor cell culture

All tumor cell lines were cultured in DMEM complete medium in tissue culture flasks (T75) at 37°C in 10% CO₂ and 95% humidity.

All manipulations were performed with sterile reagents under a laminar flow hood. Cell number and viability was determined by Trypan blue staining. Cell suspensions were mixed with 0.5% Trypan blue in PBS at appropriate dilutions and counted in a Neubauer hemocytometer under the microscope.

5.2 Immunological methods

5.2.1 Enzyme-linked immunosorbent assay (ELISA)

ELISA is a method to detect cytokines or other proteins in samples from *in vitro* or *in vivo* assays by enzyme-linked antibodies. Proteins of interest in samples were bound by the respective plate-bound capture antibody followed by a second, biotinylated detection antibody which will bind streptavidin coupled to a horse radish peroxidase (HRP). This enzyme catalyzes the oxidation of 3,3',5,5' – tetramethylbenzidine (TMB) with hydrogen peroxide to a blue chromogen.

The detection of the chemokine CXCL10, the cytokine TGF- β and the protein Galectin-1 was performed with kits including all necessary reagents according to the manufacturer's instructions. Cell culture samples for CXCL10 were diluted 1:2, and undiluted for TGF- β . Serum samples for Galectin-1, IFN- α and TNF- α were diluted 1:5, for CXCL10 samples were diluted 1:10.

5.2.2 Western Blot

Cells were washed twice with cold PBS and lysed in an appropriate volume of lysis buffer for 30 min on ice. Samples were spun down for 10 min at 14 000 g, 4°C. The supernatant was transferred to a fresh Eppendorf tube and the protein concentration was determined by Bradford assay. Samples were mixed with 6 x Laemmli buffer and incubated at 95°C of 5 min. 50 μ g whole cell lysate of each sample was loaded on a 10-15 % SDS gel, depending on the size of the protein of interest. As a standard, 5 μ l of PageRuler™ Plus Prestained Protein Ladder (Thermo Scientific) was loaded. The gel was run at 100 V for 90 min. Proteins were transferred to a nitrocellulose membrane using the Mini Trans-Blot® Electrophoresis Transferecell (Biorad) in 1 x transfer buffer. The electrophoretic transfer was performed at 350 mA for 60 min at RT. Membranes were blocked with 5% BSA/TBST for 60 min at RT. Primary antibodies were diluted in blocking solution and incubated overnight at 4°C with

gentle shaking. Afterwards they were washed with TBST three times for 10 min and then incubated with the appropriate secondary antibody for 60 min at RT rotating. Membranes were washed three times for 10 min with TBST and developed using chemiluminescence substrate ECL (Thermo Scientific), according to the manufacturer's instructions. The membranes were exposed with the Western Blot analyzer LAS4000 mini.

5.2.3 Histology

5.2.3.1 Fixation, paraffin embedding and microtoming of mouse tumors

Organs were fixed in 10% phosphate-buffered formalin (Thermo Shandon) overnight at RT, followed by 9 h automated processing with a series of dehydration steps, and then they were embedded in paraffin wax. Paraffin blocks were sectioned with a microtome and 5 μ m sections were floated on a water bath at 50°C, transferred to glass slides, dried overnight at 37°C and stored at RT until staining.

5.2.3.2 Hematoxylin and eosin staining

The general immunohistochemistry protocol for paraffin embedded tissue sections included the following steps. Paraffin-embedded sections were deparaffinized by two rinses with xylene for 15 min and three rinses with alcohol (100, 96, and 70%, each 3 min), followed by two rinses in distilled water for 5 min. Afterwards, the nuclei were stained with Mayer's hemalaun coloring nuclei blue, followed by a 5 min washing step under running tap water. Then, a 1 min counter staining with an alcoholic solution of eosin Y coloring the cytoplasm and eosinophilic structures in various shades of red, pink and orange was performed and rinsed with tap water three to four times. Finally, the sections were dehydrated in an increasing ethanol series (two times 95% and 100%, each 5 min) and twice in xylene for 15 min followed by mounting the sections with xylene based DPX.

5.2.3.3 Masson's Trichrome staining

Staining of collagen fibers to visualize tumor stroma was performed with the Masson's Trichrome Staining kit according to the manufacturer's instructions. Briefly, paraffin embedded sections were rehydrated and mordant in Bouin's solution for 1 min at 750W in a microwave and cooled down for 15 min at RT. Sections were washed in running tap water for 5 min with a subsequent staining of nuclei with Weigert's hematoxylin for 7 min (nuclei colored blue), washed under running tap water for 5 min and rinsed in distilled water. Afterwards, cytoplasm and erythrocytes were stained with Biebrich Scarlet-Acid Fuchsin solution for 5 min and slides were rinsed in distilled water. To allow uptake of Aniline Blue, sections were placed in Phosphomolybdic/Phosphotungstic Acid Solution for 10 min and directly transferred to Aniline Blue for 7 min (blue staining of collagen) and rinsed in distilled water. Finally, sections were placed into an 1% Acetic acid solution for 3 min to render the shades of color more delicate and transparent and after the dehydration to xylene they were mounted with DPX.

5.2.3.4 Alcian Blue staining

The Alcian Blue 8G dye is a basic dye, which preferably stains acid mucosubstances and acetic mucins when given the right pH and salt concentrations. The presumed basis of the staining is its positive charge attracted to negative structures (e.g. acidic sugars), bulkiness (width 2.5–3 nm, compared to toluidine blue ~0.7 x 1.1 nm (Toluidine)), which makes its diffusion very slow in less permeable parts of the tissue and thus prevent it from staining highly negative compact structures such as chromatin (DAKO). Precursor lesions of pancreatic cancer (PanIN) show strong accumulation of acetic mucins. Strongly acidic mucosubstances will be stained blue, nuclei become visible pink to red and cytoplasm will be stained pale pink. Formalin-fixed paraffin embedded tumor sections were deparaffinized and hydrated to distilled water. Staining with Alcian Blue solution (pH 2.5) for 30 min with a subsequent washing step for 2 min under running tap water was performed. Sections were rinsed in distilled water, counterstained in 0.1% nuclear fast red solution for 5 min and washed for 1 min in running tap water. After dehydration to xylene, sections were mounted in xylene based DPX.

5.2.3.5 Immunohistochemistry

The method employed in this work is the Avidin-Biotin-Complex (ABC) method. This technique uses the strong binding affinity of avidin to biotin. Three steps are involved. Firstly, a purified and unlabeled primary antibody binds the specific antigen in the tissue section. Secondly, a biotinylated secondary antibody reacts with the primary antibody and thirdly an avidin-coupled peroxidase binds specifically to biotin in order to form a strong avidin-biotin-peroxidase complex. To visualize the complex, a specific substrate like DAB (3,3'-diaminobenzidine, brown), AEC (3-amino-9-ethylcarbazole, red) or TMB (3,3' 5,5' tetramethyl benzidine, blue) can be used to develop the peroxidase producing different colorimetric end products. The detection systems used within this study were Vectastain ABC Elite rabbit-IgG and rat-IgG kit with DAB as a substrate for the peroxidase.

The general immunohistochemistry protocol includes the following steps. Deparaffinization of the tissue sections with xylene twice 15 min, rehydration in a decreasing ethanol series (100, 95 and 70%, each 3 min) and washing twice 5 min in distilled water. For some antibodies it is necessary to unmask their specific antigens. The tissue sections were dunked into sodium citrate buffer, pH 6.0 and microwaved 30 min at 750W. Evaporated buffer had to be replaced after the first 15 min. The slides were cooled down for 20 min at RT and washed twice with PBS for 5 min. Blocking of endogenous peroxidases was performed by incubation in 7.5% hydrogen peroxide (H₂O₂) for 10 min, followed by a 10 min washing step with tap water and two times PBS for 5 min. Afterwards, sections were blocked with normal serum from two different Vectastain ABC Elite kits (see chapter 4.5) for 20 min and incubated with the appropriate primary antibody, diluted in blocking buffer in a humidified chamber (Incubation times for the different primary antibodies differed in some aspects, see Table 5-1).

Table 5-1: Incubation times of primary antibodies in immunohistochemistry

Antibody	Detection system	Incubation time	Incubation temperature	Dilution
α -SMA	rabbit-IgG	1 hour	RT	1:400
CD3	rabbit-IgG	overnight	4°C	1:250
CD31	rabbit-IgG	overnight	4°C	1:1.000
Galectin-1	rat-IgG	1 hour	37°C	1:20.000
IDO	rabbit-IgG	overnight	4°C	1:50
Isotype	rabbit-IgG	depending on primary antibody		
Isotype	rat-IgG _{2b}	depending on primary antibody		

Binding of the primary antibodies was followed by some washing steps with PBS/0.05% Tween 20 and PBS (each 5 min) and 30 min incubation with biotinylated secondary antibody. After washing with PBS/0.05% Tween 20 and PBS (each 5 min), antibody binding was detected using the Vectastain Elite ABC reagent (avidin coupled peroxidase) following the instructions of the manufacturer. Finally, the sections were counterstained with Mayer's hemalaun for 90 sec, washed 5 min with tap water and rinsed 2 min in distilled water. Dehydration of the tissue sections was performed by increasing ethanol series (95%, 100% each twice 5 min) and twice 15 min xylene. Slides were covered with xylene based mounting medium DPX, dried overnight and analyzed using the Axiovert200M.

5.2.3.6 Immunocytochemistry

Panc02 cancer cells (1×10^4 per well) were seeded over night at 37°C in a sterile chamber slide, which was coated before with rat tail tendon collagen (1:100 with distilled water) for 1 h at 37°C. Cells were fixed with 4% paraformaldehyde (PFA) for 10 min at 37°C and permeabilized with 0.2% TritonX-100 for 15 min at RT. Afterwards, cells were blocked with 2% BSA for 30-60 min at RT (or overnight at 4°C). Primary antibodies in blocking solution were incubated for 60 min at RT, followed by a 45 min incubation of secondary antibody in blocking solution. Nuclei were stained with Hoechst-stain (1:200) for 5 min at RT. After every step, a washing step with PBS followed. Finally, the chamber was removed from the slide and cells were coverslipped with Vectashield mounting medium. Slides could be stored at -20°C until analysis with confocal microscopy (TCS SP5 II).

5.2.4 Flow cytometry

The detection of surface molecules as well as intracellular molecules can be done with directly fluorochrome labeled primary antibodies or with unlabeled primary antibodies, which than can be detected by fluorochrome-labeled secondary antibodies. The different emissions of the fluorochromes can be detected by flow cytometry (FACS). Additionally, the refracted light from cells is detected and therefore the size and granularity of cells can be determined.

Table 5-2: Spectral properties of the used fluorochromes in flow cytometric experiments

Fluorochrome	Excitation peak [nm]	Emission peak [nm]	Laser FACSCanto II [nm]	Filter FACSCanto II
APC	650	660	633	660/20
APC-Cy7	650	785	633	780/60
CFSE	492	517	488	530/30
FITC	495	525	488	530/30
Pacific blue	404	455	405	450/50
PE	564	575	488	585/42
PE-Cy7	564	767	488	780/60
PerCP	482	678	488	670
PI	493	619	488	610/20

The analysis was made with the flow cytometer BD FACSCantoII, which uses three different lasers: a blue laser (488 nm, air-cooled, 20 mW solid state), a red laser (633 nm, 17 mW HeNe) and a violet laser (405 nm, 30 mW solid state). These lasers with their adequate filter bands give the possibility to measure emissions of different fluorochromes at the same time. One has to pay attention that the spectral overlap of the emissions of the used fluorochromes is as low as possible. In a simultaneous analysis the compensation of the different emissions has to be done by samples, which are separately stained with each fluorochrome. With the help of the compensation controls, positive and negative populations can be detected and used to define the exact compensation level by hand or with the help of software (BD FACSDiva). Staining of the compensation controls was done by using the same cells as in the sample itself. These cells were washed once with 200 μ l FACS acid buffer and then stained with the fluorescent labeled antibody in the same dilution as in the sample to be analyzed. The controls were incubated for 30 min at 4°C in the dark. The measuring procedure could take place after a final washing step with 200 μ l FACS acid buffer.

5.2.4.1 Surface staining

For the surface staining, cells were distributed in a 96-well-plate or in FACS tubes and washed once with FACS acid buffer. Afterwards, cells were resuspended in buffer and spun down for 5 min at 400g. The supernatant was discarded and staining with the antibodies was performed. The dilution of each antibody was tested before and the right volume was pipetted to the cell suspension. The samples were mixed with a multi channel pipette and incubated for 30 min at 4°C in the dark. Finally, cells were washed with 200 μ l FACS acid buffer and resuspended in 150 μ l for analysis.

If the cells were not measured immediately after the surface staining, the cells would have been fixed with 200 μ l of 1% paraformaldehyde (PFA). The cells were incubated darkened for 20 min at 4°C and afterwards washed with 200 μ l PBS.

5.2.4.2 Intracellular staining

To achieve an intracellular staining, the antibodies have to pass the cell membrane. Therefore, cells were permeabilized with 200 μ l of 0.5% saponine solution for 20 min at 4°C. The antibodies were pipetted into 0.5% saponine solution and incubation was done for 30 min at 4 °C in the dark. If the primary antibody was unlabeled, a secondary fluorochrome-labeled antibody would be added after a washing step with 0.5% saponine solution. After an incubation time of 30 min the cells were washed with 200 μ l FACS acid buffer and fixed using 200 μ l 1% PFA. The cells were stored in 1% PFA until the measurement was done.

5.2.5 T cell assays

5.2.5.1 T cell proliferation assay

Isolated untouched Pan T cells (chapter 5.4.2.2) were labeled with CFSE using the Cell Trace™ CFSE Cell Proliferation Kit, a cell-tracing reagent (carboxyfluorescein diacetat succinimidyl ester), which diffuses passively into cells. The label is inherited by daughter cells after each cell division. Isolated T cells were washed twice with PBS and resuspended in 5 ml PBS. 2.5 μ l 5 mM CFSE (final 2.5 μ M) was mixed with 5 ml PBS and added to the T cells. After incubation for 4 min at RT labeling was stopped with 50 ml PBS/10%FBS, centrifuged for 5 min at 400g and resuspended in T cell medium. T cells were then mixed with mouse T-activator CD3/CD28 Dynabeads® to stimulate their proliferation by mimicking *in vivo* T cell activation from antigen-presenting cells. Beads were washed in T cell medium and mixed 5 sec on a vortexer. Due to magnetic properties of DynaBeads, they were placed into a magnetic field for 1 min to remove supernatant. Dynabeads were resuspended in the same volume as before and mixed with the T cell suspension. In this assay, 1×10^5 T cells were incubated with 2 μ l of CD3/CD28 Dynabeads® in a final volume of 200 μ l medium in a 96-well-plate for 72 h at 37°C. Afterwards, proliferation of T helper cells (CD3⁺CD4⁺) and cytotoxic T cells (CD3⁺CD8⁺) in the absence or presence of defined concentrations of tumor supernatant was analyzed by flow cytometry (CFSE dilution method).

5.2.5.2 T cell degranulation assay

In the degranulation assay the proteins CD107a (LAMP-1) and CD107b (LAMP-2) can be tapped with the help of fluorochrome conjugated antibodies on the cell surface. CD107a and CD107b are lysosomal membrane proteins, which reach the cell surface when cytotoxic T cells or NK cells exocytose their lytic granules after contact with target cells. Isolated CD8⁺ T cells from spleens of OT-1 mice were preincubated with 50% tumor supernatant of Panc02 and T110299 cells or T cell medium for 2 h at 37°C. After that, the pretreated T cells were separated into two different stimulation conditions, DC without peptide and DC pulsed with SIINFEKL peptide. The ratio of SIINFEKL-DC and T cells was 1:2. Additionally, in each condition 0.1 μ g CD107a-FITC and 0.5 μ g CD107b-FITC

antibody was added. Each condition contained 5×10^5 T cells per well in a 96-well plate with or without 25% tumor supernatant and in the absence or presence of DCs for 5 h at 37°C. The CD107 antibodies in the incubation conditions marked CD107 molecules which had reached the cell surface. After 5 h, the degranulation was stopped by adding FACS acid buffer and staining of the surface marker CD8 and additional CD107a and CD107b was performed.

5.3 Molecular biology methods

5.3.1 *In vitro* transcription

siRNA against galectin-1 was designed according to published guidelines and was purchased from Eurofins MWG Operon (Reynolds et al., 2004). 5'ppp-modified siRNA was established by *in vitro* transcription (IVT). The DNA template used to generate a triphosphate hairpin siRNA targeting galectin-1 had the following sequence:

5'**GATGGAGACTTCAAGATTACTCGAGTAATCTTGAAGTCTCCATCTATAGTGAGTCGTA**3'

The green sequence consists of nucleotides, which are responsible for galectin-1 gene silencing. The red nucleotides form the hairpin structure and the blue nucleotides are the TATA-box to anneal the T7 promotor primer sequence.

The first step of the IVT procedure was to prepare DNA template for transcription. This step consisted of the annealing of the T7 promotor primer to the DNA template and the synthesis of a double stranded DNA template. For the annealing step, the same amount of DNA template and T7 promotor primer plus DNA hybridization buffer was pipetted to a final volume of 14 μ l and incubated for 10 min at 75°C with subsequent incubation for 1 h at RT for cooling. The synthesis of double stranded DNA was performed using the Exo-Klenow DNA polymerase (14 μ l Template, 2 μ l Klenow Fill-In buffer (10x), 2 μ l dNTP mix (2.5 mM) and 2 μ l Exo-minus Klenow DNA polymerase (10 U/ μ l)). After incubation at 37°C for 30 min, the Exo-minus Klenow DNA polymerase was inactivated by heating it for 10 min at 75°C. The second step of the IVT procedure was the IVT itself, which was done with the HiScribe™ T7 *In Vitro* Transcription Kit according to the manufacturer's protocol for short templates (50-300 nucleotides). Incubation took place for 6 h at 42°C. The last step was to isolate the 5' modified ppp-RNA, which was subdivided into three steps. The first step included the digestion of DNA using DNaseI. 2 μ l of Turbo-DNase were added to the IVT preparation for 30 min at 37°C. Afterwards, 30 μ l of ammonium acetate were added, mixed well and the tube was washed with 230 μ l PCR-grade water. In the second step, the RNA was purified by phenol-chloroform extraction, followed by the precipitation of the RNA adding twice the volume of 99% ethanol and by incubation at -20°C over night. The third and last purification step started with a 30 min centrifugation at 14.000 rcf at 4°C to pellet the RNA. After drying, the RNA was resuspended in 100 μ l PCR-grade water and further purified by Mini quick spin columns. Finally, the amount of 5'ppp-RNA was

measured photometrically using the Nano Drop[®] and tested *in vitro* for its stimulation ability (induction of CXCL10, apoptosis or up-regulation of MHC-I expression on tumor cells).

5.3.2 Transfection of siRNAs

In vitro transfection of tumor cells was performed using Lipofectamine RNAiMAX. One day before transfection, cells were plated in a medium without antibiotics. A 50 to 60% confluence at the time of transfection was recommended. The Lipofectamine-siRNA-complexes were prepared in two separate Eppendorf tubes. The siRNA (50 μ l per well) as well as the transfection reagent Lipofectamine RNAiMAX (50 μ l per well) was diluted in Opti-MEM medium and incubated for 5 min at RT. After incubation, Lipofectamine RNAiMAX was mixed 1:1 with the siRNA and incubated for another twenty min at RT to build up liposome complexes. Finally, 100 μ l of complexes were added to each well containing cells and 1400 μ l medium for 6-well plates.

5.3.3 RNA isolation

RNA isolation was performed using the peqGOLD Total RNA isolation kit from peqlab according to the manufacturer's instructions. Samples were first lysed and homogenized in the presence of a highly denaturing guanidine-thiocyanate-containing buffer, which immediately inactivates RNases to ensure purification of intact RNA. As a second step, samples were applied to a DNA removing column and afterwards mixed with the same volume of 70% ethanol, in order to provide appropriate binding conditions. The sample was then applied to a PerfectBind RNA column, where the total RNA binds to the membrane and where contaminants were efficiently washed away with two different washing buffers. Subsequently, RNA was then eluted in 50 μ l RNase free water. The procedure provides enrichment for mRNA since most RNAs <200 nucleotides (rRNA, tRNA) are selectively excluded. The concentration of total RNA was determined photometrically by Nano Drop[®].

5.3.4 cDNA transcription

cDNA transcription was done with the RevertAID[™] First strand cDNA Synthesis kit from Thermo Scientific according to manufacturer's instructions. The kit used the RevertAid[™] M-MuLV reverse transcriptase for cDNA synthesis and the RiboLock[™] RNase inhibitor to protect RNA from degradation. Oligo(dT)₁₈ primer, which anneal selectively to the 3'-end of poly(A)RNA, were used to synthesize cDNA only from poly(A) tailed mRNA.

In the first step, 0.1 ng – 5 μ g of the isolated RNA was incubated for 60 min at 42°C for amplification with the following components: 1 μ l oligo(dT)₁₈ primer, nuclease-free water to a final volume of 12 μ l, 4 μ l Reaction Buffer (5x), 1 μ l RiboLock[™] RNase inhibitor (20 U/ μ l), 2 μ l dNTP mix (10 mM)

and 1 μl RevertAidTM M-MuLV reverse transcriptase (200 U/ μl). The reaction was terminated by heating at 70°C for 5 min.

5.3.5 Quantitative *real time* – polymerase chain reaction

Real-time PCR is a quantitative PCR method for the determination of the copy number of PCR templates such as DNA or cDNA in a PCR. It monitors the increase of cDNA as it is amplified via fluorescence, which is emitted during the reaction and functions as an indicator. The method used in this work is the probe-based PCR, which requires in addition to PCR primers a fluorochrome-labeled probe, which is an oligonucleotide with both, a fluorescent reporter at one end, and a quencher of fluorescence, at the opposite end. The 5' \rightarrow 3' activity of the Taq polymerase breaks down the probe resulting in the breakdown of the reporter-quencher proximity which allows unquenched emission of fluorescence. An increase in the product targeted by the reporter probe at each PCR cycle therefore causes a proportional increase in fluorescence due to the breakdown of the probe and release of the reporter.

For the PCR reaction the KAPA PROBE FAST qPCR Kit from peqlab was used. The appropriate gene primers were generated with respect to the Roche Library as the probes were purchased from Roche. The procedure was performed according to the manufacturer's instructions except for the total volume of each approach, which was scaled down from 20 μl to 10 μl , summarized in Table 5-3.

Table 5-3: Components for one RT-PCR approach

Content	Function	Volume/well [μl]
Water, PCR-grade	Adjust the final reaction volume	1,5
KAPA PROBE FAST Universal qPCR Master Mix (2X)	KAPA Taq HotStart DNA polymerase, KAPA PROBE FAST qPCR buffer, dNTP mix and 5 mM MgCl_2 and stabilizers	5,0
Primer forward [100 μM]	1:10 diluted	0,2
Primer reverse [100 μM]	1:10 diluted	0,2
Probe mix, 10x conc.		0,1

The detection format was 'mono color hydrolysis probes' and the program setting described in Table 5-4 was used. The analysis was done by LightCycler[®] 480 software Version 1.5.

Table 5-4: program setting

Program name	Cycles	Analysis mode	Temperature [$^{\circ}\text{C}$]
Pre-incubation	1	none	95
Amplification	45	quantification	60
Cooling	1	None	40

5.4 Animal experiments

5.4.1 Animals

C57BL/6 mice were purchased from Janvier (St. Berthevin Cedex, France). Transgenic OT-I mice were kindly provided by Dr. Reinhard Obst (Institute of Immunology, Ludwig-Maximilian University Munich, Germany).

The mice were 6 to 10 weeks of age at the onset of experiments. They were anesthetized with isoflurane for blood withdrawal and subcutaneous (s.c.) tumor cell inoculation. For orthotopic tumor cell inoculation into the pancreas, mice were narcotized with 100 μ l narcotic mixture intraperitoneal (i.p.) (Table 5-5) and antagonized with 100 μ l i.p. and 100 μ l s.c. antidote (Table 5-6). All animal studies were approved by the local regulatory agency (Regierung von Oberbayern, Munich, Germany), animal experimentation application number for Galectin-1 experiments 55.2-1-54-2531-143-09, and orthotopic tumor transplantation of T110299 were performed under the experimentation application number 55.2-1-54-2532-175-12.

Table 5-5: Narcotic mixture for orthotopic tumor cell injection

Name	concentration	Mass	Function
Midazolam	5 mg/ml	10 mg	Benzodiazepine; sedation
Temgesic (Buprenorphin)	0.3 mg/ml	0.3 mg	Opioide; analgic
Dorbene (Medetomidine)	1 mg/ml	0.2 mg	α_2 adrenergic agonist; sedation, analgic

Table 5-6: Antidote mixture for orthotopic tumor cell injection

Name	concentration	Mass	Function
Flumazenil	0.1 mg/ml	0.5 mg	Benzodiazepine receptor antagonist
Naloxone	0.4 mg/ml	1.2 mg	Opioide inverse agonist
Antisedan (Atipamezole)	5 mg/ml	2.5 mg	α_2 adrenergic antagonist

5.4.2 Organ and single cell preparation

5.4.2.1 Preparation of serum and isolation of peripheral blood mononuclear cells

For the detection of Galectin-1 in the serum, blood was collected from the retro-orbital sinus with a glass capillary pipette. To collect serum, 300 μ l of blood was collected in an Eppendorf tube and centrifuged at 1000g for 10 min. Serum (the supernatant) was carefully taken and stored at -20°C until further analysis. For the collection of PBMCs, 300 μ l blood were collected in an Eppendorf tube containing 50 μ l heparin, mixed immediately, and kept on ice. 1 ml of PharmLyse ammonium chloride buffer (1x) was added to lyse erythrocytes, and samples were incubated for 5 min at RT before being transferred into a falcon tube with 10 ml PBS with subsequent centrifugation (400g, 5 min) and

washed with PBS to remove remaining lysed red blood cells. Cells were then stained with fluorochrome-labeled antibodies and analyzed by flow cytometry.

5.4.2.2 Isolation of T cells from mouse spleen

For the isolation of mouse T cells (untouched Pan or CD8⁺ T cells), the MACS T cell isolation kit from Miltenyi Biotech was used according to manufacturer's instructions. This system is used for the isolation of untouched T cells from mouse spleen or lymph nodes. The principle is negative selection by depleting the cell suspension of non-T cells or CD8⁺ T cells (CD4⁺ T cells, NK cells, B cells, dendritic cells, macrophages, granulocytes and erythroid cells). In a first step, a single cell suspension was prepared. To remove cell clumps from dissected splenocytes the cell suspension was passed over a 40 µm nylon mesh. Cells were spun down for 5 min at 400g, resuspended in 5 ml lysing buffer to remove erythrocytes and incubated for 5 min at RT. After adding 50 ml PBS, cells were spun down for 5 min at 400g and washed with MACS-Buffer. A further washing step followed and then, cells were counted and resuspended in MACS-Buffer, 40 µl per 10⁷ cells. Next, non-T cells or -CD8⁺ T cells were magnetically labeled to biotin-conjugated monoclonal antibodies with 10 µl antibody-cocktail (CD8 T cell isolation kit, (Miltenyi Biotech) or Pan T cell isolation kit (Miltenyi Biotech)) per 10⁷ cells and incubated on ice for 15 min. The antibodies included in the CD8 T cell isolation kit are directed against CD4, CD11b, CD11c, CD19, CD45R (B220), CD49b (DX5), CD105, Anti-MHC class II, and Anti-Ter-119, whereas the Pan T cell isolation kit lacks the CD4 antibody. Again 30 µl per 10⁷ cells MACS-buffer was added. In a second step, 20 µl per 10⁷ cells anti-biotin labeled monoclonal antibodies, conjugated to MicroBeads, were added and incubated 20 min on ice. After a further washing step with MACS-buffer the cell suspension was passed through a MACS column (LS column for up to 10⁸ labeled cells) in a magnetic field where magnetically labeled non-T cells or -CD8⁺ T cells were bound to the column. The unlabeled Pan T cells or CD8⁺ T cells passed through the column (negative fraction). The purity of isolated T cell populations was checked by flow cytometric analysis.

5.4.2.3 Generation of bone marrow-derived dendritic cells

Bone marrow-derived dendritic cells (BMDCs) were isolated from murine tibia and femur. After removing muscles, bones were put in 70% ethanol for 2 min. Epiphyses were cut off and bones were flushed with a culture medium with a syringe. Bone marrow cells were flushed through a 40 µm mesh and centrifuged for 5 min at 400 g. Supernatant was discarded and cell suspension was depleted from erythrocytes with 3 ml of red cell lysis buffer for 3 min. After another centrifugation step for 5 min at 400g, cells were resuspended in 15 ml medium mixed with 20 ng/ml of murine GM-CSF and 20 ng/ml of murine IL-4, plated in 6-well plate and incubated at 37°C for six to seven days. Medium was changed every two days. One day before using the cells 1 µg/ml lipopolysaccharide (LPS) was added to activate the DC.

5.4.3 *In vivo* experiments

5.4.3.1 Tumor models

Before injecting tumor cells s.c. or orthotopically, cells had to be prepared by washing three times with PBS to remove fetal calf serum.

For s.c. tumor models, 5×10^5 Panc02 and 9×10^5 T110299 cancer cells were injected in a volume of 100 μ l PBS. Tumor growth was measured every two days with a caliper rule. Mice were sacrificed when tumor size reached 150 mm², tumors ulcerated or mice were distressed.

Orthotopic tumors were induced by surgical implantation of 2×10^5 Panc02 and 4×10^5 T110299 cancer cells in 40 μ l PBS into the tail of the pancreas after narcotization of mice as described in chapter 5.4.1. Eyes were protected from drying with a salve for eyes and noses (Bepanthen[®], Bayer Vital GmbH, Leverkusen, Germany). After tumor cell injection, peritoneum and skin were sutured with Prolene 5-0 (Ethicon). The antidote (Table 5-6) was administered (100 μ l i.p., 100 μ l s.c.) and the mice were kept under red light until every mouse had wakened up. Postoperative analgesia was performed per protocol and mice were regularly checked for signs of distress.

5.4.3.2 Therapy with siRNAs

50 μ g OH-RNA or OH-Gal-1 siRNA was complexed with *in vivo*-JetPEI at an N/P ratio of 6 in 5% glucose solution for tail vein injection. siRNAs were injected as indicated in the experiments. For survival experiments, a therapeutic application of RNA (OH-RNA, OH-Gal-1, ppp-Gal-1) was performed twice weekly over three weeks.

5.5 Statistical analysis

Data represent mean plus standard deviation (SD) for *in vitro* data or standard error of the mean (SEM) for *in vivo* data. Significant differences were analyzed by unpaired, one-way analysis of variance (ANOVA), including Bonferroni correction (multiple comparisons). Survival curves were analyzed with the Mantel-Cox test. Statistical analysis was conducted using GraphPad Prism software (version 5.02); P-values <0.05 were considered significant.

6 Results

6.1 Histological characterization of murine pancreatic cancer models

Four different murine pancreatic cancer models were characterized by histology: two syngenic models induced orthotopically in the pancreas of C57BL/6 mice (Panc02 and T110299) and two GEMM based on mutant Kras and p53 (Pdx-1-Cre, LSL-Kras^{G12D/+}, LSL-Trp53^{R172H/+}, thereafter named KPC; and Pdx-1-Cre, LSL-Kras^{G12D/+}, LSL-Trp53^{fl/-}, thereafter named KPfC). The T110299 cell line was generated from primary tumors of KPC mice.

The general composition of the tumors was visualized via hematoxylin and eosin (H&E) staining. Additional staining analyzed collagen composition to study tumor stroma, blood vessel formation and PanIN precursor lesions of PDAC. Tumor infiltrating T cells, the expression of Galectin-1 and IDO were analyzed by IHC.

6.1.1 H&E staining

Histological analysis of orthotopic Panc02 tumors (Figure 6-1 A and B) revealed a poorly differentiated morphology with large areas of necrosis in the tumor center (asterisk) and a sarcomatoid architecture. In contrast, orthotopic T110299 tumors (Figure 6-1 C and D) showed a moderately well-differentiated morphology organized in glandular structures typical for adenocarcinoma (arrows). Tumors from KPC mice (Figure 6-1 E and F) as well as KPfC mice (Figure 6-1G and H) demonstrated a well-differentiated morphology organized in glandular architecture with abundant tumor stroma (arrowhead), closely resembling human disease. Figure 6-1 E revealed early pancreatic tumors (arrow) in the head of the pancreas in close proximity to duodenum (asterisk). The star marks acinus cells of the pancreas. The biological difference between both GEMM is that KPfC mice develop adenocarcinomas (Figure 6-1 G and H asterisk) much earlier than KPC mice (Mazur and Siveke, 2011), which showed at the time of necropsy mainly PanIN lesions (Figure 6-1 F asterisk).

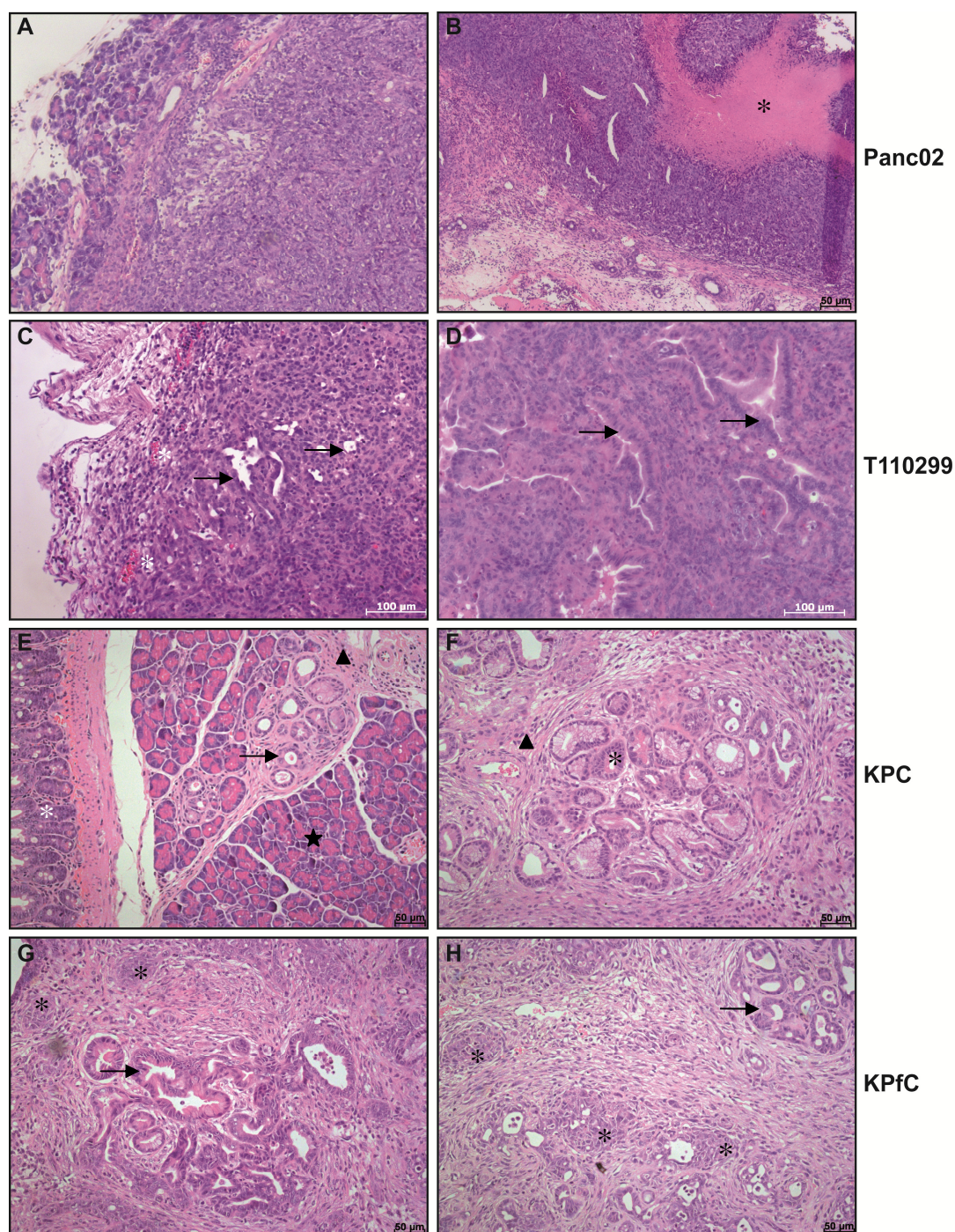


Figure 6-1: H & E staining of murine primary pancreatic carcinoma models.

H&E staining performed for orthotopic Panc02 (A and B) and T110299 (C and D) tumor model, as well as primary KPC and KPfC tumors (E-H). **A and B:** poorly differentiated pancreatic carcinoma with large amount of necrotic tissue (B, asterisk) and sarcomatoid structure (100x). **C and D:** moderately well-differentiated glandular PDAC with tumor blood vessels in the periphery (C, asterisk) (200x). **E-H:** well-differentiated morphology of PDAC with abundant tumor stroma (arrows) (200x). **E and F** show PanIN lesions and tumors in KPC mice (E, arrow) in close proximity to duodenum (E, asterisk) and acinus cells of the pancreas (E, star). These triple mutant mice develop numerous PanIN lesions (F, asterisk). **G and H** show tumors of KPfC mice (200x), with PanINs (arrows) and overt adenocarcinoma (asterisk).

6.1.2 Collagen staining of tumor stroma

Staining of collagen fibers in pancreatic carcinoma reveals tumor stroma. Panc02 tumors showed very little tumor stroma, whereas T110299 tumors exhibited areas with large amount of stroma within the tumor (Figure 6-2 A and B). Both, KPC and KPfC tumors were characterized by extensive stroma formation (Figure 6-2 C and D).

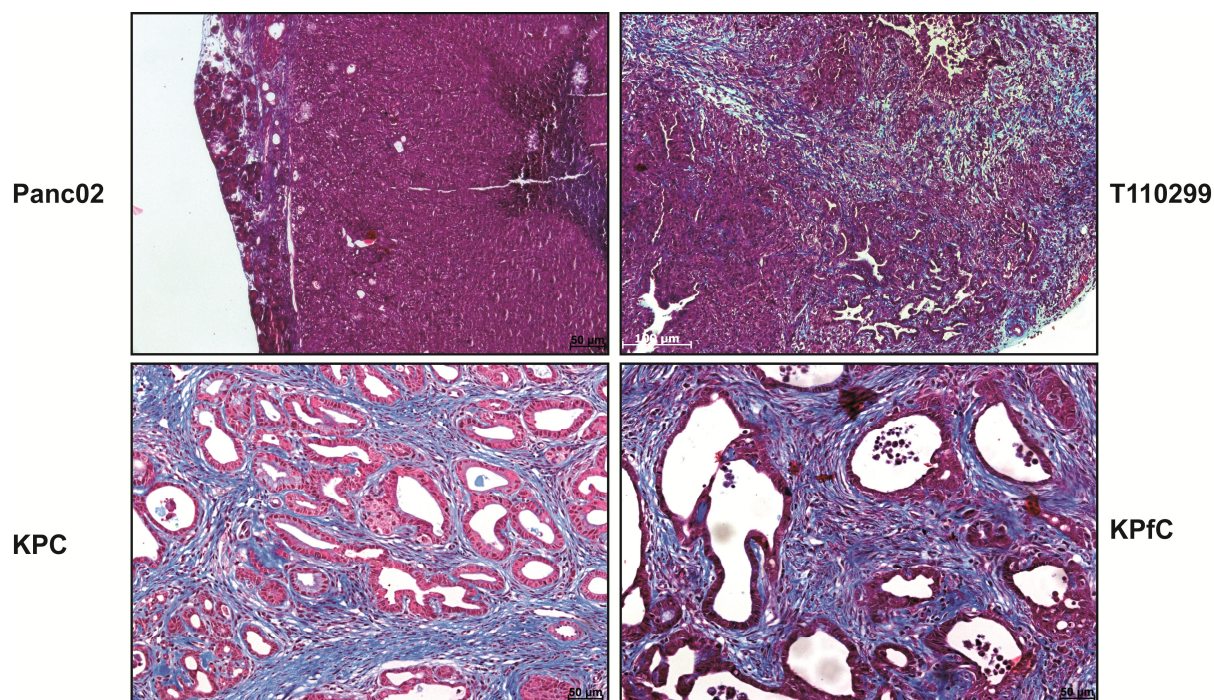


Figure 6-2: Collagen staining of pancreatic tumors.

Visualization of collagen fibers in tumor stroma was performed with Masson's Trichrome. Collagen fibers are depicted in blue, nuclei in black, cytoplasm and erythrocytes in red. **A:** Orthotopic Panc02 tumors contain very little tumor stroma (100x). **B:** Orthotopic T110299 tumors show areas with large amounts of tumor stroma in the periphery as well as within the tumor (100x). **C and D:** Tumors from KPC and KPfC mice exhibit extensive stroma formation (200x).

6.1.3 Differentiation of PDAC and PanIN lesions

Precursor lesions leading to PDAC are called PanINs. These lesions are characterized by conversion of the duct epithelial cells to a columnar phenotype with mucin accumulation (Hingorani et al., 2003, Hingorani et al., 2005). To visualize PanINs in the different mouse models, Alcian blue staining was performed (Figure 6-3). PanIN lesions are graded into three different stages. The mucin content decreases with decreasing differentiation status. Formation of papillary architecture and luminal budding was observed, with loss of polarity and appearance of atypical nuclei. Differentiation of tumors is separated into three stages, from grade 1 well-differentiated to grade 3 poorly differentiated tumors. Panc02 tumors did not show any precursor lesions (Figure 6-3 A), resembling a grade 3 tumor. T110299 tumors revealed glandular structure and stained weakly for mucin-containing PanIN-like lesions with Alcian blue (Figure 6-3 B). Therefore these tumors depicted grade 2 tumors. Tumors

from KPC mice showed strong Alcian blue staining; KPC tumors (Figure 6-3 C) demonstrated more mucin rich PanIN lesions than KPfC tumors, both resemble grade 1 tumors.

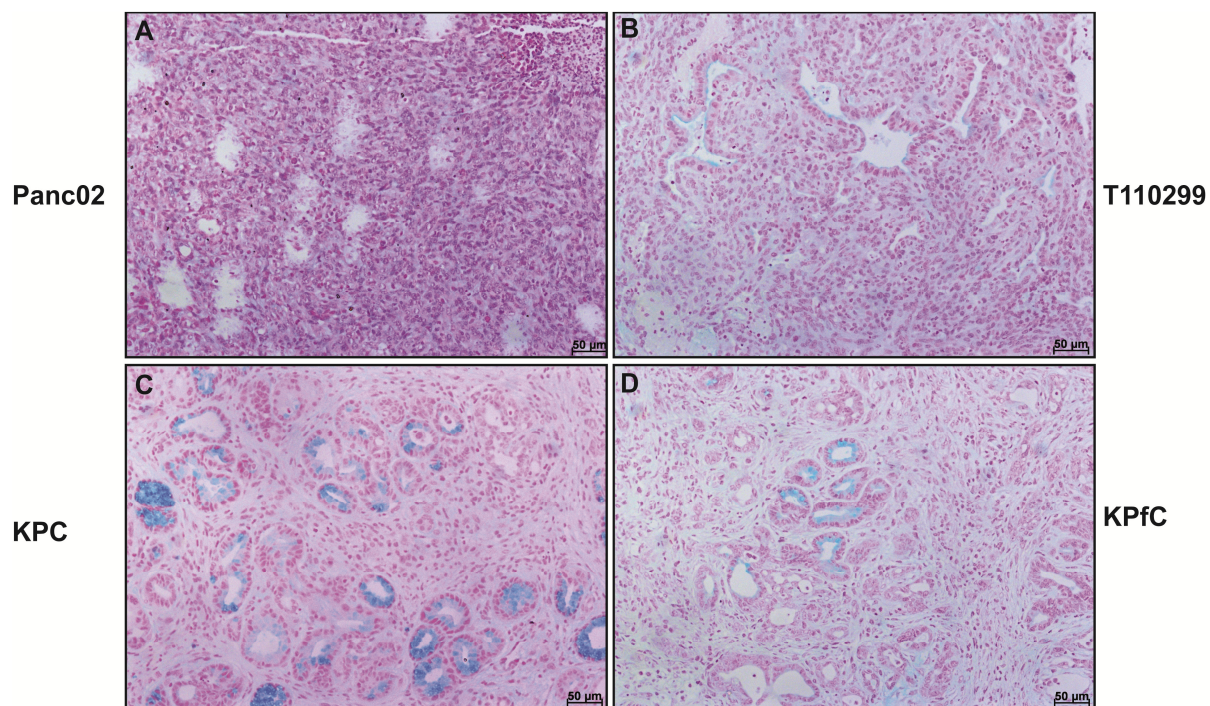


Figure 6-3: Alcian blue staining reveals differentiation status of pancreatic carcinoma.

Visualization of differentiation was performed with Alcian Blue staining. Mucin rich lesions are depicted in blue, cytoplasm in light red and nuclei in dark red. **A:** Orthotopic Panc02 tumors show differentiation of a grade 3 tumor. **B:** Orthotopic tumors from T110299 cell line reveal weak mucin staining in some tumor areas, indicative of grade 2 tumors. **C:** Early stage PanIN rich tumors from KPC mice with a differentiation status of grade 1. **D:** PanIN rich tumors from KPfC tumors with low Alcian Blue staining, depict low differentiation of grade 1 tumors. All pictures were taken with a magnification of 200x.

6.1.4 Tumor blood vessels

The formation of tumor blood vessels gives rise to a better supply of oxygen and nutrients for the tumor. Blood vessels were examined with the help of the marker CD31, which stains endothelial cells. All tumors showed pronounced blood vessel formation in the periphery of the tumor (Figure 6-4 A-D). Differences between the tumor models became visible in the central tumor regions (c). In Panc02 tumors blood vessels could be detected in the periphery (p), whereas tumor centers contained only few chaotic CD31 positive spots (Figure 6-4 A). Similarly, T110299 tumors showed formation of blood vessels in the tumor periphery, however in central tumor regions CD31 expression was sparse (Figure 6-4 B). In sections of KPC tumors blood vessels were visible (Figure 6-4 C) at the tumor periphery, whereas in tumors of KPfC mice blood vessels occurred around adenocarcinoma structures (Figure 6-4 D asterisk). In general, the architecture of the blood vessels in the tumors was chaotic compared to areas in the tumor periphery. In general, all PDAC model were hypovascular.

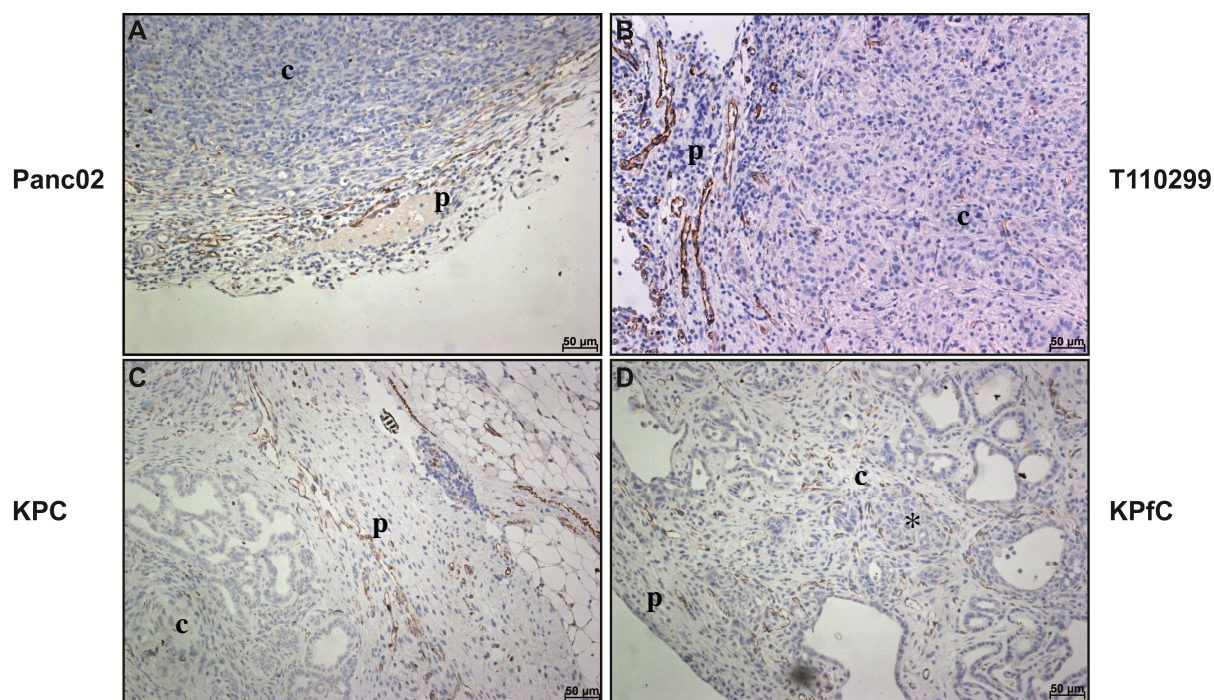


Figure 6-4: Tumor blood vessels in the periphery and center of pancreatic carcinoma.

Tumor blood vessels were visualized via staining of the endothelial marker CD31 (polyclonal rabbit IgG, 1:1000). Analyses were done for the periphery and central tumor regions. **A:** The periphery (p) of orthotopic Panc02 tumors are highly interspersed with blood vessels compared with central tumor parts (c) where almost no CD31 expression is detectable. **B:** Orthotopic T110299 tumors show abundant blood vessels at the tumor margin, whereas CD31 was almost absent in central regions. **C and D:** Tumors of KPC (C) and KPfC mice (D) demonstrate tumor blood vessel formation at the tumor border. Blood vessels were sparse in areas of adenocarcinoma (D, asterisk). All pictures were taken with a magnification of 200x.

6.1.5 Infiltrating T cells

T cell infiltrates of the orthotopic and spontaneous tumor models were investigated histologically by IHC. In orthotopic Panc02 tumors (Figure 6-5 A and B) and T110299 tumors (Figure 6-5 C and D) the infiltration with T cells was relatively high in comparison to the KPC and KPfC tumor models (Figure 6-5 E-H). Most T cells accumulated at the border of the tumor (Figure 6-5 B, D, E and G). The central regions of Panc02 and T110299 tumors (Figure 6-5 A and C) also contained a brisk lymphocyte infiltrate. In central tumor parts of KPC mice the infiltration with T cells was very sparse (Figure 6-5 F, G and H). In some areas T cell clustering in tumors could be recognized (Figure 6-5 H).

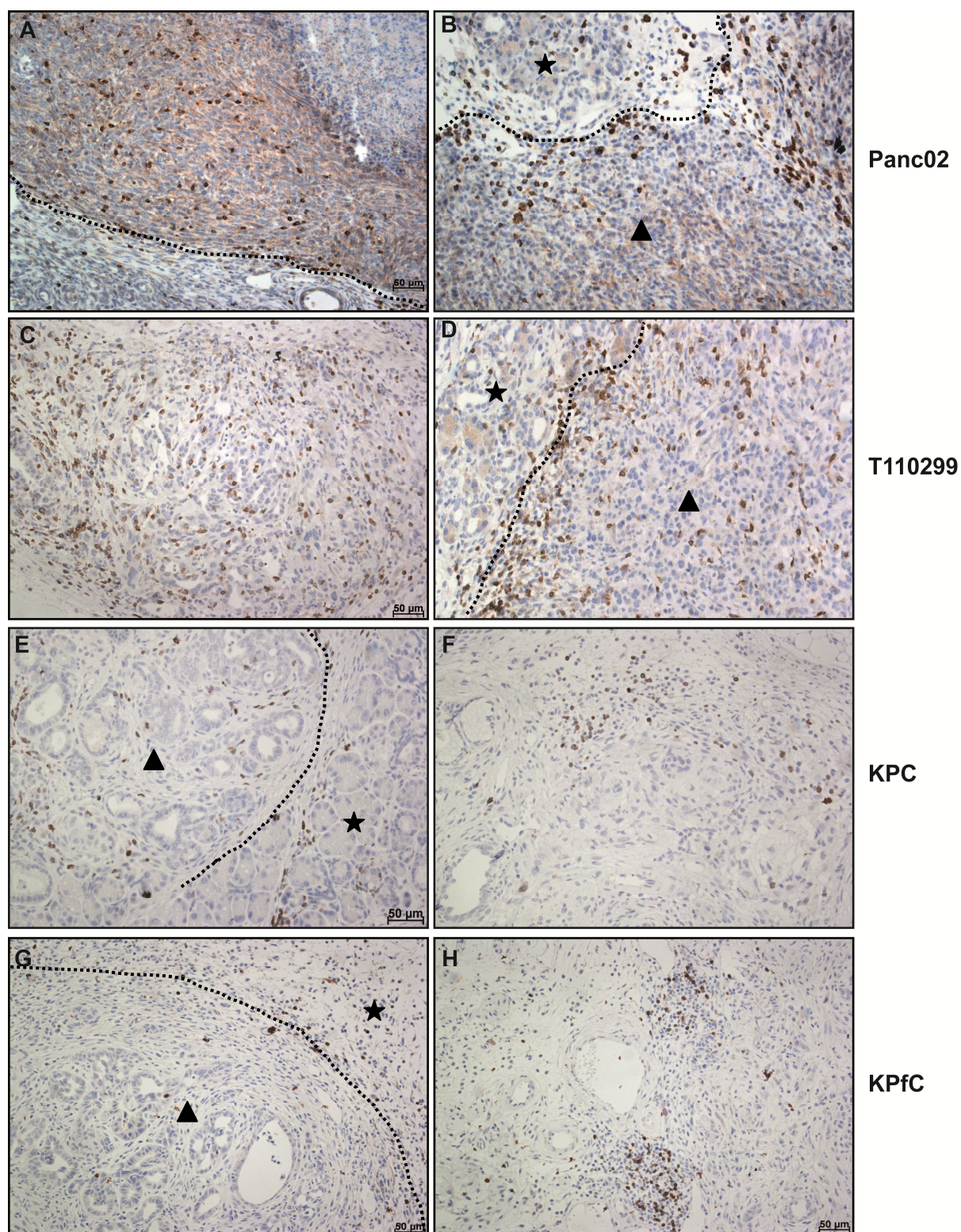


Figure 6-5: Infiltrating T cells in the periphery and center of pancreatic carcinoma.

T cells were detected with an antibody against CD3 (monoclonal rabbit IgG [SP7], 1:250). Stars mark normal pancreatic tissue, arrowheads mark tumor regions. **A and B:** Orthotopic Panc02 tumors show clustering of T cells at the tumor border and a dense infiltration in the tumor center. **C and D:** Orthotopic T110299 tumors exhibit an accumulation of T cells at the tumor periphery but also in central regions. **E and F:** Tumors from KPC mice have sparse T cell infiltrates, but show T cells clustering at the tumor border. **G and H:** Tumors from KpFC mice are sparsely infiltrated with T cells in central regions (G) but show accumulation at the periphery of the tumor (G) and in some cases aggregation of T cells within the tumor was detectable (H). All pictures were taken with a magnification of 200x.

A quantification of T cells in the four tumor models was performed by counting CD3⁺ cells per 10 high power fields (HPF). For this purpose tumors from KPC and KPfC mice were pooled. These tumors revealed a mean CD3⁺ count of about 52 cells per HPF whereas Panc02 tumors were significantly more infiltrated with T cells (mean CD3⁺ count 129) (Figure 6-6). Tumors from T110299 cell line showed a very heterogeneous infiltration with T cells. The mean value of CD3⁺ T cells per HPF was 257. Both, T110299 and Panc02 tumors were significantly more densely infiltrated with T cells as tumors from KPC mice, whereas the difference between T110229 and Panc02 tumors was not statistically significant.

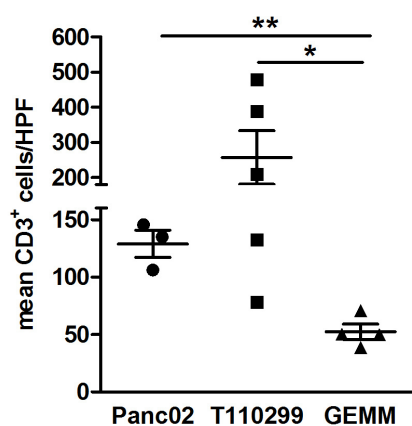


Figure 6-6: Quantitative analysis of infiltrating T cells in pancreatic carcinoma.

Tumors from KPC mice show the lowest infiltration with CD3⁺ T cells (mean value 52/HPF). In comparison, orthotopic tumors from Panc02 and T110299 cell lines were densely infiltrated with T cells with mean values of 129 and 257/HPF, respectively. T110299 tumors were heterogeneously infiltrated by CD3⁺ T cells. On the contrary, Panc02 and GEMM tumors are more homogeneously infiltrated with CD3⁺ T cells. Quantification of T cells was done by counting 10 HPF per tumor section. P value was calculated with student's unpaired t test. Significant differences are marked with * = P<0.05, ** = P<0.005. GEMM = genetically engineered mouse model (KPC and KPfC).

6.1.6 Galectin-1 and α -smooth muscle actin

One of the immunosuppressive molecules investigated in this study is galectin-1. The expression of galectin-1 in murine pancreatic carcinoma models was investigated and compared with the expression of α -smooth muscle actin (α -SMA), a marker of fibroblasts and cells with fibroblastic origin like pancreatic stellate cells (PSCs). In the literature, PSCs located in tumor stroma have been described to express galectin-1 (Tang et al., 2011, Xue et al., 2011). As shown in Figure 6-7, all four tumor models express galectin-1 and α -SMA, but cellular distributions vary. Galectin-1 is expressed in the cytoplasm as well as in nuclei of stromal cells in KPC mice (Figure 6-7 G). α -SMA expression can be detected solely in the cytoplasm of elongated, fibroblast-like cells (Figure 6-7, H). As depicted in Figure 6-7 A and B Panc02 tumor cells have a strong expression of galectin-1 but α -SMA expression was not detectable, correlating with lack of tumor stroma. In T110299 tumors (Figure 6-7 C and D) the expression of both proteins was very distinctive whereas the tumors of KPC mice had a weaker expression (Figure 6-7 E and F). However, tumors of KPfC mice displayed a strong expression of galectin-1 and α -SMA (Figure 6-7 G and H).

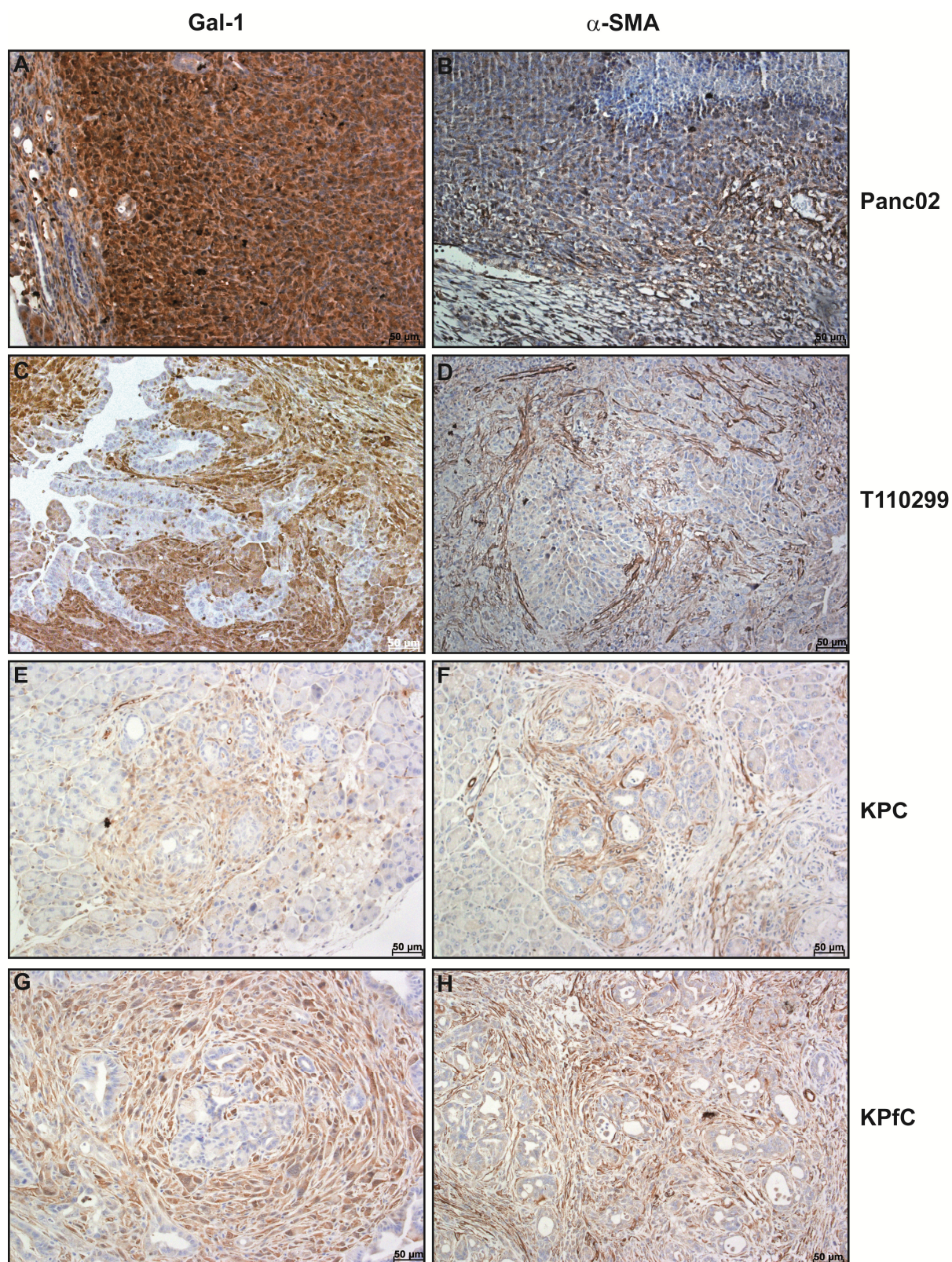


Figure 6-7: Expression of galectin-1 and α -SMA in murine pancreatic carcinoma.

Galectin-1 and α -SMA are expressed in the cytoplasm of stromal cells (PSC). Galectin-1 was also expressed in nuclei of these types of cells. Galectin-1 was stained with a monoclonal antibody rat IgG2b [201002] (1:20.000). α -SMA staining was performed with a polyclonal rabbit IgG antibody (1:400). **A and B:** Orthotopic tumors from cell line Panc02 show strong expression of galectin-1 in tumor cells but no expression of α -SMA was detectable. **C and D:** Orthotopic T110299 tumors display strong expression of galectin-1 in tumor stroma, but not in carcinoma cells. **E-H:** The expression of both galectin-1 and α -SMA is weaker in KPC (E and F) tumors as compared to KPfC tumors (G and H). All pictures were taken with a magnification of 200x.

6.1.7 Indoleamine 2,3-dioxygenase

Another immunosuppressive molecule, which was examined histologically, was indoleamine 2,3-dioxygenase (IDO). As shown in Figure 6-8 this protein was expressed primarily in the cytoplasm of carcinoma cells. Acinus cells from healthy pancreatic tissue also displayed IDO expression (Figure 6-8 C asterisks). Panc02 tumors (Figure 6-8 A) revealed a strong expression of IDO. Little IDO expression was detectable in cells located in the tumor stroma in any of the tumor models. Interestingly, PanIN lesions of KPC and KPfC mice revealed apical polarity of IDO expression (Figure 6-8 C and D).

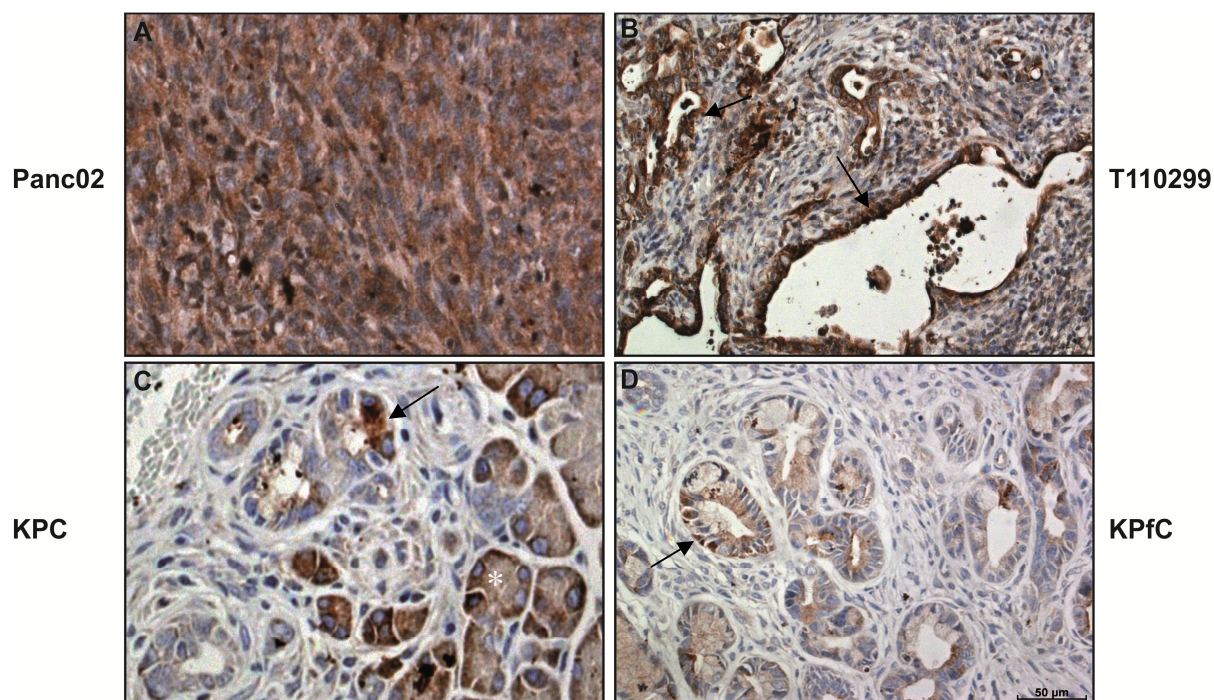


Figure 6-8: Indoleamine 2,3-dioxygenase expression in murine pancreatic carcinoma.

IDO is primarily expressed in the cytoplasm of epithelial cells, cells with epithelial origin and acinus cells of the pancreas. IDO was stained with a polyclonal antibody rabbit IgG (1:50). **A:** Panc02 tumors show a distinct expression of IDO (200x). **B:** Tumors from T110299 cell line revealed expression of IDO in tumor cells (arrows). Tumor stroma, which consists of fibroblasts, fibroblast-like cells and collagen fibers, show less IDO expression (100x). **C and D:** Tumors from KPC and KPfC mice display IDO expression tumor cells and in PanIN lesions in an apical polarity (200x).

6.1.8 Survival of mice bearing orthotopic Panc02 or T110299 tumors

The murine pancreatic cancer cell lines Panc02 and T110299 were further characterized *in vivo* with regard to survival. Therefore, tumor cells were injected orthotopically into the head of the pancreas in C57BL/6 mice as it is described in chapter 5.4.3.1. Mice were euthanized when showing signs of distress or behavioral abnormalities. Both tumor models showed aggressive tumor biology. Mice with Panc02 tumors had a median survival of 31 days (n=6) whereas in mice with T110299 tumors the median survival was 23 days (n=7), however the difference was not significant (P=0.2598) (Figure 6-9).

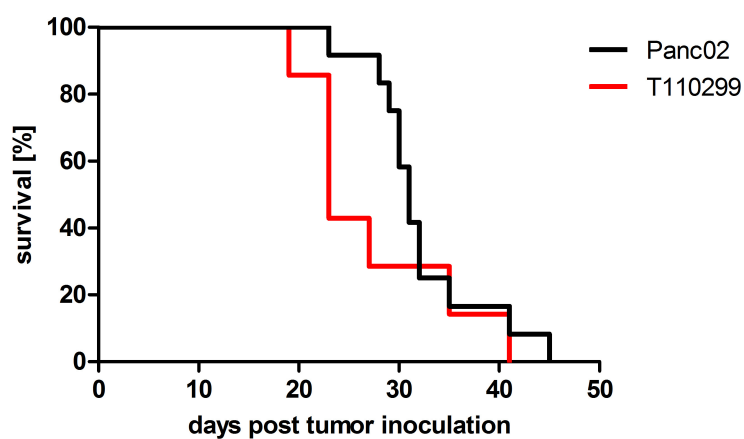


Figure 6-9: Survival of mice bearing orthotopic Panc02 and T110299 tumors.

For survival, tumor cells of Panc02 (2×10^5 cells) and T110299 (4×10^5 cells) were injected orthotopically into the head of the pancreas of C57BL/6 mice. The median survival of mice with Panc02 tumors was 31 days ($n=12$), with T110299 tumors 23 days ($n=7$). Pooled data with statistical analysis from two independent experiments with 7 to 12 mice per group are depicted.

6.2 Immunotherapy with siRNA targeting galectin-1 in the Panc02 tumor model

Therapeutic application of 5'ppp-modified siRNA (ppp-Gal-1) and unmodified siRNA (OH-Gal-1) targeting galectin-1 was one of the aims of this study. First, *in vitro* assays were performed to validate the expression of galectin-1 and intact RIG-I signaling in pancreatic cancer. In a second step, *in vivo* studies were conducted to assess the effect of OH-Gal-1 and ppp-Gal-1 in the Panc02 tumor model regarding influence on tumor growth and galectin-1 expression. In addition, the expression profiles of specific cytokines in the serum and status of immune cell activation were assessed.

6.2.1 Murine Panc02 pancreatic carcinoma cells express functional RIG-I

The first question that had to be answered was if pancreatic carcinoma cell lines express functional RIG-I as a prerequisite for successful treatment with bifunctional ppp-siRNA. RIG-I is a cytoplasmic receptor, which recognizes viral RNA with a 5'triphosphate end. RIG-I expression is regulated by type I IFNs. Initially, untreated, IFN- α or IFN- β treated Panc02 and T110299 cells were analyzed for RIG-I expression by qRT-PCR. Both cell lines displayed basal expression levels of RIG-I mRNA that were up-regulated upon stimulation with type I IFNs (Figure 6-10 A). Furthermore, treatment of Panc02 cells with the RIG-I ligand ppp-RNA resulted in the secretion of CXCL10 and IFN- β as well as up-regulation of MHC-I expression on the cell surface. In contrast, stimulation of T110299 cells with ppp-RNA induced lower levels of secreted CXCL10 and no induction of IFN- β and MHC-I could be detected (Figure 6-10 B-D). In line with intact RIG-I signaling, Panc02 cells phosphorylated the transcription factor IRF3 upon ppp-RNA stimulation. However, this was not observed for T110299 cells, indicative of defective RIG-I signaling (Figure 6-10 E). Furthermore, ppp-RNA induced apoptosis in Panc02 tumor cells, as assessed by Annexin V/PI staining, whereas viability of T110299 cells was not affected (Figure 6-10 F).

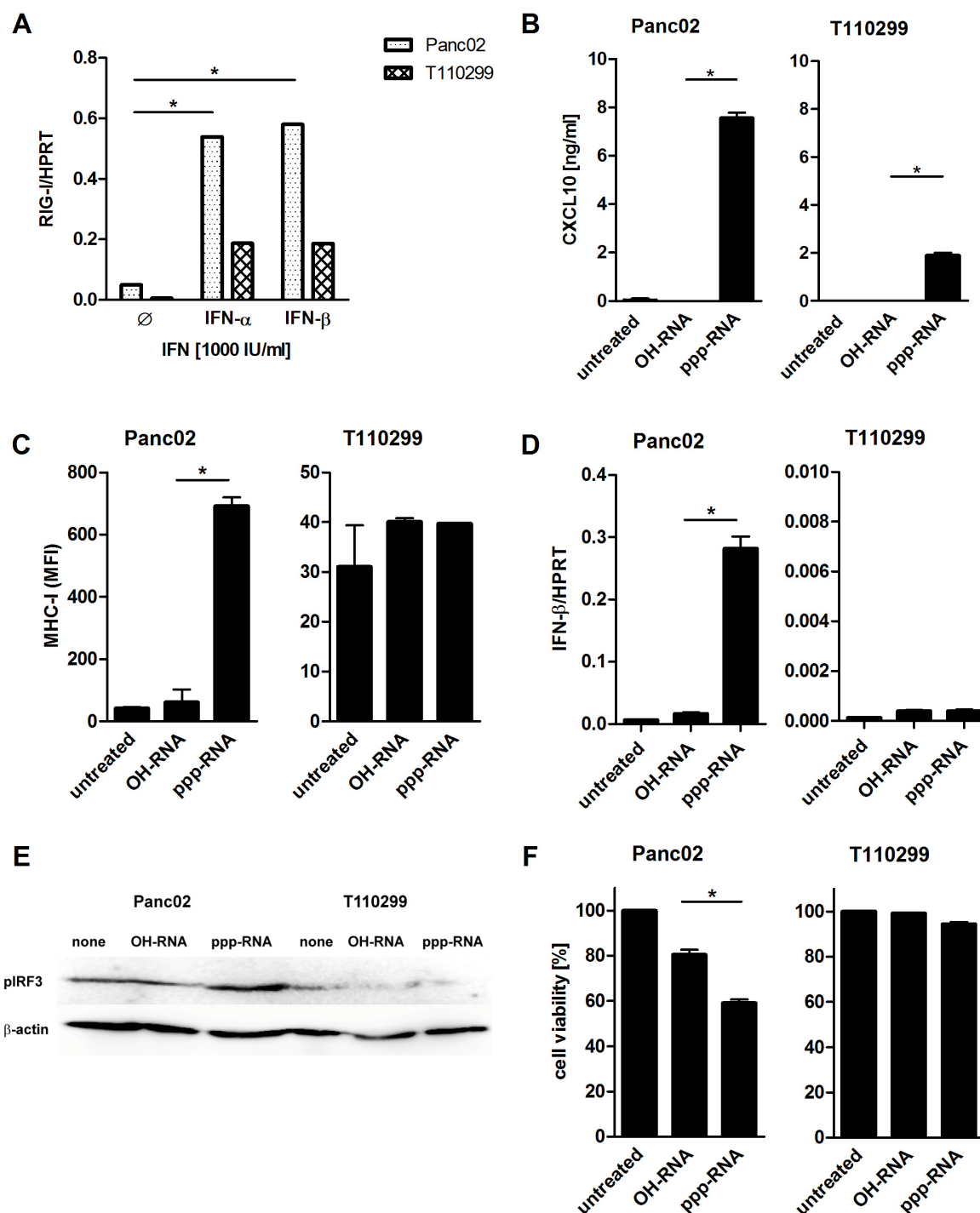


Figure 6-10: Murine Panc02 but not T110299 PDAC cells express functional RIG-I.

A: Panc02 and T110299 cells were cultured in the absence or presence of 1000 IU/ml IFN- α or IFN- β for 12 h. RIG-I expression was determined by qRT-PCR and normalized to HPRT. **B and C:** Panc02 and T110299 cells were stimulated with 500 ng/ml OH-RNA or ppp-RNA for 24 h or left untreated. CXCL10 secretion was analyzed by ELISA. MHC-I expression was determined by flow cytometry and depicted as mean fluorescence intensity (MFI). **D:** Tumor cells were stimulated with 500 ng/ml OH-RNA or ppp-RNA for 12 h or left untreated. IFN- β mRNA was determined by qRT-PCR. **E:** Phosphorylation of IRF3 in Panc02 and T110299 cells stimulated with OH-RNA or ppp-RNA for 2 h was assessed by Western Blot analysis. **F:** Tumor cell viability was measured after treatment with 3 μ g/ml OH-RNA or ppp-RNA for 48 h by Annexin V/PI staining. Viable cells were defined as Annexin V⁻PI⁻ cells. Graphs represent one of three independent experiments. Asterisks indicate * $P < 0.05$.

To confirm that ppp-RNA-induced up-regulation of CXCL10 and MHC-I expression is mediated by the RIG-I signaling pathway, RNAi was used to silence RIG-I expression before stimulation. Panc02 cells were transfected with siRNA targeting RIG-I or scrambled siRNA. After 24 h tumor cells were stimulated with OH-RNA or ppp-RNA. Up-regulation of MHC-I expression and CXCL10 secretion were analyzed by FACS (Figure 6-11 A) and ELISA (Figure 6-11 B), respectively. As expected, silencing of RIG-I expression abolished both MHC-I up-regulation and CXCL10 secretion induced by ppp-RNA.

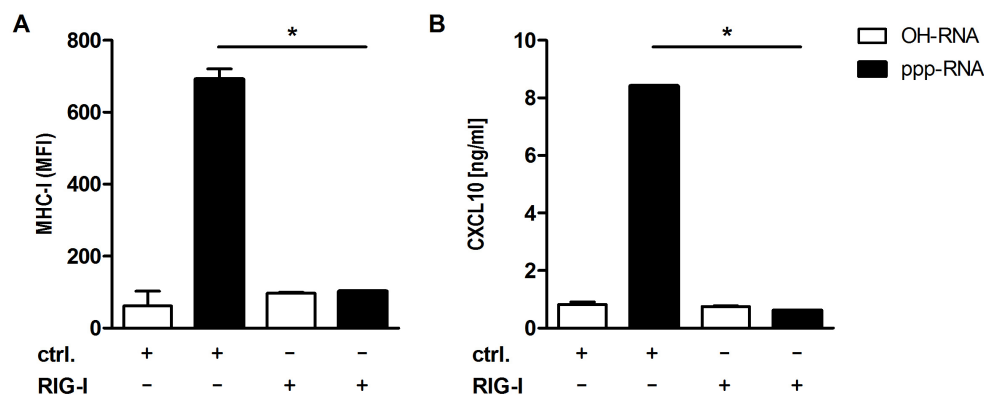


Figure 6-11: ppp-RNA-induced up-regulation of MHC-I expression and CXCL10 secretion is mediated by RIG-I.

Panc02 tumor cells were transfected with 500 ng/ml siRNA targeting RIG-I or scrambled siRNA. After 24 h cells were stimulated with 500 ng/ml of indicated RNAs. **A:** Expression of MHC-I on Panc02 tumor cells was determined by flow cytometry. **B:** CXCL10 levels in tumor supernatant were measured by ELISA. Representative data of three independent experiments are shown. Bars represent mean + SD from duplicates. Significant differences were analyzed by unpaired student's t-test. Asterisks indicate * $P < 0.05$.

6.2.2 *In vitro* actions of unmodified and 5'ppp-modified siRNA targeting galectin-1

The novel ppp-siRNA technology allows combining RIG-I activation with RNAi-mediated gene silencing in one molecule. Galectin-1 targeting siRNA (OH-Gal-1) was selected and the corresponding ppp-siRNA (ppp-Gal-1) was generated by *in vitro* transcription using a DNA template of the same sequence containing the T7 RNA polymerase promoter sequence. To verify the knockdown efficiency of both unmodified OH-Gal-1 as well as 5'ppp-modified ppp-Gal-1, qRT-PCR analysis was performed. As shown in Figure 6-12 A OH-Gal-1 induced a significant knockdown of galectin-1 mRNA expression of 80% and 50% in Panc02 and T110299 cells, respectively. In Panc02 cells galectin-1 silencing with ppp-Gal-1 was not as efficient as with OH-Gal-1 (knockdown efficacy 50%). In contrast, in T110299 cells the knockdown of galectin-1 was similarly efficient for both ppp-modified and unmodified siRNA. Treatment with ppp-RNA and ppp-Gal-1 influenced cell morphology from spindle-shaped towards round-shaped cells, indicative of apoptosis induction (Figure 6-12 B).

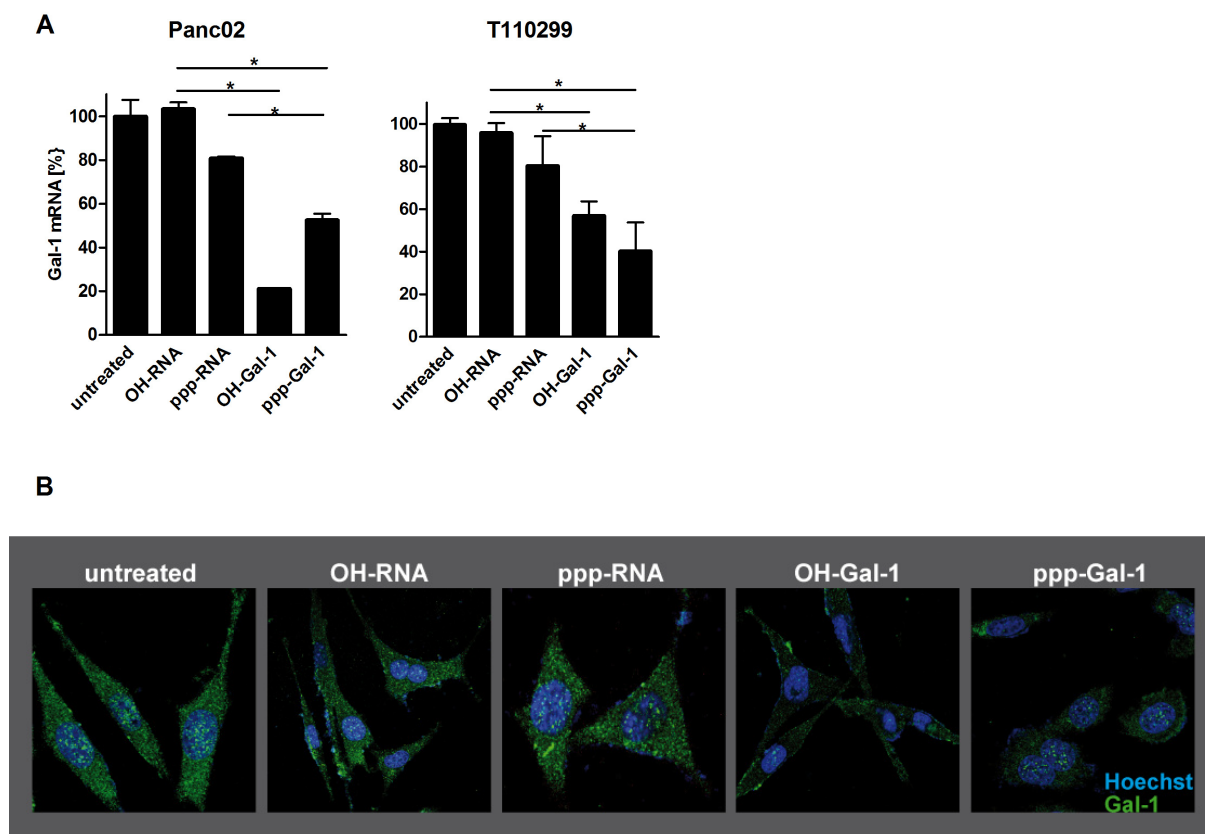


Figure 6-12: Silencing of galectin-1 expression in Panc02 and T110299 cells with unmodified and 5'ppp-modified siRNA.

A: Panc02 and T110299 cells were treated twice with 500 ng/ml OH-Gal-1 or ppp-Gal-1 for 12 h. Expression of Gal-1 mRNA was determined by qRT-PCR and is depicted as relative expression compared to untreated cells. Representative data of three independent experiments are depicted. Asterisks indicate $P < 0.05$. **B:** Panc02 cells were treated once with 500 ng/ml OH-Gal-1 or ppp-Gal-1 for 24 h. Galectin-1 immunofluorescence staining was performed with a primary mouse polyclonal antibody rabbit IgG (1:100) against Gal-1 and a secondary anti-rabbit antibody AF488 (1:100). Nuclei were counterstained with Hoechst (1:200).

Next, activation of RIG-I by the bifunctional ppp-Gal-1 molecule was validated. 24 h after stimulation with OH-Gal-1 or ppp-Gal-1, Panc02 and T110299 cells were analyzed with respect to CXCL10 secretion and MHC-I expression. In both cell lines transfection with OH-Gal-1 or scrambled OH-RNA induced no CXCL10 secretion (Figure 6-13 A). In contrast, stimulation with ppp-RNA (irrelevant siRNA sequence) and ppp-Gal-1 resulted in CXCL10 secretion in both cell lines. As observed before, CXCL10 levels were significantly higher in Panc02 cells compared to T110299 cells (Figure 6-13 A). Moreover, ppp-Gal-1 induced similar levels of MHC-I and IFN- β expression as well as apoptosis as control ppp-RNA in Panc02 cells. Again, T110299 cells showed no signs of RIG-I activation (Figure 6-13 B-D).

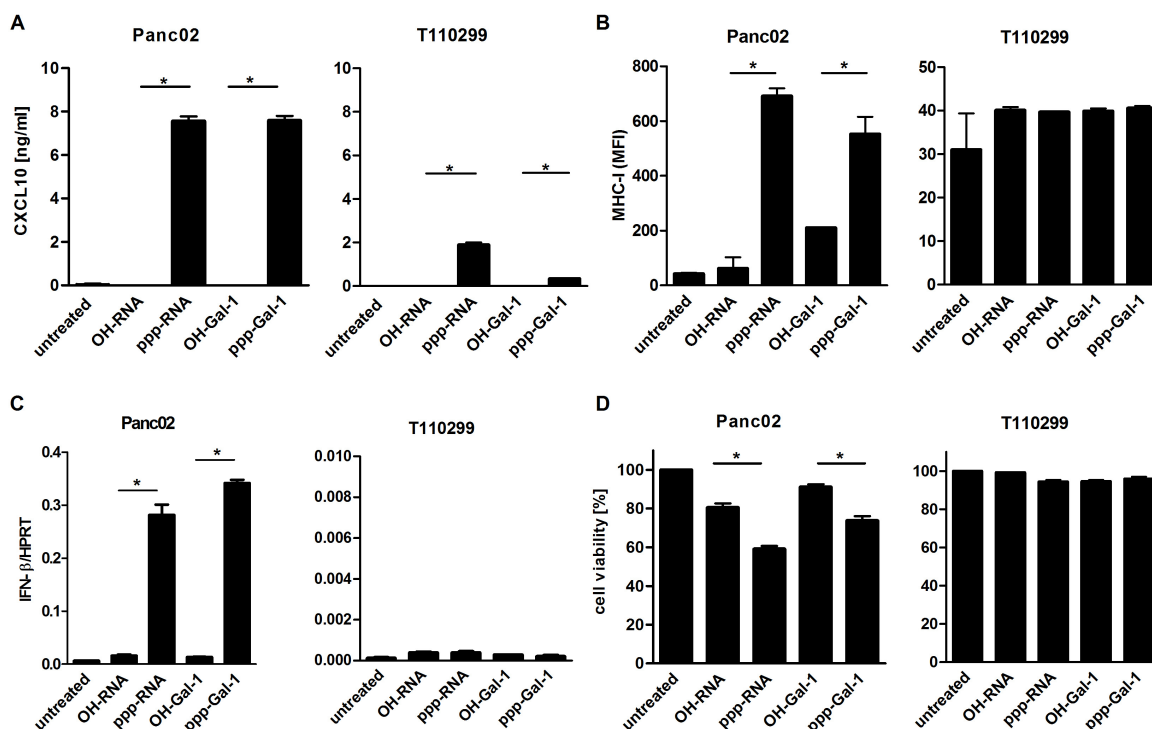


Figure 6-13: 5' ppp-modified siRNA targeting galectin-1 combines gene silencing with RIG-I signaling. **A and B:** Panc02 and T110299 cells were treated with 500 ng/ml OH-Gal-1 or ppp-Gal-1 for 24 h. CXCL10 secretion was measured by ELISA and MHC-I expression was analyzed by flow cytometry. **C:** Expression levels of IFN- β mRNA were determined by qRT-PCR after stimulation of tumor cells with 3 μ g/ml of indicated RNA for 12 h and normalized to HPRT. **D:** FACS analysis of cell viability by AnnexinV/PI staining 48 h after transfection with 3 μ g/ml of RNAs. Representative data of three independent experiments are depicted. Asterisks indicate $P < 0.05$.

6.2.3 *In vivo* actions of unmodified and 5' ppp-modified siRNA targeting galectin-1

Based on the *in vitro* studies demonstrating intact RIG-I signaling only in Panc02 cells, *in vivo* studies were performed in the Panc02 tumor model. In first experiments, Panc02 cells were injected subcutaneously in the flank of wild-type C57BL/6 mice. Serum was collected weekly over six weeks to determine galectin-1 levels during progressive tumor growth. As shown in Figure 6-14, galectin-1 serum levels significantly correlated with tumor size ($p < 0.005$).

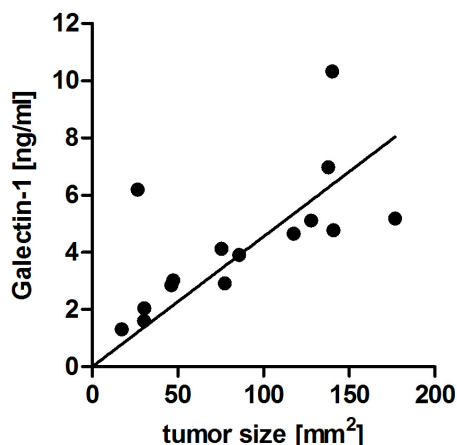


Figure 6-14: Galectin-1 serum levels in mice with Panc02 tumors correlate with tumor size.

Panc02 cancer cells were injected subcutaneously in the right flank of C57BL/6 mice (n=5). Tumor size was measured every other day. Serum was collected once weekly and galectin-1 levels were determined by ELISA. Correlation was significant (Pearson $r = 0.6571$).

Next, tumor tissue and sera of mice treated with OH-Gal-1 were analyzed in regards to galectin-1 levels. Mice with orthotopic Panc02 tumors showed similar galectin-1 mRNA expression levels after treatment with 50 μg of scrambled siRNA or OH-Gal-1 repeated three times every 48 h (Figure 6-15 A). No significant galectin-1 reduction in tumor tissue could be achieved by systemic OH-Gal-1 application via the tail vein. Galectin-1 serum levels increased significantly in mice with Panc02 tumors (Figure 6-15 B). Treatment with OH-RNA had no influence on galectin-1 serum levels. OH-Gal-1 treated mice showed reduced galectin-1 serum levels as compared to untreated or OH-RNA treated mice, however this reduction missed statistical significance (2-3 mice per group).

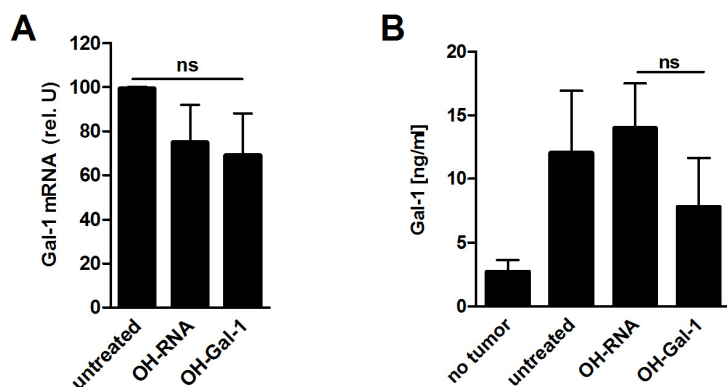


Figure 6-15: Galectin-1 mRNA levels in tumors and serum protein levels in mice with orthotopic Panc02 tumors after treatment with siRNA targeting galectin-1.

Panc02 cells were injected orthotopically in the pancreas of wild-type C57BL/6 mice. Animals were treated three times every 48 h with 50 μg of the indicated RNAs complexed with *in vivo* jetPEI via the tail vein. Mice were sacrificed 24 h after the last injection and serum and tumor tissue were collected. **A:** Galectin-1 mRNA expression in tumor tissue was analyzed by qRT-PCR. **B:** Galectin-1 serum levels were measured by ELISA. Data from two to three mice per group are represented as mean \pm SEM.

Next, the therapeutic efficacy of treatment with OH-Gal-1 and ppp-Gal-1 was investigated in the subcutaneous and orthotopic Panc02 tumor model (Figure 6-17). Treatment started at day 10 after

tumor induction and was repeated twice weekly over three weeks with 50 μ g siRNA via the tail vein. Systemic treatment with ppp-Gal-1 led to enhanced serum levels of IFN- α , CXCL10 and TNF- α (Figure 6-16 A). In addition, splenic CD4⁺ and CD8⁺ T cell, B cells, NK cells and NKT cells up-regulated CD69 expression, indicative of systemic RIG-I activation (Figure 6-16 B).

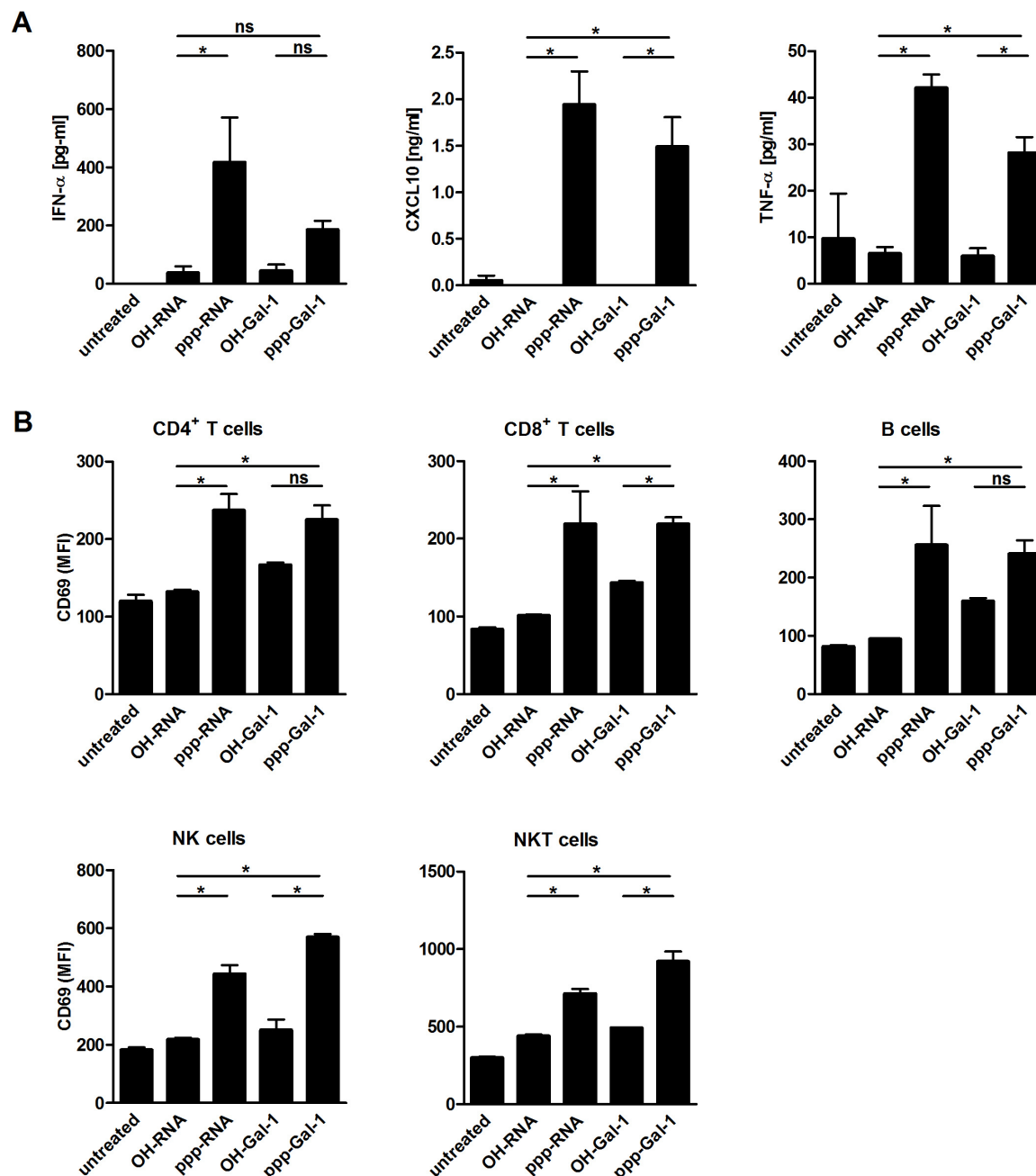
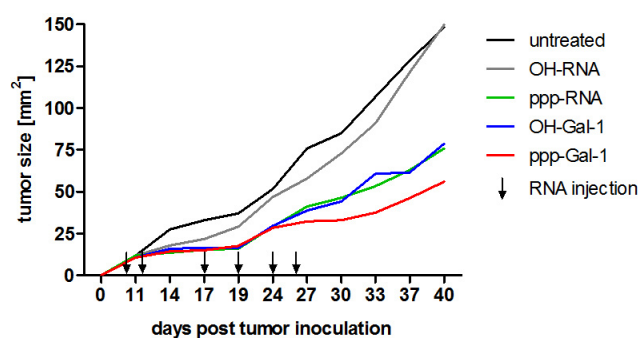


Figure 6-16: Systemic treatment of Panc02 tumor-bearing mice with unmodified and modified 5'ppp-RNA silencing galectin-1.

Mice with subcutaneous Panc02 tumors were treated with RNA ten days after tumor induction. Mice were treated twice weekly over three weeks with 50 μ g of indicated RNA via the tail vein. Serum was analyzed 6 h post third RNA injection. **A:** Levels of IFN- α , CXCL10 and TNF- α were analyzed by ELISA. **B:** Activation status of peripheral lymphocytes was determined by staining of CD69 and analyzed by flow cytometry. Pooled data from 4 to 5 mice per group are represented as mean + SEM. P-values < 0.05 were considered significant.

In the subcutaneous tumor model all mice without treatment or treated with OH-RNA had to be sacrificed by day 37 due to progressive tumor growth. At this time point, mice treated with control ppp-RNA or OH-Gal-1 showed a significantly delayed tumor growth (52% size reduction compared to untreated mice). Mice in the ppp-Gal-1 group showed the best tumor control (64% size reduction compared to untreated mice). In the orthotopic tumor model, all mice without treatment or treated with scrambled OH-RNA had to be sacrificed within 40 days after tumor induction caused by progressive tumor growth (median survival 33 and 29 days, respectively). Mice treated with OH-Gal-1 showed no significantly prolonged survival (median survival 35 days), whereas treatment with control ppp-RNA (same sequence as scrambled OH-RNA) resulted in a significantly extended survival (median survival 41 days). Mice treated with ppp-Gal-1 showed the best survival (median survival 49 days). Of note, 20 % of mice treated with ppp-Gal-1 rejected their tumor and stayed tumor free for an observation period of 100 days as compared to 8 % of mice treated with ppp-RNA and 0 % in the other therapy groups.

A



B

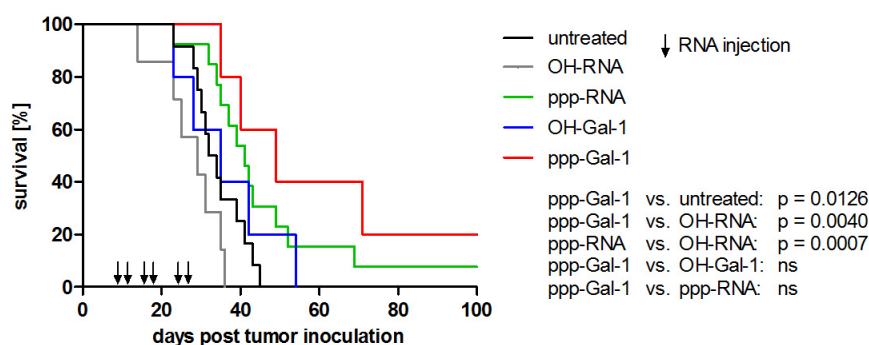


Figure 6-17: Survival of subcutaneous and orthotopic Panc02 tumor-bearing mice after treatment with unmodified and modified 5'ppp-RNA silencing galectin-1.

Mice with subcutaneous or orthotopic Panc02 tumors were treated with RNA ten days after tumor induction. Mice were treated twice weekly over three weeks with 50 μ g of indicated RNA via the tail vein. **A:** Tumor size of subcutaneous tumors was measured every three days by caliper (n=4-5/group). **B:** Survival in the orthotopic model was monitored. Experiments were terminated after 100 days. Median survival of untreated mice: 33 days (n=12); OH-RNA: 29 days (n=7); ppp-RNA: 41 days (n=13); OH-Gal-1: 35 days (n=5); ppp-Gal-1: 49 days (n=5). Pooled data with statistical analysis from two independent experiments with 4-5 mice per group in the subcutaneous and 5 to 13 mice per group in the orthotopic model are depicted. P-values for statistical comparisons are shown in the graph.

6.3 Tumor immune escape mechanisms in pancreatic ductal adenocarcinoma

T cells play an important role in tumor control by the immune system. Lymphocyte infiltrations in pancreatic tumors represent a good prognostic factor, however usually only few T cells can be found in the tumors. In addition, these T cells are often dysfunctional (Garbe et al., 2006, Mukherjee et al., 2001). Identifying the mechanisms leading to tumor immune escape in pancreatic cancer are important for the development of effective immunotherapeutic strategies. Here, general mechanisms like the influence of the tumor cells on T cell proliferation and degranulation were investigated and possible immunosuppressive molecules like galectin-1, TGF- β and IDO were analyzed with respect to their expression level in tumor cells and contribution to T cell inhibition.

6.3.1 Soluble factor(s) in tumor supernatant inhibit T cell proliferation

As an initial experiment T cell proliferation induced by CD3 and CD28 ligation via mAb coated beads in the absence or presence of PDAC cell supernatant was assessed. Therefore, primary isolated T cells from mouse spleen were labeled with CFSE, stimulated with beads and incubated with tumor supernatant for 72 h. Proliferation of CD4⁺ and CD8⁺ T cells was analyzed by flow cytometry. The tumor supernatant was generated by plating 5×10^5 tumor cells per well in a 6-well plate with 2 ml T cell medium for 24 h. As shown in Figure 6-18, supernatant of both Panc02 and T110299 cells inhibited the proliferation of both CD4⁺ and CD8⁺ T cells in a dose-dependent manner. This inhibition was very efficient; as little as 0.75% of tumor supernatant decreased T cell proliferation by approximately 50% (Figure 6-18). The inhibitory effect was more pronounced for CD4⁺ T helper cells. However, 25% of supernatant almost completely abolished proliferation of both T cell types.

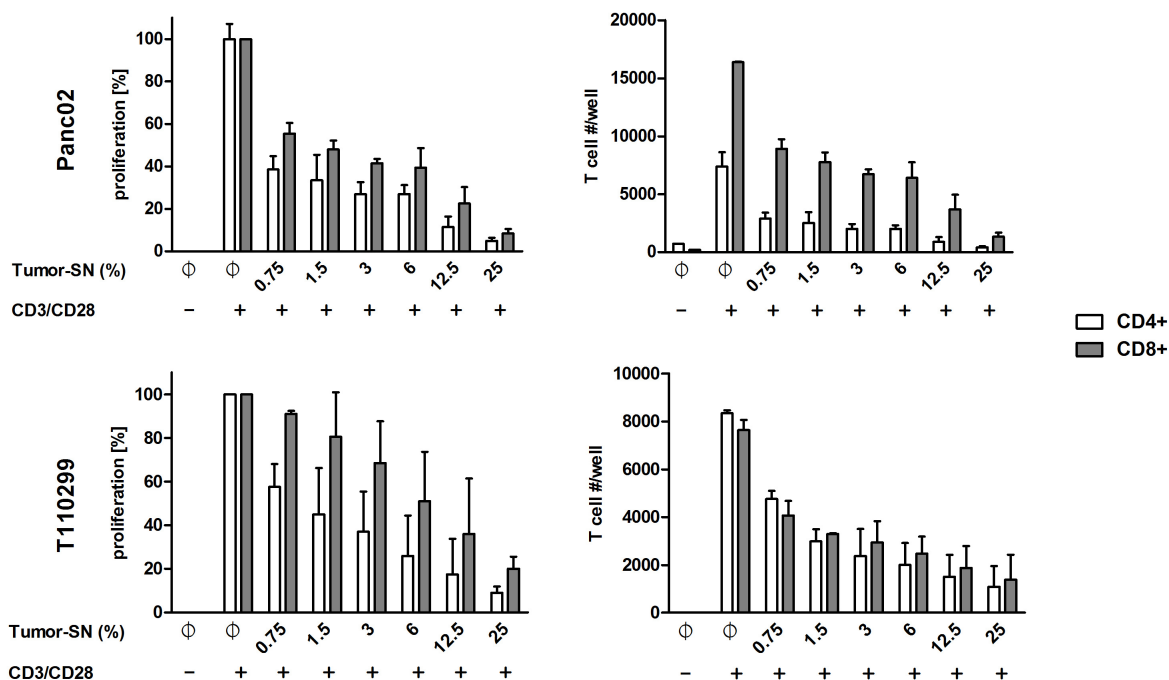


Figure 6-18: Inhibition of T cell proliferation by tumor supernatant from murine PDAC cell lines.

Primary isolated untouched T cells from mouse spleen were labeled with 2.5 μ M CFSE, stimulated with anti-CD3/CD28 Dynabeads and incubated in the absence or presence with indicated percentages of tumor supernatant (Tumor-SN) for 72 h. T cell proliferation was analyzed by flow cytometry. Proliferation of T cells in medium without tumor supernatant was normalized to 100%. Representative data of three independent experiments are shown. Bars represent mean \pm SD from duplicates.

The inhibitory effect on T cell proliferation was next assessed using antigen-specific T cells. Splenic CD8⁺ T cells were isolated from OT-1 mice and labeled with CFSE. These T cells are transgenic for a T cell receptor recognizing the ovalbumin epitope SIINFEKL in the context of MHC-I molecules. To stimulate the T cells SIINFEKL-pulsed DCs were added to the T cell culture. Proliferation of CD8⁺ T cells was analyzed by flow cytometry. T cell proliferation of OT-1 CD8⁺ T cells was significantly inhibited by tumor supernatant from both Panc02 and T110299 cells (Figure 6-19).

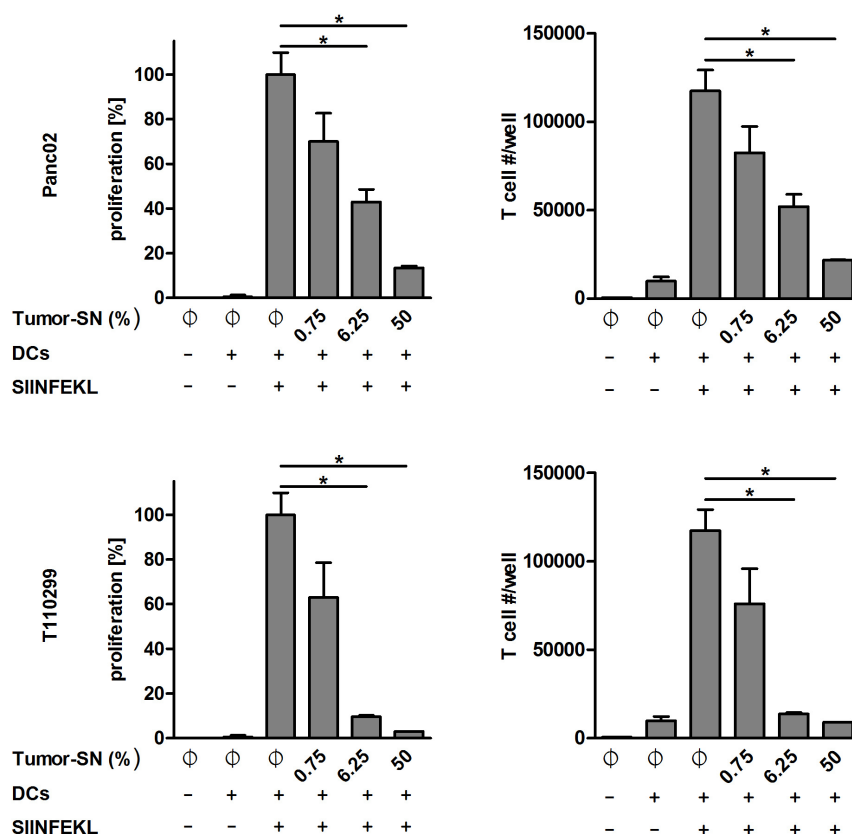


Figure 6-19: Suppression of OT-1 T cell proliferation by tumor supernatant.

Primary isolated untouched CD8⁺ T cells from OT-1 mouse spleen were labeled with 2.5 μ M CFSE, stimulated with SIINFEKL-pulsed DCs and incubated in the absence or presence of tumor supernatant (Tumor-SN) for 72 h. T cell proliferation was analyzed by flow cytometry. T cell proliferation in the absence of tumor supernatant was normalized to 100%. Representative data of three independent experiments are shown. Bars represent mean \pm SD from duplicates. Significant differences were analyzed by one-way ANOVA including Bonferroni correction. P-values < 0.05 were considered significant.

6.3.2 Tumor supernatant induces T cell apoptosis

To address the question whether tumor supernatants induces T cell apoptosis, T cells were incubated with 6.25% tumor supernatant for 72 h in the presence of T cell stimulator beads and analyzed by flow cytometry using the Annexin V/PI assay. As depicted in Figure 6-20 A, cell viability of unstimulated T cells (no beads) and T cells cultured with tumor supernatant of Panc02 and T110299 cells decreased significantly up to 80%. In addition, T cells cultured in the presence of tumor supernatant significantly up-regulated expression of the death receptor Fas (CD95) (Figure 6-20 B). Interestingly, T cells that were first stimulated with beads for 24 or 48 h before addition of tumor supernatant were not affected in their proliferative response and did not undergo apoptosis (Figure 6-20 C). This indicates that soluble factor(s) present in the tumor supernatant of PDAC cells inhibit proliferation only of naïve, not previously activated T cells.

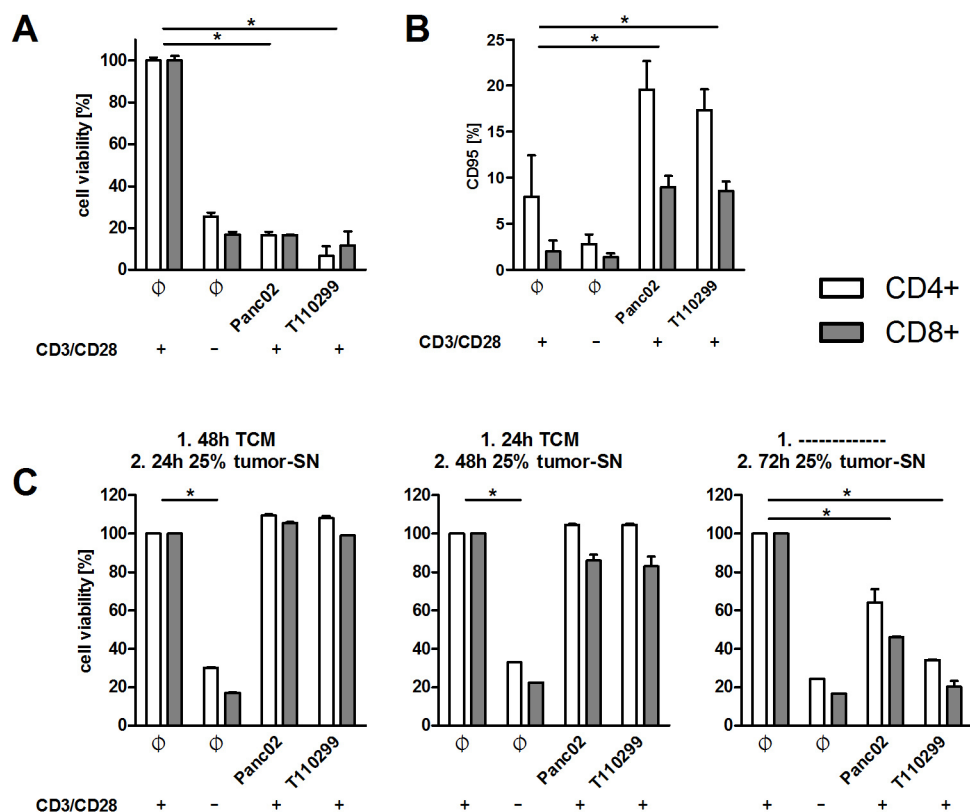


Figure 6-20: T cell apoptosis induced by tumor supernatant of murine PDAC cells.

A: Primary untouched T cells (white bars CD4⁺, gray bars CD8⁺) from mouse spleen were stimulated with anti-CD3/CD28 Dynabeads and incubated in the absence or presence of 6.25% tumor supernatant for 72 h. Annexin V/PI staining was analyzed by flow cytometry. Viability was defined as Annexin V⁻/PI⁻ cell population and normalized to 100% of stimulated T cells in the absence of supernatant. **B:** Stimulated T cells were cultured in the absence or presence of 6.25% tumor supernatant for 72 h. Fas (CD95) expression was analyzed by flow cytometry. **C:** T cells were stimulated with anti-CD3/CD28 Dynabeads and cultured in the absence or presence of 25% tumor supernatant. (1) 48 h preincubation with T cell medium followed by 24 h incubation with tumor supernatant. (2) 24 h preincubation with T cell medium followed by 48 h incubation with tumor supernatant and (3) 72 h incubation with tumor supernatant. Representative data of three independent experiments are shown. Bars represent mean \pm SD from duplicates. Significant differences were analyzed by one-way ANOVA including Bonferroni correction. P-values < 0.05 were considered significant.

6.3.3 Soluble factors do not impair cytotoxic T cell degranulation

An important function of cytotoxic T cells is degranulation with release of perforin and granzyme B to induce target cell killing. During this process intracellular granules filled with perforin and granzyme B fuse with the cell membrane of T cells for secretion into the extracellular space. Perforin generates pores in the cell membrane of target cells while granzyme B triggers apoptotic processes. On the inner membrane of these granules the molecules CD107a and CD107b, also referred as LAMP-1 and LAMP-2, reach the surface and can be bound by antibodies as indirect measurement of degranulation. To assess whether tumor supernatant affects T cell degranulation, primary cytotoxic T cells isolated from OT-1 mice were stimulated with SIINFEKL-pulsed DCs and incubated with 6.25% tumor supernatant for 5 h. As shown in Figure 6-21, the degranulation of cytotoxic T cells was not reduced by soluble factors in PDAC supernatants.

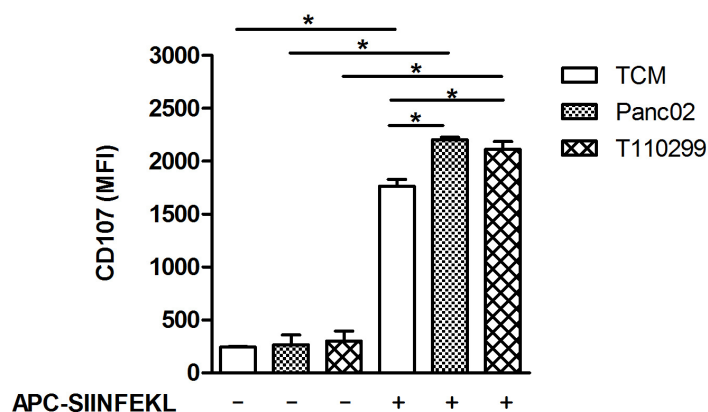


Figure 6-21: Soluble factors do not impair cytotoxic T cell degranulation.

Primary isolated untouched CD8⁺ T cells from OT-1 mouse spleen were incubated with fluorochrome-labeled CD107a/b antibodies in the absence or presence of tumor supernatant (6.25%) for 5 h. T cell stimulation was done by SIINFEKL-pulsed antigen presenting cells (APC-SIINFEKL). CD107 expression was analyzed by flow cytometry. Representative data of three independent experiments are shown. Bars represent mean \pm SD from duplicates. Significant differences were analyzed by one-way ANOVA including Bonferroni correction. P-values < 0.05 were considered significant.

6.3.4 T cell inhibition is mediated by a tumor-derived soluble protein

Next, the question was addressed how PDAC cells mediated T-cell inhibition. One important pathway in T cell function that is accountable for T cell homeostasis and peripheral tolerance is the PD-1/PD-L1 axis. PD-1 is upregulated on T cells when they are activated to regulate T cell responses (Chen and Flies, 2013). PD-L1, the ligand for PD-1, is normally expressed on antigen presenting cells, but can also be expressed on tumor cells (Okudaira et al., 2009, Nomi et al., 2007, Dong et al., 2002, Butte et al., 2007). There is also evidence that PD-L1 can be released by tumor cells (Frigola et al., 2012, Frigola et al., 2011). Therefore, it was investigated if soluble PD-L1 could be responsible for T cell inhibition in tumor supernatants. Western blot analysis of tumor supernatants revealed that both cell lines secrete PD-L1 (Figure 6-22 A). However, blocking PD-1 or B7-1, another receptor for PD-L1, on T cells using monoclonal antibodies did not restore T cell proliferation (Figure 6-22 B and C), ruling out a major contribution of this pathway in our experimental setting.

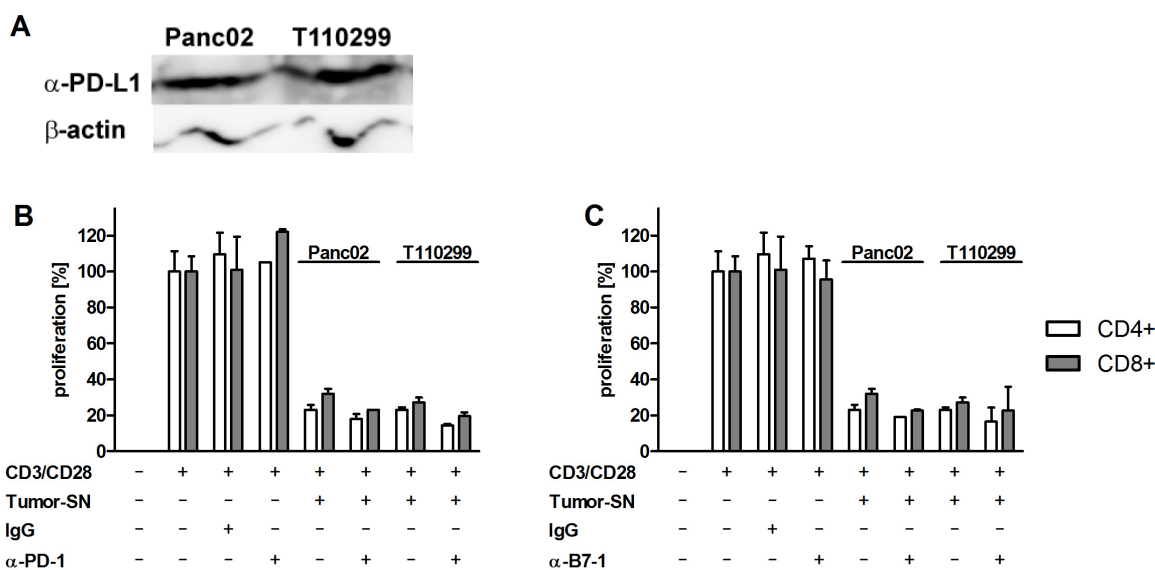


Figure 6-22: Murine PDAC cells secrete PD-L1, but the PD-1/PD-L1 axis is not responsible for tumor supernatant-induced T cell inhibition.

A: Western Blot analysis of PD-L1 from tumor supernatants of Panc02 and T110299 cell lines using a CD274 mAb (clone MIH5, 1:1000). **B:** Effect of PD-1 blocking on primary T cells with anti-CD279 mAb (clone J43, 5 μ g/ml) in a T cell proliferation assay. **C:** Effect of blocking B7-1 on primary T cells with anti-CD80 mAb (clone 16-10A1, 5 μ g/ml). Representative data of three independent experiments are shown. Bars represent mean \pm SD from duplicates.

To gain further insight into the possible mechanisms leading to T cell suppression, 50 IU/ml of IL-2 were added to the T cell culture as an attempt to rescue T cell proliferation. Moreover, benzonase, a nuclease degrading immunosuppressive nucleotides, was added. Neither IL-2 nor benzonase rescued T cell suppression mediated by tumor cell supernatants (Figure 6-23 A). However, heating of the tumor supernatant to 95°C for 10 min resulted in a complete restoring of T cell proliferation (Figure 6-23 A). Instability to heating argues that the immunosuppressive factor may be a protein that was denatured by boiling. To verify if a tumor-derived protein is responsible for T cell inhibition, tumor supernatant was treated with Proteinase K before adding to the T cells. Proteinase K treatment lead to a significant increase in T cell proliferation (Figure 6-23 B), indicating that a tumor-derived soluble protein mediates T cell inhibition.

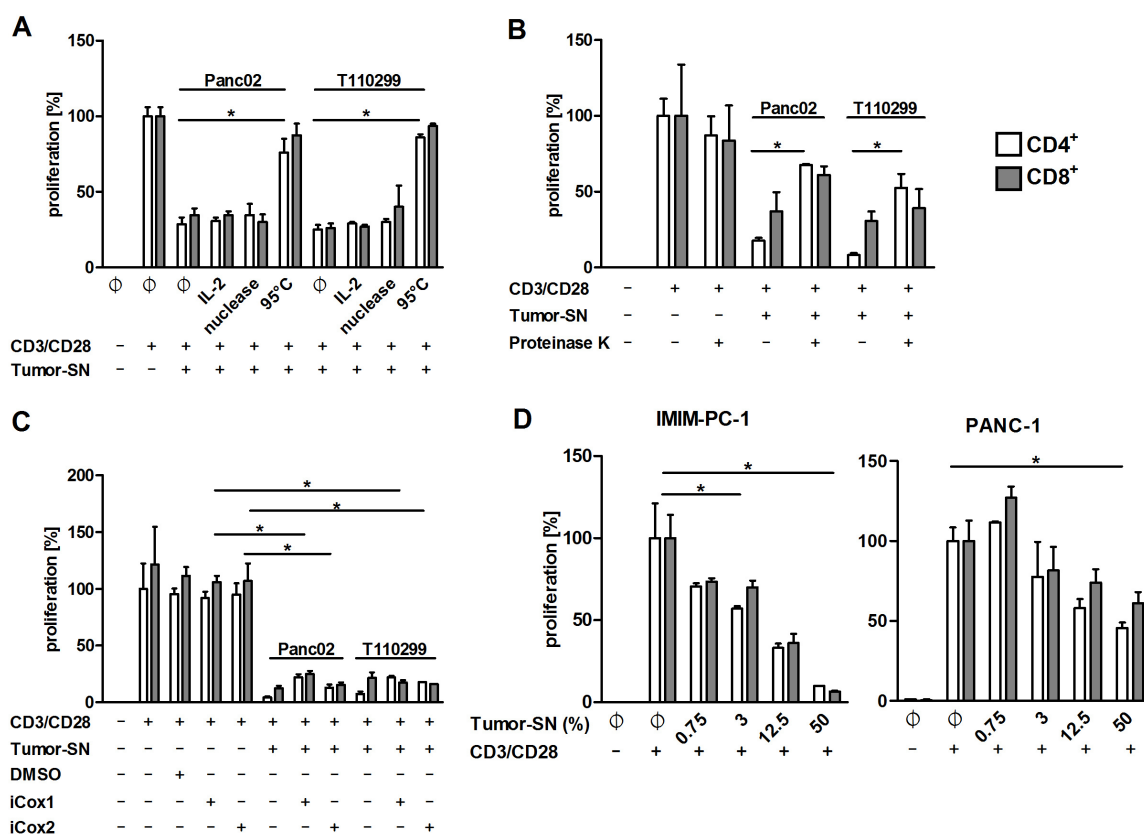


Figure 6-23: T cell inhibition is mediated by a tumor-derived protein, whereas nucleotides or prostaglandins are dispensable.

Freshly isolated splenic T cells were labeled with CFSE and incubated in the absence or presence of CD3/CD28 Dynabeads for 72 h and T cell proliferation was analyzed by flow cytometry. **A:** Tumor supernatants (6.25%) of Panc02 and T110299 cells were treated either with 50 IU/ml IL-2 or 50 IU/ml benzonase (nuclease) or boiled for 10 min before adding to T cells. **B:** Tumor supernatant was treated with Proteinase K beads (5 mg/ml) for 2 h. 6.25% tumor supernatant was added to T cells. **C:** Tumor cells were treated either with 10 μ M SC-560, an inhibitor of COX1 (iCox1), or 20 μ M Celecoxibe, an inhibitor of COX2 (iCox2), for 24 h. 25% supernatant of treated or untreated tumor cells was used for T cell proliferation assay. **D:** Murine T cells were incubated with tumor supernatant from human pancreatic cancer cells (PANC-1 and IMIM-PC-1). Representative data of three independent experiments are shown. Bars represent mean \pm SD from duplicates. Significant differences were analyzed by one-way ANOVA including Bonferroni correction. P-values < 0.05 were considered significant.

Prostaglandins are known for their immune regulatory role via inhibiting T cell function (Loose and Van de Wiele, 2009). Prostanoids are generated by the enzymes cyclooxygenase 1 and 2 (COX1 and 2). To analyze if tumor-derived prostanoids play a role in T cell inhibition, PDAC cells were pretreated with the COX1 inhibitor SC-560 or COX2 inhibitor Celecoxibe for 24 h and supernatants collected. As shown in Figure 6-23 C, COX inhibition did not affect T cell proliferation.

To gain further information regarding the nature of the inhibitory factor, it was assessed whether the factor is also produced by human PDAC cells and if the factor is species cross-reactive. To this end, supernatant from human IMIM-PC1 and PANC-1 cell lines were collected and added to murine T cell proliferation assays (Figure 6-23 D). These assays could clearly show that human PDAC cells are also capable of suppressing proliferation of murine T cells.

Taken together, PDAC cells produce a T cell proliferation suppressing factor, that is a) soluble, b) heat-labile, c) likely a protein (prostanoids and nucleotides were ruled out) and d) capable of cross-reacting between mice and humans. Thus, likely candidates that were investigated in subsequent studies were a) TGF- β which shares close homology in different species, b) galectin-1 which is produced in high levels by PDAC cells, and c) IDO which produces tryptophan catabolites leading to T cell apoptosis in both human and murine T cells.

6.3.5 T cell inhibition is not mediated by galectin-1

A molecule with T cell inhibitory function, which can be produced by tumor cells, is galectin-1. Therefore, the expression of galectin-1 was analyzed in cell lysates as well as supernatants of Panc02 and T110299 cells by ELISA. As shown in Figure 6-24, galectin-1 was expressed in high levels by PDAC cells. Moreover, galectin-1 could be found in tumor supernatants, although at significantly lower levels.

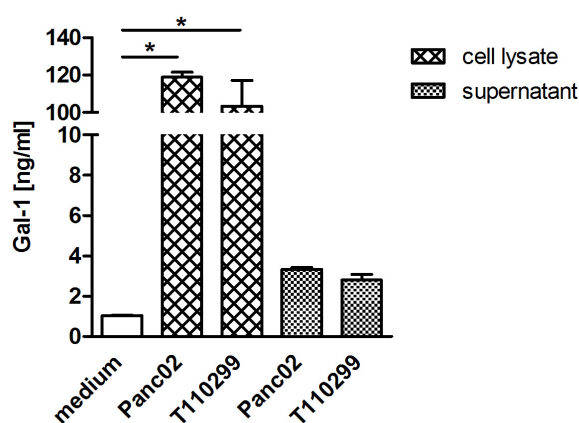


Figure 6-24: Galectin-1 content in cell lysate and supernatant of murine PDAC cells.

Panc02 and T110299 cells were plated in a 96-well plate for 24 h. Supernatant was collected and pelleted cells were lysed with 60 μ l lysis buffer for 10 min on ice. Galectin-1 content was measured by ELISA. Representative data of three independent experiments are shown. Bars represent mean + SD from duplicates. Significant differences were analyzed by one-way ANOVA including Bonferroni correction. P-values < 0.05 were considered significant.

To assess the possible contribution of secreted galectin-1 on T cell inhibition, T110299 cells were treated with specific siRNA targeting Gal-1 and supernatants collected. Although galectin-1 silencing resulted in 50% reduced mRNA expression levels (Figure 6-12 A), this had no effect on T cell inhibition mediated by T110299 cells (Figure 6-25).

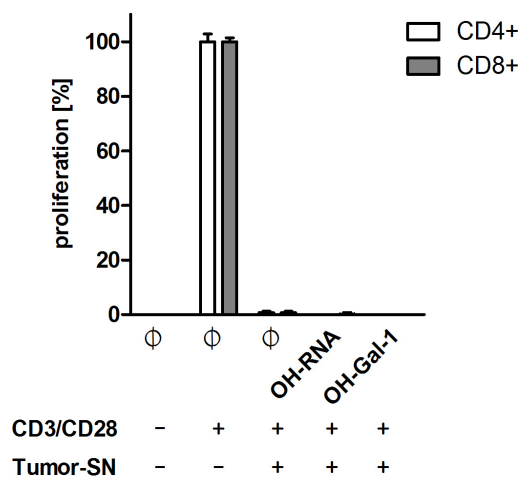


Figure 6-25: T cell inhibition is not affected by siRNA based silencing of galectin-1 in T110299 cells.

T110299 cells were plated in a 96-well plate (4×10^4 cell per well) and galectin-1 expression was silenced with 500 ng/ml OH-Gal-1. After 24 h 50% of tumor supernatant (Tumor-SN) was used for T cell proliferation assay. CFSE labeled T cells were incubated in the absence or presence of CD3/CD28 Dynabeads with or without tumor supernatant for 72 h and analyzed by flow cytometry. Representative data of three independent experiments are shown. Bars represent mean + SD from duplicates. Significant differences were analyzed by one-way ANOVA including Bonferroni correction. P-values < 0.05 were considered significant.

To exclude, that RNAi-mediated galectin-1 silencing was insufficient, two different inhibitors of galectin-1 were used: β -lactose, a natural inhibitor of galectin-1, and Thiodigalactoside (TDG), a synthetic and metabolically stable inhibitor (Ito et al., 2011). Treatment with 50 mM β -lactose in 25% tumor supernatant had no effect on T cell inhibition and apoptosis, respectively (Figure 6-26 A and B). Similarly, treatment with TDG demonstrated that galectin-1 was not involved in T cell inhibition (Figure 6-26 C) as CD4⁺ and CD8⁺ T cells showed the same proliferation rate compared to untreated or sucrose (control) treated tumor supernatant, respectively.

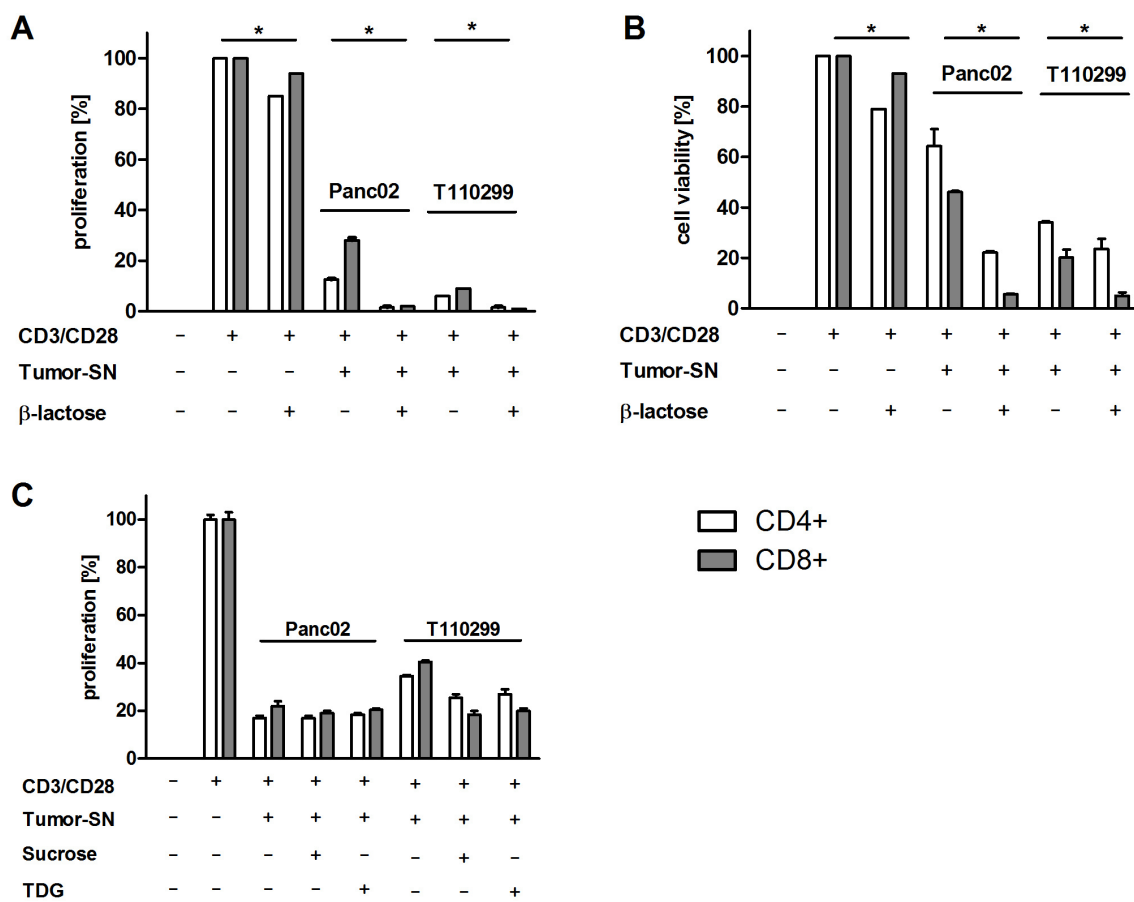


Figure 6-26: Galectin-1 inhibition does not restore inhibition of T cell proliferation.

Primary untouched T cells were incubated in the absence or presence of CD3/CD28 Dynabeads and proliferation was analyzed by flow cytometry. Inhibitors of galectin-1 were added to tumor supernatants (25%) of Panc02 and T110299 cells. **A:** T cell proliferation assay with 50 mM β -lactose in tumor supernatant. **B:** T cell viability was determined by Annexin V/PI staining after 72 h. Viable cells were defined as Annexin V⁻/PI⁻. **C:** T cells were incubated with 12.5% tumor supernatant of Panc02 and T110299 cells, which were treated with 10 mM Thiodigalactoside (TDG) or 10 mM sucrose as negative control for 72 h in a T cell proliferation assay. Representative data of three independent experiments are shown. Bars represent mean \pm SD from duplicates. Significant differences were analyzed by one-way ANOVA including Bonferroni correction. P-values < 0.05 were considered significant.

6.3.6 Blocking TGF- β receptor signalling partially restores T cell proliferation

Panc02 tumor cells have previously been shown to secrete TGF- β into tumor supernatant and serum levels of TGF- β were progressively elevated in Panc02 tumor-bearing mice (Ellermeier et al., 2013). As TGF- β is a potent immune suppressive molecule and is cross-reactive between different species due to its highly conserved sequence, the role of this cytokine in regards to tumor supernatant-mediated T cell inhibition was analyzed. Initially, silencing of TGF- β ₁ was performed using siRNA technology. Panc02 cells were treated twice with 500 ng/ml siRNA targeting TGF- β ₁ and 24 h after the second transfection the tumor supernatant (6.25%) was used for T cell proliferation assays (Figure 6-27). Silencing of TGF- β ₁ did not restore T cell proliferation, but silencing efficacy was only partly effective with reduction of TGF- β ₁ mRNA between 50-70% (data not shown). Another problem of this

approach might be that the siRNA targets only a single TGF- β isoform, but not two other isoforms, TGF- β_2 and TGF- β_3 .

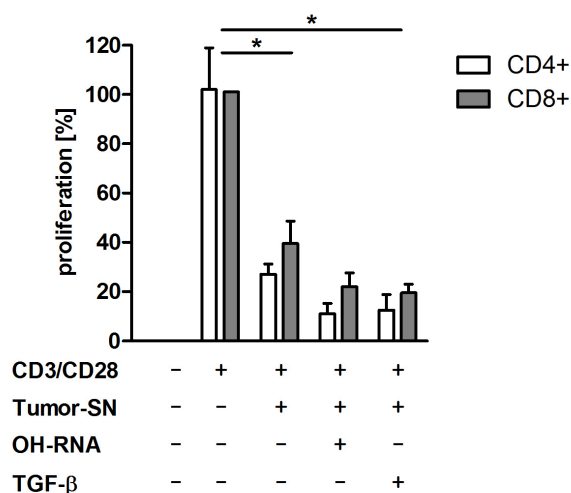


Figure 6-27: T cell inhibition is not influenced by siRNA based silencing of TGF- β_1 .

Panc02 cells were incubated with siRNAs (2 x 500 ng/ml) with or without silencing activity against TGF- β for 24 h or left untreated. 6.25% tumor supernatant (Tumor-SN) was used in T cell proliferation assay and T cell proliferation was analyzed after 72 h by flow cytometry. Representative data of three independent experiments are shown. Bars represent mean \pm SD from duplicates. Significant differences were analyzed by one-way ANOVA including Bonferroni correction. P-values < 0.05 were considered significant.

Taking these considerations into account, the competitive TGF- β receptor 1 kinase inhibitor SD-208 was used for subsequent experiments. T cells were incubated with 10 μ M SD-208 for 2 h before addition of 6.25% tumor supernatant for further 72 h. As depicted in Figure 6-28, treatment with SD-208 significantly restored T cell proliferation in cultures exposed to either Panc02 or T110299 supernatant. Interestingly, the CD8⁺ T cell population was more affected than the CD4⁺ T cell population. While T cells exposed to supernatant of Panc02 cells regained 50% proliferation capacity with respect to CD8⁺ T cells and 20% for CD4⁺ T cells, the T cells exposed to T110299 tumor supernatant displayed approx. 70% recovered proliferation for CD8⁺ T cells and 30% for CD4⁺ T cells.

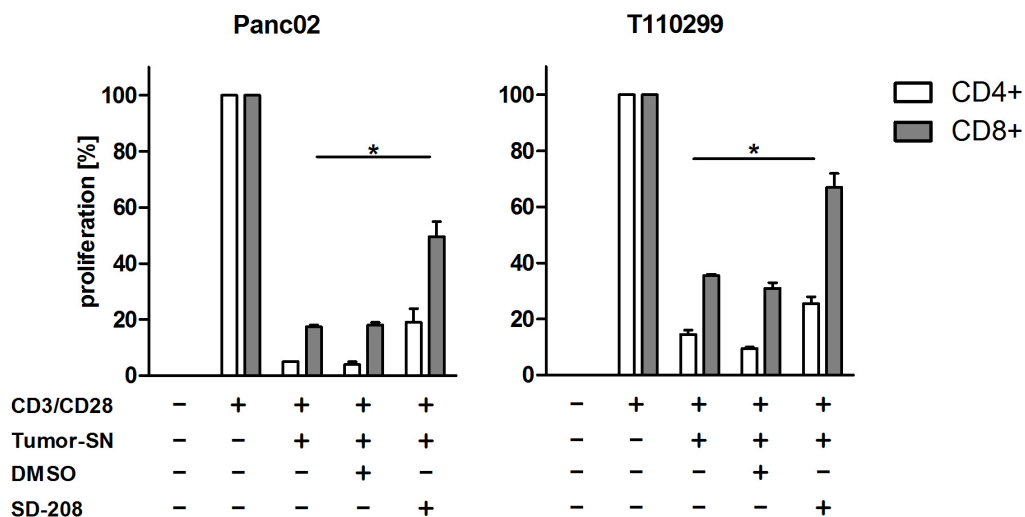


Figure 6-28: Inhibition of TGF- β -receptor signaling partially restores T cell proliferation.

Primarily CFSE labeled T cells from mouse spleen were stimulated with anti-CD3/CD28 Dynabeads and incubated in the absence or presence of 10 μ M of the TGF- β receptor 1 kinase inhibitor SD-208 for 2 h. DMSO served as vehicle control. Subsequently, 6.25% tumor supernatant (Tumor-SN) was added to the T cells for additional 72 h. Analysis of proliferation was performed by flow cytometry. Representative data of three independent experiments are shown. Bars represent mean \pm SD from duplicates. Significant differences were analyzed by one-way ANOVA including Bonferroni correction. P-values < 0.05 were considered significant.

6.3.7 Blocking IDO activity partially restores T cell proliferation

Although TGF- β signaling in T cells seems to be important for tumor-mediated inhibition of T cell proliferation, there are probably additional factors impacting T cell function, as evidenced by only partial recovery of T cell proliferation by SD-208.

Several studies have shown that IDO is highly expressed in pancreatic cancer (Lee et al., 2002, Johnson et al., 2009, Katz et al., 2008). To analyze if IDO could be an additional factor that negatively influences T cell proliferation in our experimental setting, Panc02 and T110299 cells were treated with the IDO inhibitor D-1-methyltryptophan (D-1-MT) before the supernatant was collected and added to T cells. As shown in Figure 6-29 A, T cells exposed to supernatant from D-1-MT treated Panc02 cells showed a significant increase of CD8⁺ T cell proliferation. In addition, inhibition of IDO revealed a trend for restoring T cell proliferation for T110299 cells, however this was statistically not significant (Figure 6-29 A). Interestingly, T cell proliferation could be further recovered when D-1-MT was added to the T cells together with the tumor supernatant (Figure 6-29 B). In this case, T cells regained approx. 90% proliferation capacity with respect to the CD8⁺ cells and 80% for the CD4⁺ cells for both PDAC cell lines, respectively. In addition, the blockade of IDO also protected T cells from undergoing apoptosis. T cells exposed to Panc02 supernatant showed significantly increased cell viability when treated with D-1-MT (Figure 6-29 C). D-1-MT treatment also increased T cell viability after exposure to T110299 supernatant. However, this effect was not statistically significant. Interestingly, T cells

upregulated expression of the death receptor Fas (CD95) after exposure to tumor supernatant (Figure 6-20 B). Of note, IDO inhibition by D-1-MT decreased Fas expression (Figure 6-29 D).

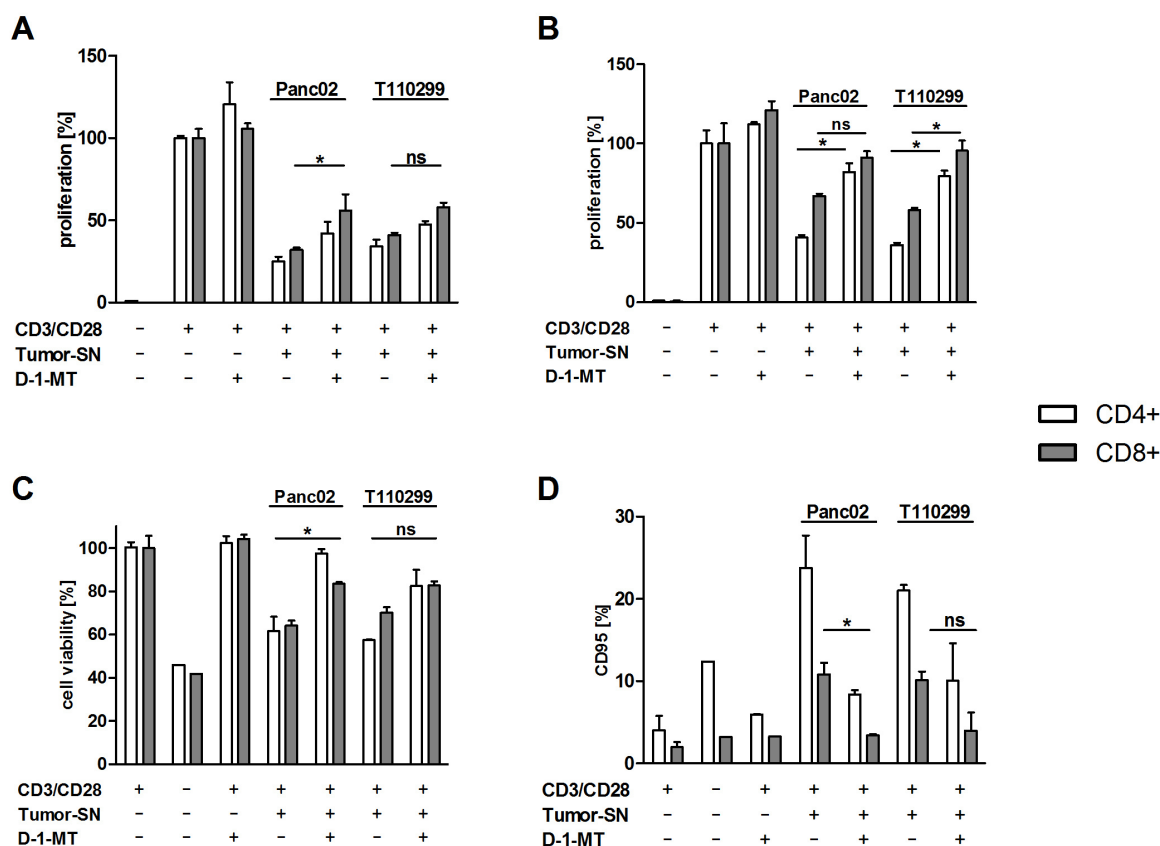


Figure 6-29: Inhibition of IDO rescues T cell from inhibition by PDAC cells.

A: Panc02 and T110299 cells were treated with the IDO inhibitor D-1-MT (2 mM) for 24 h. Afterwards, tumor supernatant (SN) was used for T cell proliferation assays. **B:** D-1-MT was added to T cells in a T cell proliferation assay together with 6.25% SN of Panc02 and T110299 cells. **C:** Cell viability of T cells was measured by Annexin V/PI staining 72 h after stimulation with CD3/CD28 beads in the absence or presence of 6.25% tumor SN and D-1-MT, respectively. **D:** T cell CD95 expression was measured 72 h after stimulation with CD3/CD28 beads in the absence or presence of 6.25% tumor SN and D-1-MT, respectively. Representative data of three independent experiments are shown. Bars represent mean \pm SD from duplicates. Significant differences were analyzed by one-way ANOVA including Bonferroni correction. P-values < 0.05 were considered significant.

These surprising results indicate that a factor in the tumor supernatant of Panc02 and T110299 cells induces IDO expression in T cells, which finally leads to tryptophan depletion and the production of kynurenine. Kynurenine are products of tryptophan metabolism produced by IDO, which inhibit protein biosynthesis and induce T cell apoptosis. To assess whether tumor supernatants of Panc02 and T110299 cells increase IDO expression in T cells, we performed qRT-PCR analysis. As shown in Figure 6-30, IFN- γ , a well-known stimulus mediating IDO up-regulation in tumor cells and antigen-presenting cells (Johnson et al.), induced to some extent IDO mRNA expression in CD4⁺ T cells, but not CD8⁺ T cells. In contrast, exposure to tumor supernatants induced pronounced up-regulation of IDO mRNA expression in both CD4⁺ as well as CD8⁺ T cells. T cell stimulation via CD3 and CD28 alone had no influence on IDO expression. These results indicate that a so far unidentified factor

secreted by PDAC cells potentially induces IDO expression in T cells, which might contribute to tumor-mediated immunosuppression in the tumor microenvironment.

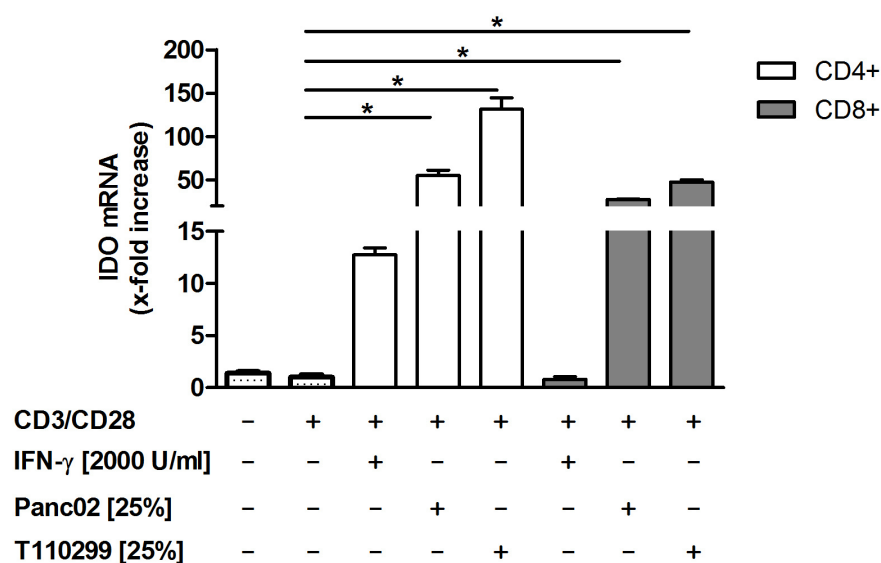


Figure 6-30: Induction of IDO mRNA expression in T cells after exposure to tumor supernatant from Panc02 and T110299 cells.

Freshly isolated CD4⁺ and CD8⁺ T cells from mouse spleen were incubated with or without tumor supernatant (25%) from Panc02 or T110299 cells or with IFN- γ (2000 U/ml) for 48 h in the presence of anti-CD3/CD28 beads. Cells were harvested for mRNA extraction and expression of IDO mRNA was analyzed by qRT-PCR. β -actin served as housekeeping gene. Representative data of three independent experiments are shown. Bars represent mean \pm SD from duplicates. Significant differences were analyzed by one-way ANOVA including Bonferroni correction. P-values < 0.05 were considered significant.

7 Discussion

7.1 T110299 cells generated from KPC tumors represent a valuable tool for studying PDAC

Pancreatic cancer research needs clinically relevant mouse tumor models. Since 1984, when Corbett et al. described the chemically induced Panc02 cell line, these cells have frequently been used to study pancreatic cancer biology and therapy *in vitro* and *in vivo* (Corbett et al., 1984). In 2003 and 2005, Hingorani et al. published the first GEMM for pancreatic cancer that reflects the human disease in many aspects (Hingorani et al., 2003, Hingorani et al., 2005). However, studies on these mouse models are laborious, time consuming and therefore not ideally suited for the study on novel therapeutic strategies at a large scale. In this respect, the transplantation of tumor cells in syngeneic animals, e.g. orthotopically into the pancreas, offers several advantages, such as better controlled tumor growth, the possibility to manipulate tumor cells *ex vivo* (e.g. transfection of the cells with specific antigens or constructs that can be used for *in vivo* imaging), and the availability of knock-out animals in order to study the contribution of specific immune-mediated mechanisms to therapy success. One option for generating tumor models that more closely reflect the human tumor biology is to generate cell lines from KPC mice. This study characterized four PDAC models with regard to tumor architecture (tumor cell differentiation, PanIN formation, stroma composition and blood vessel formation), T cell infiltration, and the expression pattern of selected immunosuppressive molecules like galectin-1 and IDO. The intention of these efforts was to identify the best suited preclinical models to investigate the interaction of tumor cells with the immune system as well as other local and systemic factors. A functional immune system is a prerequisite for the research on tumor cell interactions with cytotoxic T cells, regulatory T cells, tumor-associated macrophages, immune cell trafficking or the inflammatory stromal reaction. Furthermore, immune competent models are more convenient for therapy studies (Partecke et al., 2011).

Tumors from Panc02 cells revealed a poorly differentiated morphology with a sarcomatoid architecture and areas of necrosis, probably due to rapid and uncontrolled tumor growth. Partecke et al. previously described that Panc02 tumors have a sarcoma-like undifferentiated growth pattern, which is rarely found in humans (Partecke et al., 2011). In contrast, tumors from T110299 cells, which were originally derived from KPC mice, were moderate to well-differentiated and exhibited duct-like structures typical for adenocarcinoma. Similar results have been reported by Partecke et al., who used a cell line derived from a GEMM tumor carrying the *Kras*^{G12D} mutation with normal p53 expression (6606PDA) (Partecke et al., 2011). The morphology showed similarities to primary KPC tumors that were investigated in this study. Primary KPC tumors have an accelerated development of metastatic well-differentiated PDAC whereas KPfC tumors have an even shorter latency and survival rate,

compared to KPC mice (Mazur and Siveke, 2011, Hingorani et al., 2005). Tuveson et al. previously reported that the tumors from KPC mice bear a high analogy to human pancreatic cancer in many different aspects (histology, pathology, genetics, etc.) (Tuveson and Hingorani, 2005).

Immunohistochemistry studies revealed that Panc02 tumors express very little tumor stroma and, as expected, no PanIN lesions (poorly differentiated grade 3 tumor), as shown by Masson's Trichrome and Alcian Blue staining, respectively. This observation exposed a critical weakness of the Panc02 tumor model, as characteristics of human pancreatic cancers are (1) the high abundance of stroma (Chu et al., 2007, Mahadevan and Von Hoff, 2007) and (2) the establishment of adenocarcinomas from precursor lesions (Hruban et al., 2008). Both KPC and KPfC tumor models showed abundant stroma and PanIN lesions (well differentiated grade 1 tumors). Interestingly, T110299 tumors were also had lots of tumor stroma. KPC tumors displayed the papillary structure with many PanIN lesions at lower stages whereas KPfC tumors represented PanIN lesions at higher stages and more adenocarcinoma structures. In comparison, tumors from the T110299 cell line showed less mucin staining, but the areas resembling PanIN lesions were well detectable and indicated that the cell line contains cells with various differentiation grades.

In tumors, formation of blood vessels is an important factor for the supply with nutrients and oxygen and therefore promotes tumor progression. In pancreatic carcinoma, van der Zee et al. showed that tumor growth is less dependent on angiogenesis (van der Zee et al., 2011). In general, the vasculature in primary pancreatic cancer in both humans and mouse is sparse (Olive et al., 2009). Orthotopic tumors from the Panc02 and T110299 cell lines as well as both KPC tumor models revealed abundant blood vessel formation in the periphery of the tumor, but in central regions very few and only distorted blood vessels could be found. Some vessels could be noticed around PanIN lesions and adenocarcinoma structures. Olive et al. showed that in transplanted tumors, blood vessels arise in close proximity to neoplastic cells, leading to a dense vascularization in the periphery. In contrast, in KPC mice and human PDAC, blood vessels were widely spaced from cancer cells and the density of blood vessels was markedly decreased (Olive et al., 2009). These anatomical features contribute to a barrier for drug delivery in PDAC and to the creation of a hypoxic environment (Hidalgo and Von Hoff, 2012). Whether the leakiness of the vasculature and drug delivery into tumors differs between the different tumor models has to be investigated in further studies.

PDAC express a variety of cancer-associated antigens that can potentially be recognized by T cells. However, these T cells are often dysfunctional after migration to the tumor site. PDAC has been recognized for the development of immune escape mechanisms, like the down-regulation of MHC class I molecules and Fas receptor, the recruitment of Tregs and MDSC, the secretion of IL-10 and TGF- β , the induction of loss of CD3 ζ by T cells (thereby inactivating T cell signaling) and the

expression of Fas-ligand on tumor cells to induce apoptosis in cancer-infiltrating effector T cells (Kleeff et al., 2007, Lunardi et al., 2013). Contrary to KPC tumors, Panc02 and T110299 tumors were significantly more infiltrated with T cells both at the tumor margin as well as in central tumor regions. Several other groups reported that in PDAC progression, the infiltration with leukocytes, especially T cells and regulatory T cells, increases (Clark et al., 2007, Ryschich et al., 2005, Fukunaga et al., 2004, Bazhin et al., 2013, Shevchenko et al., 2013). Regulatory T cells can prevent an immune response against the tumor by competitive consumption of IL-2 and the induction of IL-10 and TGF- β (Zou, 2006). Shevchenko et al. demonstrated in an orthotopic Panc02 tumor model that these tumors were highly infiltrated with regulatory T cells with an effector/memory phenotype, suggesting their enhanced suppressive activity and higher proliferation capacity (Shevchenko et al., 2013). In KPC tumors, it is possible that T cells reach the tumor border attracted by the inflammatory milieu found in stroma, but due to the immunosuppressive milieu within the tumor and the fortress built by stromal components, only few T cells reach the central tumor regions. A predominant T cell clustering around preinvasive lesions has been observed (Clark et al., 2007). The high infiltration with CD3⁺ T cells in Panc02 tumors is largely attributed to regulatory T cells, reaching up to 40% of all T cells within the tumor (Jacobs et al., 2011). Similarly, T110299 tumors are infiltrated with regulatory T cells and far less with CD8⁺ T cells (data not shown). A possible reason for higher T cell infiltration in transplanted tumors may be seen in the inflammatory milieu created by injecting tumor cells, which causes a wound, due to the injection, and cell death at the injection site.

A possible explanation for the reduced numbers of tumor infiltrating T cells could be seen in apoptosis induction through the immunosuppressive milieu in pancreatic cancer. A likely candidate for inducing T cell apoptosis is Galectin-1 (Kovacs-Solyom et al., 2010, Banh et al., 2011). It has been described that galectin-1 in PDAC is expressed by activated PSCs, which are characterized by strong α -SMA expression (Tang et al., 2011, Xue et al., 2011). Activated PSCs are located adjacent to and surrounding cancer cells whereas in healthy pancreatic tissue PSCs remain in a quiescent state with no α -SMA expression. Galectin-1 is strongly expressed in activated PSCs which form a barricade between tumor and other stromal compartments (Tang et al., 2011). It was also shown that galectin-1 expression significantly increased from dysplastic pancreatic tissue to PDAC progression. This could also be observed in this study when comparing tumors from KPC and KPfC mice. KPfC tumors contain more adenocarcinoma structures correlating with enhanced galectin-1 and α -SMA protein expression in stroma. Tumors from the T110299 cell line also revealed a strong galectin-1 and α -SMA expression in stromal cells surrounding cancer cells. In contrast, galectin-1 was strongly expressed in Panc02 tumor cells. As stroma was virtually absent in Panc02 tumors, collagen and α -SMA staining was faint. Tang et al. described that few CD3⁺ T cells infiltrate in the parenchyma surrounding the tumor, correlating with galectin-1 staining in the mesenchymal cell population around the tumor. These observations, which are in line with this study, suggest that galectin-1 might comprise an

immunological barrier. Banh et al. and Kovás-Sólyom et al. reported that galectin-1 promotes T cell apoptosis, tumor growth and metastasis (Banh et al., 2011, Kovacs-Solyom et al., 2010). Galectin-1 may further contribute to the immunosuppressive microenvironment in PDAC by suppressing transendothelial migration of effector T cells to the tumor site (Yang et al., 2008, Cedeno-Laurent and Dimitroff, 2011, Toscano et al., 2007). On the one hand, Chen et al. found that lower expression levels of stromal galectin-1 in pancreatic cancer patients are a positive prognostic factor (Chen et al., 2012). On the other hand, overexpression of galectin-1 has been documented in many different tumor types, including breast carcinoma, hepatocellular carcinoma and oral squamous cell cancer, among others, and often correlated with tumor aggressiveness and metastatic phenotypes (Daroqui et al., 2007, Spano et al., 2010, Zhong et al., 2010).

Another immunosuppressive molecule that was investigated in this study is IDO. IDO was strongly expressed in Panc02 tumors but also in non-transformed acinus cells. Witkiewicz et al. reported that IDO is expressed in the cytoplasm of well-differentiated pancreatic adenocarcinomas from human cell lines but is not expressed in healthy pancreatic tissue (Witkiewicz et al., 2008). In a subsequent study, the same authors showed that IDO2 is equally overexpressed and an active target in pancreatic cancer (Witkiewicz et al., 2009). In T110299 and both KPC tumor models IDO was expressed in the cytoplasm of tumor cells, but was also found in some cells located in the stroma. As IDO is expressed by APCs in tumors, those cells might represent infiltrating APCs (Grohmann et al., 2003, Katz et al., 2008). Further studies are required to better define IDO expressing stromal cells in these tumor models.

In summary, the histological results suggest that the Panc02 tumor model differs substantially from the majority of human PDAC, whereas KPC models more closely reflect the situation found in human pancreatic cancer in regard to stroma production, tumor cell differentiation (including the presence of PanINs), as well as expression patterns of Galectin-1 and IDO. The orthotopic T110299 tumor model may be a valuable tool for the research on novel treatments for PDAC. Tumor growth is very reliable and homogeneous. In addition, tumor cell morphology, tumor stroma and the expression of immunosuppressive molecules closely resemble primary tumors in KPC mice, and thus the human disease.

7.2 Treatment with 5'ppp-modified siRNA targeting galectin-1 prolongs survival in the Panc02 tumor model

Pancreatic cancer is mostly diagnosed at an advanced stage. Therefore, surgical resection can be performed in only a small number of patients and even after resection, recurrence occurs in the majority of the patients. Although adjuvant treatment with both chemotherapy and radiation therapy

has been investigated demonstrating some improvements in disease-free and overall survival rates, new therapeutic approaches are urgently needed (Koido et al., 2011).

The aim of cancer immunotherapy is to activate the immune system for therapeutic benefit. Immune responses against viruses and tumors share common principles, such as T cell-mediated killing of target cells and immune evasion. A strategy for tumor immunotherapy could be to mimic a viral infection for boosting immunity against the tumor cells. In this study, a combination of two antiviral principles was used to treat experimental pancreatic cancer. Firstly, a sequence specific degradation of mRNA by RNAi; and secondly, the activation of the pattern recognition receptor RIG-I to initiate a type I IFN driven immune response. This study could confirm RIG-I receptor expression in PDAC cells (Ellermeier et al., 2013). Both murine cell lines, Panc02 and T110299, up-regulated RIG-I expression when stimulated with type I IFNs, but Panc02 cells were more sensitive in this respect. Upon RIG-I activation with ppp-RNA, Panc02 tumor cells secreted high levels of CXCL10, a chemokine attracting lymphocytes, and up-regulated IFN- β expression. In addition, the surface expression of MHC-I molecules was induced. Thus, intratumoral RIG-I activation has the potential to attract lymphocytes to the tumor site and to activate T_H1 cells and cytotoxic T cells for more efficient tumor cell killing. In contrast, T110299 cells transfected with ppp-RNA secreted lower levels of CXCL10 and no IFN- β and MHC-I up-regulation was observed. Moreover, the phosphorylation of the transcription factor IRF3 and the induction of apoptosis was seen in Panc02 but not T110299 cells, indicating that RIG-I signaling is defective in this cell line derived from KPC mice. Further studies are needed to assess whether RIG-I signaling is defective in all tumor cell lines derived from the KPC model, or whether this a unique feature of this particular cell line. This is an important issue regarding the choice of the best-suited tumor model for immunotherapy studies. Of note, all human PDAC cell lines tested so far do express functional RIG-I and undergo apoptosis in response to ppp-RNA treatment (Ellermeier et al., 2013).

Next, this study evaluated a novel bifunctional ppp-siRNA silencing galectin-1 for the treatment of murine pancreatic cancer. The treatment of Panc02 and T110299 tumor cells with ppp-Gal-1 revealed an efficient knockdown of galectin-1 expression reaching similar levels as an unmodified OH-Gal-1 siRNA. However, as described for the control ppp-RNA RIG-I mediated effects, such as IFN- β production, MHC-I up-regulation and apoptosis induction, were only observed in Panc02, but not T110299 cells.

Therefore, these *in vitro* results guided us to explore ppp-Gal-1 based immunotherapy in the Panc02 tumor model *in vivo*. Interestingly, in mice with Panc02 tumors galectin-1 serum levels correlated with tumor size, indicating that galectin-1 is tumor derived, or at least induced by the tumor. Disappointingly, the systemic treatment of these mice with OH-Gal-1 had no significant influence on galectin-1 expression in tumor tissue. A reason for this failure might be that the treatment was either

too short or, more likely, that RNA levels deposited at the tumor site were too low. New strategies optimizing siRNA delivery to the tumors are warranted and are the focus of future studies in our working group. However, galectin-1 serum levels decreased upon treatment, although statistical significance was not reached. Whether this decrease of galectin-1 levels reflects true RNAi-mediated silencing in the tumor or simply reduced viability of the tumor cells, which seem to be the main source of galectin-1 production in the Panc02 model, remains an open question. In the survival experiment the systemic treatment with OH-Gal-1 and ppp-Gal-1 included a total of six injections over the course of three weeks. The treatment with OH-Gal-1 showed no significant effect on tumor-specific survival (35 days) whereas ppp-Gal-1 extended median survival up to 49 days. Maybe even more importantly, 20% of the mice rejected their tumor and had no signs of residual tumor mass after an observation period of 100 days. Thus, ppp-Gal-1 appears to be a highly effective novel molecule for the treatment of murine pancreatic cancer. No significant toxicity was observed during treatment with ppp-Gal-1, indicative of a broad therapeutic window (data not shown). These results are in line with a previous report from our group in which systemic treatment with ppp-RNA targeting TGF- β induced effective tumor cell apoptosis *in vivo*, whereas normal pancreas or other organs showed no signs of histopathology (Ellermeier et al., 2013). A likely reason for low toxicity is the observation that tumor cells are highly susceptible to RIG-I mediated apoptosis whereas non-malignant cells are protected via Bcl-xL expression (Besch et al., 2009, Meng et al., 2013). Another possibility is an enhanced CD95 (Fas) expression of tumor cells exposed to ppp-RNA rendering them sensitive towards killing via Fas-FasL interaction by activated lymphocytes ((Meng et al., 2013) and own unpublished observations). A long-term survival of some of the ppp-Gal-1 treated mice is indicative that RIG-I-based treatment induces a tumor-specific adaptive immune response leading to efficient tumor control. In a follow-up study, our group could demonstrate that RIG-I activation induces immunogenic tumor cell death resulting in efficient antigen uptake and presentation by DCs. As a result, CD8⁺ T cells acquire a killing function leading to further antigen release in the tumor and thereby entertaining an anti-tumor immunity cycle (Düwell et al., manuscript submitted).

Together, these data suggest that treatment with ppp-Gal-1 is a new valuable strategy for immunotherapy of PDAC, deserving further evaluation, e.g. in the KPC tumor model. As galectin-1 is highly expressed in the tumor stroma of KPC mice, ppp-Gal-1 therapy may contribute to the reduction of tumor stroma. Tumor stroma has recently been identified as an interesting target for treatment of PDAC (Neesse et al., 2011). In this regard, it will be of interest to assess whether PSC are susceptible to RIG-I mediated apoptosis and the extent of PSC-mediated immune suppression. Further improvements of this ppp-siRNA strategy are urgently needed, such as a large-scale synthetic generation of the 5'ppp-modification to avoid *in vitro* transcription via the T7 polymerase and RNA formulation tools for more effective RNA delivery into the tumors. In addition, combination therapies

with chemotherapy are currently being investigated by our group for enhancing therapeutic efficacy of ppp-RNA-based immunotherapy.

7.3 Murine pancreatic cancer cells induce potent T cell inhibition via TGF- β and IDO

Several reports by independent groups have found that T cells infiltrating PDAC are dysfunctional through a variety of immunosuppressive mechanisms present in the tumor microenvironment (Kleeff et al., 2007, Lunardi et al., 2013). This study now shows that the proliferation of both CD4⁺ and CD8⁺ T cells was significantly inhibited through soluble factors present in the tumor supernatant of Panc02 and T110299 cell lines *in vitro*. T cell suppression was highly effective, since addition of as little as 1% of tumor supernatant to complete T cell media led to a 50% reduction of the T cell proliferative response mediated by CD3 and CD28 ligation. Naïve T cells also underwent apoptosis whereas effector functions, such as degranulation of cytotoxic CD8⁺ T cells, were not impaired. To characterize the mechanisms leading to T cell inhibition in PDAC, this study investigated different soluble or secreted factors that are capable of impairing T cell proliferation.

T cell homeostasis is critical for an intact immune system and is regulated by different mechanisms. Two naturally occurring “T cell brakes” are CTLA-4 and PD-1 expressed by T cells, which bind to B7-1 (CD80/CD86) and PD-L1 (CD274/B7-H1) on APCs, respectively (Chen and Flies, 2013, Butte et al., 2007). Freeman et al. reported that PD-L1 reduced T cell proliferation when co-immobilized on plastic beads with anti-CD3 mAb (Freeman et al., 2000). Latchman et al. found that PD-1/PD-L1 signals inhibited T cell proliferation by blocking cell cycle progression but not by increasing cell death (Latchman et al., 2001). Then again, others showed that PD-L1 can be expressed by cancer cells leading to apoptosis of activated T cells (Dong et al., 2002). The expression of PD-L1 on murine and human pancreatic cancer cell lines has been reported (Okudaira et al., 2009, Nomi et al., 2007). Notably, the expression of PD-L1 can be induced by IFN- γ , a cytokine thought to have anti-tumor activity. Frigola et al. identified a soluble form of PD-L1 in cell-supernatants of PD-L1-positive tumor cell lines that retains immunosuppressive activity (Frigola et al., 2011). The same group could demonstrate that soluble PD-L1 induced apoptosis in CD4⁺ and CD8⁺ T cells (Frigola et al., 2012). These observations prompted us to investigate the presence of soluble PD-L1 in tumor supernatant of Panc02 and T110299 cells. Both cell lines expressed PD-L1 on the cell surface and PD-L1 protein was found in the supernatants of the tumor cells. However, neutralizing PD-1 expressed on T cells using an anti-PD-1 mAb did not influence the T cell inhibitory effect mediated by tumor supernatants T cell proliferation, indicating that other mechanisms than the PD-1/PD-L1 axis are likely to be more important.

Immunosuppressive prostanoids, especially prostaglandins, are other possible tumor-derived factors leading to T cell inhibition. Prostanoids are generated by the enzymes cyclooxygenase 1 and 2 (COX1

and 2). COX1 is constitutively expressed by many cell types and plays an active role in colon carcinogenesis (Wu et al., 2009), while COX2 is usually induced and overexpressed in pancreatic cancers, possibly playing a role in tumor progression (Colby et al., 2008, Hill et al., 2012). Here, selective inhibitors for COX1 (SC-560) and COX2 (Celecoxibe) were used to treat pancreatic cancer cell lines before tumor supernatant was collected for T cell proliferation assays. Neither COX1 nor COX2 inhibition had a significant influence on the T cell suppressive effect of tumor supernatants, suggesting that prostanoids are not involved in this phenomenon.

A focus of this study was galectin-1, which can overwhelm T cell effector functions by modulation of effector T cell survival (Rubinstein et al., 2004). Perillo et al. and other groups showed that galectin-1 inhibits T cell activation, induces growth arrest and apoptosis of activated T cells, mainly T_H1 , T_H17 and $CD8^+$ T cells (Rabinovich et al., 2002, Perillo et al., 1995, Salatino et al., 2008, Kovacs-Solyom et al., 2010, Banh et al., 2011) and suppresses the secretion of pro-inflammatory cytokines (IL-2, TNF- α , IFN- γ) leading to a T_H2 cytokine profile (Rabinovich et al., 1999, Salatino et al., 2008). The induction of regulatory T cells is another mechanism how secreted galectin-1 promotes an immunosuppressive milieu in tumors (Ito et al., 2012, Garin et al., 2007). Galectin-1 is expressed in various cancer cell types like pancreatic cancer, breast cancer, glioma, colon carcinoma and thyroid carcinoma, but also in non-malignant cells, such as PSC (Satelli et al., 2008, Dalotto-Moreno et al., 2013, Xue et al., 2011, Chen et al., 2012). Immunohistochemistry demonstrated the expression of galectin-1 in both Panc02 and T110299 cell lines. Furthermore, the galectin-1 content in cell lysates and supernatants from both tumor cell lines supported the hypothesis that galectin-1 may be responsible for inducing T cell inhibition in the T cell proliferation assays. Surprisingly, neither silencing of galectin-1 via siRNA nor inhibition with β -lactose or TDG had a significant effect on T cell inhibition by tumor supernatants. These results are in contrast to reports by other groups which could show that galectin-1 silencing and inhibitors alter T cell inhibition (Dalotto-Moreno et al., 2013, Tang et al., 2011, Ito and Ralph, 2012, Ito et al., 2011). Based on these experiments one has to conclude that other factors present in the tumor supernatant of PDAC cells are far more effective T cell suppressors than galectin-1. In contrast, these *in vitro* experiments were not designed to rule out a role for galectin-1 in T cell inhibition at the tumor site *in vivo*, as induction of T cell apoptosis may require intimate cell-cell contact between tumor cells and T cells for translocation of tumor cell-bound galectin-1 to T cells (Kovacs-Solyom et al., 2010).

Our group recently reported that murine pancreatic cancer cells produce high levels of TGF- β and that serum levels were significantly increased in Panc02-tumor-bearing mice (Ellermeier et al., 2013). TGF- β is well known for causing immunosuppression by inducing (1) regulatory T cells from $CD4^+$ T cells and (2) apoptosis in T effector cells, (3) inhibiting cytokine production of cytotoxic T cells and (4) down-regulating IL-2R on T cells (de Visser and Kast, 1999, Rubtsov and Rudensky, 2007). Thus,

TGF- β is a likely candidate for mediating the observed T cell suppression in proliferation assays. To investigate this, TGF- β_1 was transiently silenced via siRNA in tumor cells. However, TGF- β_1 silencing did not restore T cell proliferation. Possible explanations could be an insufficient silencing activity of the siRNA (50-80%) or that other isoforms of TGF- β (e.g. TGF- β_2) are compensating for reduced TGF- β_1 levels. To rule these possibilities out, the small molecule inhibitor SD-208 was used in T cell proliferation assays. SD-208 is a potent 2,4-disubstituted pteridine, ATP-competitive TGF- β -RII kinase inhibitor that blocks the biological effects of both TGF- β_1 and TGF- β_2 (Uhl et al., 2004). Gaspar et al. previously demonstrated that SD-208 blocks TGF- β dependent Smad2 phosphorylation and expression of TGF- β inducible proteins in pancreatic cancer cells, leading to reduced tumor growth and decreased incidence of metastasis (Gaspar et al., 2007). Interestingly, T cell proliferation was significantly restored when TGF- β signaling was blocked in T cells by SD-208. The T cells also secreted more pro-inflammatory cytokines, such as IFN- γ (data not shown), in line with observations made by Uhl et al. (Uhl et al., 2004). Thus, SD-208 treatment has potential for rescuing T cell proliferation in pancreatic cancer. Nonetheless, T cell proliferation was only partially restored by SD-208, suggesting that other factors in tumor supernatant significantly contribute to T cell inhibition.

Another potentially interesting factor leading to T cell inhibition is IDO. IDO is highly expressed in pancreatic cancer and its activity can be further induced by IFN- γ (Lee et al., 2002, Johnson et al., 2009, Katz et al., 2008). To investigate the contribution of IDO in regard to T cell inhibition, 1-methyl-tryptophan (1-MT), a specific, competitive inhibitor of IDO, was used. 1-MT had been applied in many studies to reveal IDO-mediated effects both *in vitro* and *in vivo* (Johnson et al., 2009). Here the D-isomer was chosen because it is more effective in reversing IDO-mediated suppression of effector T cell responses *in vitro* and slowing the growth of transplantable tumors in mice via T cell-dependent mechanisms (Johnson et al., 2009). This study revealed that tumor supernatant from Panc02 and T110299 cell lines induced IDO mRNA expression in T cells and that D-1-MT significantly restored T cell proliferation. Interestingly, the inhibitory effect was more pronounced when D-1-MT was given to T cells as compared to the tumor cells, indicating that T cell-derived or soluble tumor-derived IDO was mainly responsible for the inhibitory effect on T cell proliferation. Furthermore, T cell viability significantly increased when IDO was blocked in T cells. Remarkably, this effect correlated with reduced Fas (CD95) expression on cytotoxic T cells. These results point towards a factor in the tumor supernatant of Panc02 and T110299 cells that induces IDO expression in T cells, which finally leads to apoptosis of T cells in an autocrine or paracrine manner. IDO enzyme activity leads to the production of kynurenine as a result of tryptophan metabolism. N-formyl-kynurenine is hydrolyzed to kynurenine, which inhibits protein biosynthesis and induces T cell apoptosis (Mellor and Munn, 1999). Known inducers of IDO are prostaglandin E2 (PGE-2) (Muller and Prendergast, 2007), IFN- γ (Taylor and Feng, 1991), LPS (TLR4 ligand), CpG ODN (TLR9 ligand) (Johnson et al., 2009) and TGF- β (Yuan et al., 1998, Fallarino et al., 2012). PGE-2 is produced by COX2; as

Celecoxibe had no effect on T cell inhibition, it is unlikely that PGE-2 is the inducer of IDO expression in T cells. INF- γ can also be ruled out as pancreatic tumor cells do not express this T cell derived cytokine. Similarly, TLR ligands released by tumor cells are also unlikely in this regard, but were not ruled out in this study. Finally, TGF- β has been shown to influence IDO activity. Fallarino et al. reviewed the interaction of IDO and TGF- β concluding that IDO responds to TGF- β by regulating gene transcription thereby amplifying its expression and maintaining a TGF- β -dominated environment (Fallarino et al., 2012). Thus, tumor derived TGF- β (and possibly other secreted factors) may induce IDO expression in T cells, thereby leading to autointoxication of T cells by kynurenine and subsequently T cell apoptosis. The blocking of TGF- β signaling by SD-208 may intervene here to stop amplification of IDO expression in T cells, thus rescuing T cells from apoptosis. This hypothesis has to be investigated in further experiments, which are currently conducted in our working group. Combinatorial therapy with SD-208 and D-1-MT may be a promising treatment strategy for pancreatic cancer that deserves further investigation in preclinical models of PDAC.

7.4 Conclusion and perspectives

This study provides evidence that the T110299 model, which is derived from the KPC tumor model, shares many histological features with both spontaneous tumors arising in KPC mice and human tumors. Especially the typical appearance of glandular structures resembling adenocarcinoma, the pronounced stroma production and poor vascularization in the center of the tumor make this cell line a valuable tool to study novel therapies for PDAC in which the tumor stroma is a therapeutic target. In addition, IDO and TGF- β expression by the tumor cells, and galectin-1 expression in PSC in the stroma make this model ideally suited to investigate immunosuppressive mechanisms, which are also active in human PDAC. However, defective RIG-I signaling in T110299 cells is an obstacle for studying RIG-I-based immunotherapies in this model. Here, the Panc02 tumor model appears to be the more suitable option, as this cell line expresses functional RIG, which is also the case in all tested human PDAC cell lines (Ellermeier et al., 2013). Interestingly, recent studies in our group could demonstrate that T110299 cells express functional MDA-5, another cytosolic helicase involved in viral recognition and immune signaling. MDA-5 ligands induced type I IFN production and mediated tumor cell apoptosis (Hannes Hölz, personal communication). Therefore, therapy with MDA-5 ligands could be investigated in this mouse model. Taken together, a detailed understanding of morphological and biological characteristics of the different tumor models is vital for the choice of the right preclinical model in order to address scientific questions, such as therapy response or immune suppressive mechanisms.

For immunotherapy of PDAC a bifunctional siRNA combining RNAi-mediated gene silencing of galectin-1 with ppp-RNA-mediated RIG-I activation (ppp-Gal-1) was designed, produced by *in vitro* transcription using the T7 polymerase and evaluated in the orthotopic Panc02 tumor model. The dual

activities of this molecule were confirmed *in vitro*, leading to reduced galectin-1 expression, production of CXCL10 and IFN- β , MHC-I up-regulation and apoptosis of tumor cells. The treatment of mice with orthotopic pancreatic tumors with ppp-Gal-1 significantly prolonged survival, as compared to unmodified OH-Gal-1 or control RNA. In addition, 20% of the mice rejected their tumors completely leading to long-term tumor control. Thus, 5'ppp-modified siRNA is a promising treatment strategy for PDAC, as previously shown for a ppp-siRNA targeting the immunosuppressive molecule TGF- β_1 or glutaminase, an enzyme critically involved in tumor cell metabolism and ROS elimination (Ellermeier et al., 2013, Meng et al., 2013). To push this novel strategy into the realm of clinical testing, further improvements have to be achieved. These include identifying delivery systems for optimal RNA cargo deposition in the tumor, optimal dosing and injection routes, and synthetic generation of 5'ppp-modified siRNA on a large scale under GMP conditions. GEMM, such as the KPC model, and derived cell lines may be helpful for future developments.

Pancreatic tumor cells employ multiple mechanisms for suppression of T cell responses. This study identified TGF- β and IDO as two potent and drugable inhibitors of T cell proliferation. Supernatants of PDAC cells effectively blocked T cell proliferation induced by CD3 and CD28 triggering. This could be partially prevented by the inhibition of TGF- β receptor signaling via SD-208 or by blocking IDO activity with D-1-MT. An interesting observation was that tumor supernatant induced pronounced up-regulation of IDO mRNA expression in T cells. Furthermore, blocking IDO activity in T cells appeared to be more effective than blocking IDO in tumor cells. This leads to a new hypothesis that factors secreted by the tumor cells (such as TGF- β) induce IDO expression in T cells, which in turn leads to autointoxication of the T cells via kynurenine production and eventually T cell apoptosis. This suicide or paracrine-mediated fratricide can potentially be prevented by either blocking TGF- β receptors, IDO or both. Nonetheless, this hypothesis needs to be confirmed in relevant *in vitro* and *in vivo* systems.

8 References

- Abbas, A.K., Lichtman, A.H. & Pillai, S. 2007. *Cellular and molecular immunology*, Philadelphia, Saunders Elsevier.
- Ambros, V. 2004. The functions of animal microRNAs. *Nature*, 431, 350-5.
- Andersen, M.H., Schrama, D., Thor Straten, P. & Becker, J.C. 2006. Cytotoxic T cells. *J Invest Dermatol*, 126, 32-41.
- Apte, M.V., Haber, P.S., Applegate, T.L., Norton, I.D., McCaughan, G.W., *et al.* 1998. Periacinar stellate shaped cells in rat pancreas: identification, isolation, and culture. *Gut*, 43, 128-33.
- Ball, H.J., Sanchez-Perez, A., Weiser, S., Austin, C.J., Astelbauer, F., *et al.* 2007. Characterization of an indoleamine 2,3-dioxygenase-like protein found in humans and mice. *Gene*, 396, 203-13.
- Banh, A., Zhang, J., Cao, H., Bouley, D.M., Kwok, S., *et al.* 2011. Tumor galectin-1 mediates tumor growth and metastasis through regulation of T-cell apoptosis. *Cancer Res*, 71, 4423-31.
- Bardeesy, N. & DePinho, R.A. 2002. Pancreatic cancer biology and genetics. *Nat Rev Cancer*, 2, 897-909.
- Bayne, L.J., Beatty, G.L., Jhala, N., Clark, C.E., Rhim, A.D., Stanger, B.Z. & Vonderheide, R.H. 2012. Tumor-derived granulocyte-macrophage colony-stimulating factor regulates myeloid inflammation and T cell immunity in pancreatic cancer. *Cancer Cell*, 21, 822-35.
- Bazhin, A.V., Shevchenko, I., Umansky, V., Werner, J. & Karakhanova, S. 2013. Two immune faces of pancreatic adenocarcinoma: possible implication for immunotherapy. *Cancer Immunol Immunother*.
- Becker, J.C., Andersen, M.H., Schrama, D. & Thor Straten, P. 2013. Immune-suppressive properties of the tumor microenvironment. *Cancer Immunol Immunother*, 62, 1137-48.
- Besch, R., Poeck, H., Hohenauer, T., Senft, D., Hacker, G., *et al.* 2009. Proapoptotic signaling induced by RIG-I and MDA-5 results in type I interferon-independent apoptosis in human melanoma cells. *J Clin Invest*, 119, 2399-411.
- Bharadwaj, U., Li, M., Zhang, R., Chen, C. & Yao, Q. 2007. Elevated interleukin-6 and G-CSF in human pancreatic cancer cell conditioned medium suppress dendritic cell differentiation and activation. *Cancer Res*, 67, 5479-88.
- Bonifaz, L.C., Bonnyay, D.P., Charalambous, A., Darguste, D.I., Fujii, S., *et al.* 2004. In vivo targeting of antigens to maturing dendritic cells via the DEC-205 receptor improves T cell vaccination. *J Exp Med*, 199, 815-24.
- Bronte, V., Serafini, P., Mazzoni, A., Segal, D.M. & Zanovello, P. 2003. L-arginine metabolism in myeloid cells controls T-lymphocyte functions. *Trends Immunol*, 24, 302-6.
- Burnet, F.M. 1970. The concept of immunological surveillance. *Prog Exp Tumor Res*, 13, 1-27.
- Burris, H.A., 3rd, Moore, M.J., Andersen, J., Green, M.R., Rothenberg, M.L., *et al.* 1997. Improvements in survival and clinical benefit with gemcitabine as first-line therapy for patients with advanced pancreas cancer: a randomized trial. *J Clin Oncol*, 15, 2403-13.
- Butte, M.J., Keir, M.E., Phamduy, T.B., Sharpe, A.H. & Freeman, G.J. 2007. Programmed death-1 ligand 1 interacts specifically with the B7-1 costimulatory molecule to inhibit T cell responses. *Immunity*, 27, 111-22.
- Cao, X. 2009. New DNA-sensing pathway feeds RIG-I with RNA. *Nat Immunol*, 10, 1049-51.
- Cedeno-Laurent, F. & Dimitroff, C.J. 2011. Galectin-1 research in T cell immunity: Past, present and future. *Clin Immunol*.
- Cedeno-Laurent, F., Opperman, M., Barthel, S.R., Kuchroo, V.K. & Dimitroff, C.J. 2012. Galectin-1 triggers an immunoregulatory signature in th cells functionally defined by IL-10 expression. *J Immunol*, 188, 3127-37.
- Chen, D.S. & Mellman, I. 2013. Oncology meets immunology: the cancer-immunity cycle. *Immunity*, 39, 1-10.
- Chen, L. & Flies, D.B. 2013. Molecular mechanisms of T cell co-stimulation and co-inhibition. *Nat Rev Immunol*, 13, 227-42.
- Chen, R., Pan, S., Ottenhof, N.A., de Wilde, R.F., Wolfgang, C.L., *et al.* 2012. Stromal galectin-1 expression is associated with long-term survival in resectable pancreatic ductal adenocarcinoma. *Cancer Biol Ther*, 13, 899-907.

- Chu, G.C., Kimmelman, A.C., Hezel, A.F. & DePinho, R.A. 2007. Stromal biology of pancreatic cancer. *J Cell Biochem*, 101, 887-907.
- Clark, C.E., Beatty, G.L. & Vonderheide, R.H. 2009. Immunosurveillance of pancreatic adenocarcinoma: insights from genetically engineered mouse models of cancer. *Cancer Lett*, 279, 1-7.
- Clark, C.E., Hingorani, S.R., Mick, R., Combs, C., Tuveson, D.A. & Vonderheide, R.H. 2007. Dynamics of the immune reaction to pancreatic cancer from inception to invasion. *Cancer Res*, 67, 9518-27.
- Colby, J.K., Klein, R.D., McArthur, M.J., Conti, C.J., Kiguchi, K., *et al.* 2008. Progressive metaplastic and dysplastic changes in mouse pancreas induced by cyclooxygenase-2 overexpression. *Neoplasia*, 10, 782-96.
- Conroy, T., Desseigne, F., Ychou, M., Bouche, O., Guimbaud, R., *et al.* 2011. FOLFIRINOX versus gemcitabine for metastatic pancreatic cancer. *N Engl J Med*, 364, 1817-25.
- Corbett, T.H., Roberts, B.J., Leopold, W.R., Peckham, J.C., Wilkoff, L.J., Griswold, D.P., Jr. & Schabel, F.M., Jr. 1984. Induction and chemotherapeutic response of two transplantable ductal adenocarcinomas of the pancreas in C57BL/6 mice. *Cancer Res*, 44, 717-26.
- Cubilla, A.L. & Fitzgerald, P.J. 1984. *Tumors of the exocrine pancreas*, Washington, D.C., Armed Forces Inst. of Pathology.
- Curiel, T.J., Coukos, G., Zou, L., Alvarez, X., Cheng, P., *et al.* 2004. Specific recruitment of regulatory T cells in ovarian carcinoma fosters immune privilege and predicts reduced survival. *Nat Med*, 10, 942-9.
- Dalotto-Moreno, T., Croci, D.O., Cerliani, J.P., Martinez-Allo, V.C., Dergan-Dylon, S., *et al.* 2013. Targeting galectin-1 overcomes breast cancer-associated immunosuppression and prevents metastatic disease. *Cancer Res*, 73, 1107-17.
- Daroqui, C.M., Ilarregui, J.M., Rubinstein, N., Salatino, M., Toscano, M.A., *et al.* 2007. Regulation of galectin-1 expression by transforming growth factor beta1 in metastatic mammary adenocarcinoma cells: implications for tumor-immune escape. *Cancer Immunol Immunother*, 56, 491-9.
- Davis, I.D., Chen, W., Jackson, H., Parente, P., Shackleton, M., *et al.* 2004. Recombinant NY-ESO-1 protein with ISCOMATRIX adjuvant induces broad integrated antibody and CD4(+) and CD8(+) T cell responses in humans. *Proc Natl Acad Sci U S A*, 101, 10697-702.
- de Visser, K.E. & Kast, W.M. 1999. Effects of TGF-beta on the immune system: implications for cancer immunotherapy. *Leukemia*, 13, 1188-99.
- Diamond, M.S., Kinder, M., Matsushita, H., Mashayekhi, M., Dunn, G.P., *et al.* 2011. Type I interferon is selectively required by dendritic cells for immune rejection of tumors. *J Exp Med*, 208, 1989-2003.
- Dodson, L.F., Hawkins, W.G. & Goedegebuure, P. 2011. Potential targets for pancreatic cancer immunotherapeutics. *Immunotherapy*, 3, 517-37.
- Dong, H., Strome, S.E., Salomao, D.R., Tamura, H., Hirano, F., *et al.* 2002. Tumor-associated B7-H1 promotes T-cell apoptosis: a potential mechanism of immune evasion. *Nat Med*, 8, 793-800.
- Elbashir, S.M., Harborth, J., Lendeckel, W., Yalcin, A., Weber, K. & Tuschl, T. 2001. Duplexes of 21-nucleotide RNAs mediate RNA interference in cultured mammalian cells. *Nature*, 411, 494-8.
- Ellenrieder, V., Alber, B., Lacher, U., Hendler, S.F., Menke, A., *et al.* 2000. Role of MT-MMPs and MMP-2 in pancreatic cancer progression. *Int J Cancer*, 85, 14-20.
- Ellermeier, J., Wei, J., Duester, P., Hoves, S., Stieg, M.R., *et al.* 2013. Therapeutic efficacy of bifunctional siRNA combining TGF-beta1 silencing with RIG-I activation in pancreatic cancer. *Cancer Res*, 73, 1709-20.
- Fallarino, F., Grohmann, U., Hwang, K.W., Orabona, C., Vacca, C., *et al.* 2003. Modulation of tryptophan catabolism by regulatory T cells. *Nat Immunol*, 4, 1206-12.
- Fallarino, F., Grohmann, U. & Puccetti, P. 2012. Indoleamine 2,3-dioxygenase: from catalyst to signaling function. *Eur J Immunol*, 42, 1932-7.
- Fallarino, F., Grohmann, U., Vacca, C., Bianchi, R., Orabona, C., *et al.* 2002. T cell apoptosis by tryptophan catabolism. *Cell Death Differ*, 9, 1069-77.
- Feig, C., Gopinathan, A., Nesses, A., Chan, D.S., Cook, N. & Tuveson, D.A. 2012. The pancreas cancer microenvironment. *Clin Cancer Res*, 18, 4266-76.

- Freeman, G.J., Long, A.J., Iwai, Y., Bourque, K., Chernova, T., *et al.* 2000. Engagement of the PD-1 immunoinhibitory receptor by a novel B7 family member leads to negative regulation of lymphocyte activation. *J Exp Med*, 192, 1027-34.
- Frigola, X., Inman, B.A., Krco, C.J., Liu, X., Harrington, S.M., *et al.* 2012. Soluble B7-H1: differences in production between dendritic cells and T cells. *Immunol Lett*, 142, 78-82.
- Frigola, X., Inman, B.A., Lohse, C.M., Krco, C.J., Chevillat, J.C., *et al.* 2011. Identification of a soluble form of B7-H1 that retains immunosuppressive activity and is associated with aggressive renal cell carcinoma. *Clin Cancer Res*, 17, 1915-23.
- Fuertes, M.B., Kacha, A.K., Kline, J., Woo, S.R., Kranz, D.M., Murphy, K.M. & Gajewski, T.F. 2011. Host type I IFN signals are required for antitumor CD8+ T cell responses through CD8 α + dendritic cells. *J Exp Med*, 208, 2005-16.
- Fukunaga, A., Miyamoto, M., Cho, Y., Murakami, S., Kawarada, Y., *et al.* 2004. CD8+ tumor-infiltrating lymphocytes together with CD4+ tumor-infiltrating lymphocytes and dendritic cells improve the prognosis of patients with pancreatic adenocarcinoma. *Pancreas*, 28, e26-31.
- Gabrilovich, D.I., Ostrand-Rosenberg, S. & Bronte, V. 2012. Coordinated regulation of myeloid cells by tumours. *Nat Rev Immunol*, 12, 253-68.
- Gabrilovich, D.I., Velders, M.P., Sotomayor, E.M. & Kast, W.M. 2001. Mechanism of immune dysfunction in cancer mediated by immature Gr-1+ myeloid cells. *J Immunol*, 166, 5398-406.
- Garbe, A.I., Vermeer, B., Gamrekelashvili, J., von Wasielewski, R., Greten, F.R., *et al.* 2006. Genetically induced pancreatic adenocarcinoma is highly immunogenic and causes spontaneous tumor-specific immune responses. *Cancer Res*, 66, 508-16.
- Garin, M.I., Chu, C.C., Golshayan, D., Cernuda-Morollon, E., Wait, R. & Lechler, R.I. 2007. Galectin-1: a key effector of regulation mediated by CD4+CD25+ T cells. *Blood*, 109, 2058-65.
- Gaspar, N.J., Li, L., Kapoun, A.M., Medicherla, S., Reddy, M., *et al.* 2007. Inhibition of transforming growth factor beta signaling reduces pancreatic adenocarcinoma growth and invasiveness. *Mol Pharmacol*, 72, 152-61.
- Gaudernack, G. 2006. Prospects for vaccine therapy for pancreatic cancer. *Best Pract Res Clin Gastroenterol*, 20, 299-314.
- Godin-Ethier, J., Hanafi, L.A., Piccirillo, C.A. & Lapointe, R. 2011. Indoleamine 2,3-dioxygenase expression in human cancers: clinical and immunologic perspectives. *Clin Cancer Res*, 17, 6985-91.
- Grohmann, U., Fallarino, F. & Puccetti, P. 2003. Tolerance, DCs and tryptophan: much ado about IDO. *Trends Immunol*, 24, 242-8.
- Hanahan, D. & Weinberg, R.A. 2000. The hallmarks of cancer. *Cell*, 100, 57-70.
- Herrerros-Villanueva, M., Hijona, E., Cosme, A. & Bujanda, L. 2012. Mouse models of pancreatic cancer. *World J Gastroenterol*, 18, 1286-94.
- Hidalgo, M. 2010. Pancreatic cancer. *N Engl J Med*, 362, 1605-17.
- Hidalgo, M. & Von Hoff, D.D. 2012. Translational therapeutic opportunities in ductal adenocarcinoma of the pancreas. *Clin Cancer Res*, 18, 4249-56.
- Hill, R., Li, Y., Tran, L.M., Dry, S., Calvopina, J.H., *et al.* 2012. Cell intrinsic role of COX-2 in pancreatic cancer development. *Mol Cancer Ther*, 11, 2127-37.
- Hingorani, S.R., Petricoin, E.F., Maitra, A., Rajapakse, V., King, C., *et al.* 2003. Preinvasive and invasive ductal pancreatic cancer and its early detection in the mouse. *Cancer Cell*, 4, 437-50.
- Hingorani, S.R., Wang, L., Multani, A.S., Combs, C., Deramaudt, T.B., *et al.* 2005. Trp53R172H and KrasG12D cooperate to promote chromosomal instability and widely metastatic pancreatic ductal adenocarcinoma in mice. *Cancer Cell*, 7, 469-83.
- Hiraoka, N., Onozato, K., Kosuge, T. & Hirohashi, S. 2006. Prevalence of FOXP3+ regulatory T cells increases during the progression of pancreatic ductal adenocarcinoma and its premalignant lesions. *Clin Cancer Res*, 12, 5423-34.
- Hornung, V., Ellegast, J., Kim, S., Brzozka, K., Jung, A., *et al.* 2006. 5'-Triphosphate RNA is the ligand for RIG-I. *Science*, 314, 994-7.
- Hornung, V., Guenther-Biller, M., Bourquin, C., Ablasser, A., Schlee, M., *et al.* 2005. Sequence-specific potent induction of IFN- α by short interfering RNA in plasmacytoid dendritic cells through TLR7. *Nat Med*, 11, 263-70.

- Howlader N, N.A., Krapcho M, Garshell J, Neyman N, Altekruse SF, Kosary CL, Yu M, Ruhl J, Tatalovich Z, Cho H, Mariotto A, Lewis DR, Chen HS, Feuer EJ, Cronin KA. 1975-2010. *SEER Cancer Statistics Factsheets: Pancreas Cancer*. National Cancer Institute. Bethesda, MD [Online]. Available: <http://seer.cancer.gov/statfacts/html/pancreas.html>.
- Hruban, R.H., Maitra, A. & Goggins, M. 2008. Update on pancreatic intraepithelial neoplasia. *Int J Clin Exp Pathol*, 1, 306-16.
- Ikemoto, T., Shimada, M., Komatsu, M., Yamada, S., Saito, Y., *et al.* 2013. Indoleamine 2,3-dioxygenase affects the aggressiveness of intraductal papillary mucinous neoplasms through Foxp3+CD4+CD25+ T cells in peripheral blood. *Pancreas*, 42, 130-4.
- Iovanna, J., Mallmann, M.C., Goncalves, A., Turrini, O. & Dagorn, J.C. 2012. Current knowledge on pancreatic cancer. *Front Oncol*, 2, 6.
- Ito, K. & Ralph, S.J. 2012. Inhibiting galectin-1 reduces murine lung metastasis with increased CD4(+) and CD8 (+) T cells and reduced cancer cell adherence. *Clin Exp Metastasis*.
- Ito, K., Scott, S.A., Cutler, S., Dong, L.F., Neuzil, J., Blanchard, H. & Ralph, S.J. 2011. Thiodigalactoside inhibits murine cancers by concurrently blocking effects of galectin-1 on immune dysregulation, angiogenesis and protection against oxidative stress. *Angiogenesis*, 14, 293-307.
- Ito, K., Stannard, K., Gabutero, E., Clark, A.M., Neo, S.Y., *et al.* 2012. Galectin-1 as a potent target for cancer therapy: role in the tumor microenvironment. *Cancer Metastasis Rev*, 31, 763-78.
- Jacobs, C., Duester, P., Heckelsmiller, K., Wei, J., Bauernfeind, F., *et al.* 2011. An ISCOM vaccine combined with a TLR9 agonist breaks immune evasion mediated by regulatory T cells in an orthotopic model of pancreatic carcinoma. *Int J Cancer*, 128, 897-907.
- Jaffee, E.M., Abrams, R., Cameron, J., Donehower, R., Duerr, M., *et al.* 1998. A phase I clinical trial of lethally irradiated allogeneic pancreatic tumor cells transfected with the GM-CSF gene for the treatment of pancreatic adenocarcinoma. *Hum Gene Ther*, 9, 1951-71.
- Janeway, C.A., Jr. & Medzhitov, R. 2002. Innate immune recognition. *Annu Rev Immunol*, 20, 197-216.
- Jarboe, J. & Saif, M.W. 2013. First line therapy for metastatic pancreatic cancer. *JOP*, 14, 340-3.
- Johnson, B.A., 3rd, Baban, B. & Mellor, A.L. 2009. Targeting the immunoregulatory indoleamine 2,3-dioxygenase pathway in immunotherapy. *Immunotherapy*, 1, 645-61.
- Katz, J.B., Muller, A.J. & Prendergast, G.C. 2008. Indoleamine 2,3-dioxygenase in T-cell tolerance and tumoral immune escape. *Immunol Rev*, 222, 206-21.
- Kleeff, J., Beckhove, P., Esposito, I., Herzig, S., Huber, P.E., Lohr, J.M. & Friess, H. 2007. Pancreatic cancer microenvironment. *Int J Cancer*, 121, 699-705.
- Koido, S., Homma, S., Takahara, A., Namiki, Y., Tsukinaga, S., *et al.* 2011. Current immunotherapeutic approaches in pancreatic cancer. *Clin Dev Immunol*, 2011, 267539.
- Kovacs-Solyom, F., Blasko, A., Fajka-Boja, R., Katona, R.L., Vegh, L., *et al.* 2010. Mechanism of tumor cell-induced T-cell apoptosis mediated by galectin-1. *Immunol Lett*, 127, 108-18.
- Latchman, Y., Wood, C.R., Chernova, T., Chaudhary, D., Borde, M., *et al.* 2001. PD-L2 is a second ligand for PD-1 and inhibits T cell activation. *Nat Immunol*, 2, 261-8.
- Lee, G.K., Park, H.J., Macleod, M., Chandler, P., Munn, D.H. & Mellor, A.L. 2002. Tryptophan deprivation sensitizes activated T cells to apoptosis prior to cell division. *Immunology*, 107, 452-60.
- Liu, K. & Nussenzweig, M.C. 2010. Origin and development of dendritic cells. *Immunol Rev*, 234, 45-54.
- Liyanage, U.K., Moore, T.T., Joo, H.G., Tanaka, Y., Herrmann, V., *et al.* 2002. Prevalence of regulatory T cells is increased in peripheral blood and tumor microenvironment of patients with pancreas or breast adenocarcinoma. *J Immunol*, 169, 2756-61.
- Loose, D. & Van de Wiele, C. 2009. The immune system and cancer. *Cancer Biother Radiopharm*, 24, 369-76.
- Lunardi, S., Muschel, R.J. & Brunner, T.B. 2013. The Stromal Compartments in Pancreatic Cancer: Are There Any Therapeutic Targets? *Cancer Lett*.
- Mahadevan, D. & Von Hoff, D.D. 2007. Tumor-stroma interactions in pancreatic ductal adenocarcinoma. *Mol Cancer Ther*, 6, 1186-97.
- Maitra, A. & Hruban, R.H. 2008. Pancreatic cancer. *Annu Rev Pathol*, 3, 157-88.

- Mazur, P.K. & Siveke, J.T. 2011. Genetically engineered mouse models of pancreatic cancer: unravelling tumour biology and progressing translational oncology. *Gut*.
- Mellman, I., Coukos, G. & Dranoff, G. 2011. Cancer immunotherapy comes of age. *Nature*, 480, 480-9.
- Mellor, A.L. & Munn, D.H. 1999. Tryptophan catabolism and T-cell tolerance: immunosuppression by starvation? *Immunol Today*, 20, 469-73.
- Meng, G., Xia, M., Xu, C., Yuan, D., Schnurr, M. & Wei, J. 2013. Multifunctional antitumor molecule 5'-triphosphate siRNA combining glutaminase silencing and RIG-I activation. *Int J Cancer*.
- Moo-Young, T.A., Larson, J.W., Belt, B.A., Tan, M.C., Hawkins, W.G., et al. 2009. Tumor-derived TGF-beta mediates conversion of CD4+Foxp3+ regulatory T cells in a murine model of pancreas cancer. *J Immunother*, 32, 12-21.
- Moore, M.J., Goldstein, D., Hamm, J., Figer, A., Hecht, J.R., et al. 2007. Erlotinib plus gemcitabine compared with gemcitabine alone in patients with advanced pancreatic cancer: a phase III trial of the National Cancer Institute of Canada Clinical Trials Group. *J Clin Oncol*, 25, 1960-6.
- Mukherjee, P., Ginardi, A.R., Madsen, C.S., Tinder, T.L., Jacobs, F., et al. 2001. MUC1-specific CTLs are non-functional within a pancreatic tumor microenvironment. *Glycoconj J*, 18, 931-42.
- Muller, A.J. & Prendergast, G.C. 2007. Indoleamine 2,3-dioxygenase in immune suppression and cancer. *Curr Cancer Drug Targets*, 7, 31-40.
- Munn, D.H., Sharma, M.D., Baban, B., Harding, H.P., Zhang, Y., Ron, D. & Mellor, A.L. 2005. GCN2 kinase in T cells mediates proliferative arrest and anergy induction in response to indoleamine 2,3-dioxygenase. *Immunity*, 22, 633-42.
- Nagata, S. 1996. Fas-mediated apoptosis. *Adv Exp Med Biol*, 406, 119-24.
- Neesse, A., Michl, P., Frese, K.K., Feig, C., Cook, N., et al. 2011. Stromal biology and therapy in pancreatic cancer. *Gut*, 60, 861-8.
- Nomi, T., Sho, M., Akahori, T., Hamada, K., Kubo, A., et al. 2007. Clinical significance and therapeutic potential of the programmed death-1 ligand/programmed death-1 pathway in human pancreatic cancer. *Clin Cancer Res*, 13, 2151-7.
- Okudaira, K., Hokari, R., Tsuzuki, Y., Okada, Y., Komoto, S., et al. 2009. Blockade of B7-H1 or B7-DC induces an anti-tumor effect in a mouse pancreatic cancer model. *Int J Oncol*, 35, 741-9.
- Olive, K.P., Jacobetz, M.A., Davidson, C.J., Gopinathan, A., McIntyre, D., et al. 2009. Inhibition of Hedgehog signaling enhances delivery of chemotherapy in a mouse model of pancreatic cancer. *Science*, 324, 1457-61.
- Omary, M.B., Lugea, A., Lowe, A.W. & Pandol, S.J. 2007. The pancreatic stellate cell: a star on the rise in pancreatic diseases. *J Clin Invest*, 117, 50-9.
- Palucka, K. & Banchereau, J. 2012. Cancer immunotherapy via dendritic cells. *Nat Rev Cancer*, 12, 265-77.
- Partecke, L.I., Sandler, M., Kaeding, A., Weiss, F.U., Mayerle, J., et al. 2011. A syngeneic orthotopic murine model of pancreatic adenocarcinoma in the C57/BL6 mouse using the Panc02 and 6606PDA cell lines. *Eur Surg Res*, 47, 98-107.
- Perillo, N.L., Pace, K.E., Seilhamer, J.J. & Baum, L.G. 1995. Apoptosis of T cells mediated by galectin-1. *Nature*, 378, 736-9.
- Petrocca, F. & Lieberman, J. 2011. Promise and challenge of RNA interference-based therapy for cancer. *J Clin Oncol*, 29, 747-54.
- Pichlmair, A., Schulz, O., Tan, C.P., Naslund, T.I., Liljestrom, P., Weber, F. & Reis e Sousa, C. 2006. RIG-I-mediated antiviral responses to single-stranded RNA bearing 5'-phosphates. *Science*, 314, 997-1001.
- Pinzon-Charry, A., Maxwell, T. & Lopez, J.A. 2005. Dendritic cell dysfunction in cancer: a mechanism for immunosuppression. *Immunol Cell Biol*, 83, 451-61.
- Poeck, H., Besch, R., Maihoefer, C., Renn, M., Tormo, D., et al. 2008. 5'-Triphosphate-siRNA: turning gene silencing and Rig-I activation against melanoma. *Nat Med*, 14, 1256-63.
- Pollard, J.W. 2004. Tumour-educated macrophages promote tumour progression and metastasis. *Nat Rev Cancer*, 4, 71-8.
- Prendergast, G.C. 2008. Immune escape as a fundamental trait of cancer: focus on IDO. *Oncogene*, 27, 3889-900.

- Pylayeva-Gupta, Y., Lee, K.E., Hajdu, C.H., Miller, G. & Bar-Sagi, D. 2012. Oncogenic Kras-induced GM-CSF production promotes the development of pancreatic neoplasia. *Cancer Cell*, 21, 836-47.
- Rabinovich, G.A., Ariel, A., Herschkoviz, R., Hirabayashi, J., Kasai, K.I. & Lider, O. 1999. Specific inhibition of T-cell adhesion to extracellular matrix and proinflammatory cytokine secretion by human recombinant galectin-1. *Immunology*, 97, 100-6.
- Rabinovich, G.A., Ramhorst, R.E., Rubinstein, N., Corigliano, A., Daroqui, M.C., Kier-Joffe, E.B. & Fainboim, L. 2002. Induction of allogenic T-cell hyporesponsiveness by galectin-1-mediated apoptotic and non-apoptotic mechanisms. *Cell Death Differ*, 9, 661-70.
- Reynolds, A., Leake, D., Boese, Q., Scaringe, S., Marshall, W.S. & Khvorova, A. 2004. Rational siRNA design for RNA interference. *Nat Biotechnol*, 22, 326-30.
- Rubinstein, N., Alvarez, M., Zwirner, N.W., Toscano, M.A., Ibarregui, J.M., *et al.* 2004. Targeted inhibition of galectin-1 gene expression in tumor cells results in heightened T cell-mediated rejection; A potential mechanism of tumor-immune privilege. *Cancer Cell*, 5, 241-51.
- Rubtsov, Y.P. & Rudensky, A.Y. 2007. TGFbeta signalling in control of T-cell-mediated self-reactivity. *Nat Rev Immunol*, 7, 443-53.
- Ruffell, B., Affara, N.I. & Coussens, L.M. 2012. Differential macrophage programming in the tumor microenvironment. *Trends Immunol*, 33, 119-26.
- Ryschich, E., Notzel, T., Hinz, U., Autschbach, F., Ferguson, J., *et al.* 2005. Control of T-cell-mediated immune response by HLA class I in human pancreatic carcinoma. *Clin Cancer Res*, 11, 498-504.
- Salatino, M., Croci, D.O., Bianco, G.A., Ibarregui, J.M., Toscano, M.A. & Rabinovich, G.A. 2008. Galectin-1 as a potential therapeutic target in autoimmune disorders and cancer. *Expert Opin Biol Ther*, 8, 45-57.
- Sallusto, F. & Lanzavecchia, A. 1994. Efficient presentation of soluble antigen by cultured human dendritic cells is maintained by granulocyte/macrophage colony-stimulating factor plus interleukin 4 and downregulated by tumor necrosis factor alpha. *J Exp Med*, 179, 1109-18.
- Satelli, A., Rao, P.S., Gupta, P.K., Lockman, P.R., Srivenugopal, K.S. & Rao, U.S. 2008. Varied expression and localization of multiple galectins in different cancer cell lines. *Oncol Rep*, 19, 587-94.
- Schmiegel, P.D.W. & Budach, P.D.W. 2011. *Krebs der Bauchspeicheldrüse. Antworten. Hilfen. Perspektiven.*, Bonn, Deutsche Krebshilfe e.V.
- Sharma, M.D., Baban, B., Chandler, P., Hou, D.Y., Singh, N., *et al.* 2007. Plasmacytoid dendritic cells from mouse tumor-draining lymph nodes directly activate mature Tregs via indoleamine 2,3-dioxygenase. *J Clin Invest*, 117, 2570-82.
- Shevchenko, I., Karakhanova, S., Soltek, S., Link, J., Bayry, J., *et al.* 2013. Low-dose gemcitabine depletes regulatory T cells and improves survival in the orthotopic Panc02 model of pancreatic cancer. *Int J Cancer*, 133, 98-107.
- Shortman, K. & Naik, S.H. 2007. Steady-state and inflammatory dendritic-cell development. *Nat Rev Immunol*, 7, 19-30.
- Spano, D., Russo, R., Di Maso, V., Rosso, N., Terracciano, L.M., *et al.* 2010. Galectin-1 and its involvement in hepatocellular carcinoma aggressiveness. *Mol Med*, 16, 102-15.
- Stathis, A. & Moore, M.J. 2010. Advanced pancreatic carcinoma: current treatment and future challenges. *Nat Rev Clin Oncol*, 7, 163-72.
- Stockwin, L.H., McGonagle, D., Martin, I.G. & Blair, G.E. 2000. Dendritic cells: immunological sentinels with a central role in health and disease. *Immunol Cell Biol*, 78, 91-102.
- Tang, D., Yuan, Z., Xue, X., Lu, Z., Zhang, Y., *et al.* 2011. High expression of Galectin-1 in pancreatic stellate cells plays a role in the development and maintenance of an immunosuppressive microenvironment in pancreatic cancer. *Int J Cancer*.
- Taylor, M.W. & Feng, G.S. 1991. Relationship between interferon-gamma, indoleamine 2,3-dioxygenase, and tryptophan catabolism. *FASEB J*, 5, 2516-22.
- Toscano, M.A., Bianco, G.A., Ibarregui, J.M., Croci, D.O., Correale, J., *et al.* 2007. Differential glycosylation of TH1, TH2 and TH-17 effector cells selectively regulates susceptibility to cell death. *Nat Immunol*, 8, 825-34.
- Tuveson, D.A. & Hingorani, S.R. 2005. Ductal pancreatic cancer in humans and mice. *Cold Spring Harb Symp Quant Biol*, 70, 65-72.

- Uhl, M., Aulwurm, S., Wischhusen, J., Weiler, M., Ma, J.Y., *et al.* 2004. SD-208, a novel transforming growth factor beta receptor I kinase inhibitor, inhibits growth and invasiveness and enhances immunogenicity of murine and human glioma cells in vitro and in vivo. *Cancer Res*, 64, 7954-61.
- van der Zee, J.A., van Eijck, C.H., Hop, W.C., van Dekken, H., Dicheva, B.M., *et al.* 2011. Angiogenesis: a prognostic determinant in pancreatic cancer? *Eur J Cancer*, 47, 2576-84.
- Von Hoff, D.D., Ervin, T., Arena, F.P., Chiorean, E.G., Infante, J., *et al.* 2013. Increased survival in pancreatic cancer with nab-paclitaxel plus gemcitabine. *N Engl J Med*, 369, 1691-703.
- Vonderheide, R.H. & Bayne, L.J. 2013. Inflammatory networks and immune surveillance of pancreatic carcinoma. *Curr Opin Immunol*, 25, 200-5.
- Weller, M., Constam, D.B., Malipiero, U. & Fontana, A. 1994. Transforming growth factor-beta 2 induces apoptosis of murine T cell clones without down-regulating bcl-2 mRNA expression. *Eur J Immunol*, 24, 1293-300.
- Witkiewicz, A., Williams, T.K., Cozzitorto, J., Durkan, B., Showalter, S.L., Yeo, C.J. & Brody, J.R. 2008. Expression of indoleamine 2,3-dioxygenase in metastatic pancreatic ductal adenocarcinoma recruits regulatory T cells to avoid immune detection. *J Am Coll Surg*, 206, 849-54; discussion 854-6.
- Witkiewicz, A.K., Costantino, C.L., Metz, R., Muller, A.J., Prendergast, G.C., Yeo, C.J. & Brody, J.R. 2009. Genotyping and expression analysis of IDO2 in human pancreatic cancer: a novel, active target. *J Am Coll Surg*, 208, 781-7; discussion 787-9.
- Wormann, S.M., Diakopoulos, K.N., Lesina, M. & Algul, H. 2013. The immune network in pancreatic cancer development and progression. *Oncogene*.
- Wu, W.K., Sung, J.J., Wu, Y.C., Li, H.T., Yu, L., Li, Z.J. & Cho, C.H. 2009. Inhibition of cyclooxygenase-1 lowers proliferation and induces macroautophagy in colon cancer cells. *Biochem Biophys Res Commun*, 382, 79-84.
- Xue, X., Lu, Z., Tang, D., Yao, J., An, Y., *et al.* 2011. Galectin-1 secreted by activated stellate cells in pancreatic ductal adenocarcinoma stroma promotes proliferation and invasion of pancreatic cancer cells: an in vitro study on the microenvironment of pancreatic ductal adenocarcinoma. *Pancreas*, 40, 832-9.
- Yang, R.Y., Rabinovich, G.A. & Liu, F.T. 2008. Galectins: structure, function and therapeutic potential. *Expert Rev Mol Med*, 10, e17.
- Yoneyama, M., Kikuchi, M., Natsukawa, T., Shinobu, N., Imaizumi, T., *et al.* 2004. The RNA helicase RIG-I has an essential function in double-stranded RNA-induced innate antiviral responses. *Nat Immunol*, 5, 730-7.
- Yuan, W., Collado-Hidalgo, A., Yufit, T., Taylor, M. & Varga, J. 1998. Modulation of cellular tryptophan metabolism in human fibroblasts by transforming growth factor-beta: selective inhibition of indoleamine 2,3-dioxygenase and tryptophanyl-tRNA synthetase gene expression. *J Cell Physiol*, 177, 174-86.
- Zhang, N. & Bevan, M.J. 2011. CD8(+) T cells: foot soldiers of the immune system. *Immunity*, 35, 161-8.
- Zhang, Y., Chen, L., Yang, J., Fleming, J.B., Chiao, P.J., Logsdon, C.D. & Li, M. 2013. Study human pancreatic cancer in mice: how close are they? *Biochim Biophys Acta*, 1835, 110-8.
- Zhong, L.P., Wei, K.J., Yang, X., Pan, H.Y., Ye, D.X., Wang, L.Z. & Zhang, Z.Y. 2010. Overexpression of Galectin-1 is negatively correlated with pathologic differentiation grade in oral squamous cell carcinoma. *J Cancer Res Clin Oncol*, 136, 1527-35.
- Zitvogel, L., Tesniere, A. & Kroemer, G. 2006. Cancer despite immunosurveillance: immunoselection and immunosubversion. *Nat Rev Immunol*, 6, 715-27.
- Zou, W. 2006. Regulatory T cells, tumour immunity and immunotherapy. *Nat Rev Immunol*, 6, 295-307.

9 Appendices

9.1 Abbreviations

AEC	3-Amino-9-ethylcarbazole
AHR	Aryl hydrocarbon receptor
APC	Allophycocyanin
APCs	Antigen presenting cells
BMDCs	Bone marrow-derived dendritic cells
BRCA2	Breast cancer type 2 susceptibility protein
CAR	Chimeric antigen receptor
CCL	Chemokine (C-C motif) ligand
CD	Cluster of differentiation
cDC	Conventional dendritic cell
cDNA	Copy deoxyribonucleic acid
CDNK2A	Cyclin-dependent kinase inhibitor 2A
CEA	Carcinoembryonic antigen
CFSE	Carboxyfluorescein diacetat succinimidyl ester
CK 19	Cytokeratin 19
COX1/2	Cyclooxygenase 1/2
CTL	Cytotoxic T lymphocyte
CTLA-4	Cytotoxic T-Lymphocyte Antigen 4
CXCL	Chemokine (C-X-C motif) ligand
DAB	3,3'-diaminobenzidine
DAPI	4',6-diamidino-2-phenylindole
DC	Dendritic cell
D-1-MT	D-1-methyltryptophan
DMEM	Dubelcco's Modified Eagle Medium
DMSO	Dimethyl sulfoxide
DTT	Dithiotreitol
ECM	Extracellular matrix
EFG	Epidermal growth factor
ELISA	Enzyme-linked immunosorbent assay

FACS	Fluorescence activated cell sorter
FBS	Fetal bovine serum
FITC	Fluorescein isothiocyanate
FoxP3	Forkhead box P3
FRET	Fluorescence resonance energy transfer
Gal-1	Galectin-1
GEMM	Genetically engineered mouse model
GM-CSF	Granulocyte macrophage-colony stimulating factor
H&E	Hematoxylin and eosin
HLA	Human leukocyte antigen
HPF	High power field
HPRT	Hypoxanthin-phosphoribosyl-transferase
HRP	Horse radish peroxidase
IDO	Indoleamine 2,3-dioxygenase
IFN	Interferon
Ig	Immunoglobulin
IHC	Immunohistochemistry
IL	Interleukin
i.p.	Intraperitoneal
IPMN	Intraductal papillary mucinous neoplasm
IP-10	Interferon gamma induced protein 10
IPS-1	Interferon beta promoter stimulator 1
IRF-3	Interferon regulatory factor 3
i.t.	Intratumoral
i.v.	Intravenous
KD	Knockdown
Kras	V-Ki-ras 2 Kirsten rat sarcoma viral oncogene homolog
LPS	Lipopolysaccheride
LSL	Lox-Stop-Lox
mAb	Monoclonal antibody
3-MCA	3-Methylcholantren

MCN	Mucinous cystic neoplasm
MDA-5	Melanoma differentiation-associated protein 5 (RIG-I-like helicase)
MDSC	Myeloid-derived suppressor cells
MFI	Median fluorescence intensity
MHC	Major histocompatibility complex
MMP	Matrix metalloproteinase
mRNA	Messenger RNA
NAD	Nicotinamide adenine dinucleotide
NK cell	Natural killer cell
NLR	Nod-like receptor
PAMPS	Pathogen-associated molecular patterns
PanIN	Pancreatic intraepithelial neoplasia
PB	Pacific blue
PBS	Phosphate buffered saline
PD-1	Programmed cell death protein 1
PDAC	Pancreatic ductal adenocarcinoma
pDC	Plasmacytoid dendritic cell
PDGF	Platelet-derived growth factor
PD-L1	Programmed cell death ligand 1
PE	Phycoerythrin
PerCP	Peridinin chlorophyll
PFA	Paraformaldehyde
PI	Propidium iodide
ppp	Triphosphate
PSC	Pancreatic stellate cell
qRT-PCR	Quantitative real time PCR
RIG-I	Retinoic acid-inducible gene-I
RISC	RNAi-induced silencing complex
RNA	Ribonucleic acid
RNAi	RNA interference
RPMI	Roswell Park Memorial Institute
s.c.	Subcutaneous

SDS	Sodium dodecyl sulfate
siRNA	Small interfering RNA
α -SMA	Alpha-smooth muscle actin
SMAC	Supramolecular activation cluster
TAA	Tumor-associated antigen
TAM	Tumor-associated macrophages
TBST	TRIS-buffered saline with Tween 20
TCR	T cell receptor
TDG	Thiodigalactoside
TGF- β	Transforming growth factor β
T _H cells	T helper cells
TIL	Tumor infiltrating lymphocyte
TLR	Toll-like receptor
TMB	3,3' 5,5' Tetramethyl benzidine
TNF- α	Tumor necrosis factor alpha
Treg	Regulatory T cell
VEGF	Vascular endothelial growth factor

9.2 List of figures

Figure 2-1: Effects of IDO-positive tumors (modified from Godin-Ethier et al.).....	17
Figure 6-1: H & E staining of murine primary pancreatic carcinoma models.	43
Figure 6-2: Collagen staining of pancreatic tumors.	44
Figure 6-3: Alcian blue staining reveals differentiation status of pancreatic carcinoma.....	45
Figure 6-4: Tumor blood vessels in the periphery and center of pancreatic carcinoma.....	46
Figure 6-5: Infiltrating T cells in the periphery and center of pancreatic carcinoma.	47
Figure 6-6: Quantitative analysis of infiltrating T cells in pancreatic carcinoma.	48
Figure 6-7: Expression of galectin-1 and α -SMA in murine pancreatic carcinoma.....	49
Figure 6-8: Indoleamine 2,3-dioxygenase expression in murine pancreatic carcinoma.	50
Figure 6-9: Survival of mice bearing orthotopic Panc02 and T110299 tumors.	51
Figure 6-10: Murine Panc02 but not T110299 PDAC cells express functional RIG-I.	53
Figure 6-11: ppp-RNA-induced up-regulation of MHC-I expression and CXCL10 secretion is mediated by RIG-I.....	54
Figure 6-12: Silencing of galectin-1 expression in Panc02 and T110299 cells with unmodified and 5' ppp-modified siRNA.....	55
Figure 6-13: 5' ppp-modified siRNA targeting galectin-1 combines gene silencing with RIG-I signaling.	56
Figure 6-14: Galectin-1 serum levels in mice with Panc02 tumors correlate with tumor size.....	57
Figure 6-15: Galectin-1 mRNA levels in tumors and serum protein levels in mice with orthotopic Panc02 tumors after treatment with siRNA targeting galectin-1.	57
Figure 6-16: Systemic treatment of Panc02 tumor-bearing mice with unmodified and modified 5' ppp-RNA silencing galectin-1.	58
Figure 6-17: Survival of subcutaneous and orthotopic Panc02 tumor-bearing mice after treatment with unmodified and modified 5' ppp-RNA silencing galectin-1.	59
Figure 6-18: Inhibition of T cell proliferation by tumor supernatant from murine PDAC cell lines. ...	61
Figure 6-19: Suppression of OT-1 T cell proliferation by tumor supernatant.....	62
Figure 6-20: T cell apoptosis induced by tumor supernatant of murine PDAC cells.....	63
Figure 6-21: Soluble factors do not impair cytotoxic T cell degranulation.....	64
Figure 6-22: Murine PDAC cells secrete PD-L1, but the PD-1/PD-L1 axis is not responsible for tumor supernatant-induced T cell inhibition.....	65
Figure 6-23: T cell inhibition is mediated by a tumor-derived protein, whereas nucleotides or prostaglandins are dispensable.	66
Figure 6-24: Galectin-1 content in cell lysate and supernatant of murine PDAC cells.....	67
Figure 6-25: T cell inhibition is not affected by siRNA based silencing of galectin-1 in T110299 cells.	68

Figure 6-26: Galectin-1 inhibition does not restore inhibition of T cell proliferation.....	69
Figure 6-27: T cell inhibition is not influenced by siRNA based silencing of TGF- β_1	70
Figure 6-28: Inhibition of TGF- β -receptor signaling partially restores T cell proliferation.	71
Figure 6-29: Inhibition of IDO rescues T cell from inhibition by PDAC cells.....	72
Figure 6-30: Induction of IDO mRNA expression in T cells after exposure to tumor supernatant from Panc02 and T110299 cells.....	73

9.3 List of tables

Table 2-1: GEMMs of pancreatic ductal adenocarcinoma (modified from Mazur et al.(Mazur and Siveke, 2011))	6
Table 4-1: Primary conjugated antibodies and reagents for flow cytometry.....	26
Table 4-2: Purified antibodies for IHC.....	27
Table 4-3: Blocking antibodies for <i>in vitro</i> assays.....	27
Table 4-4: Western Blot antibodies.....	27
Table 4-5: siRNA sequences for RNAi.....	28
Table 4-6: DNA-template sequences for IVT	28
Table 4-7: Primer sequences for qRT-PCR.....	29
Table 5-1: Incubation times of primary antibodies in immunohistochemistry.....	33
Table 5-2: Spectral properties of the used fluorochromes in flow cytometric experiments.....	34
Table 5-3: Components for one RT-PCR approach	38
Table 5-4: program setting	38
Table 5-5: Narcotic mixture for orthotopic tumor cell injection	39
Table 5-6: Antidote mixture for orthotopic tumor cell injection.....	39

9.4 Publications

9.4.1 Original publications

Jonathan Ellermeier, Jiwu Wei, Peter Duewell, Sabine Hoves, Mareike R. Stieg, **Tina Adunka**, Daniel Noerenberg, Hans-Joachim Anders, Doris Mayr, Hendrik Poeck, Gunther Hartmann, Stefan Endres, and Max Schnurr.

Therapeutic efficacy of bifunctional siRNA combining TGF- β_1 silencing with RIG-I activation in pancreatic cancer

Cancer Research 2013 March 15; 73(6): 1709-1720 (JIF: 8.65)

9.4.2 Oral presentations

Galectin-1 and -3 as potential targets for immunotherapy of pancreatic carcinoma with bifunctional ppp-siRNAs

Deutscher Pankreasklub 2011, Marburg

TGF- β secreted from pancreatic ductal adenocarcinoma (PDAC) cells induces potent inhibition of CD4⁺ and CD8⁺ T cell proliferation and is a promising target for tumor immunotherapy

Deutscher Pankreasklub 2012, Leipzig

Effective restoring of CD4⁺ and CD8⁺ T cell responses through inhibition of secreted TGF- β by pancreatic ductal adenocarcinoma (PDAC)

CIMT 2013, Mainz

9.5 Acknowledgements

I would like to thank Prof. Dr. med. Max Schnurr, who was an excellent supervisor and not only offered technical and professional advice but also helped with everyday problems. I would like to thank him particularly for his trust, constant encouragement and not selling me down the river when I revealed him my pregnancy.

I am very grateful to Professor Dr. Stefan Endres for giving me the opportunity to work on my thesis in close collaboration with the Division of Clinical Pharmacology. His constant support and encouragement provides the basis for the pleasant atmosphere in the lab that made me enjoy my time as a PhD student very much.

I would also like to thank the Deutsche Forschungsgemeinschaft for providing funding as stipend of the Graduiertenkolleg 1202 “Oligonucleotides in cell biology and therapy”. The program of the Graduiertenkolleg 1202 contained research and soft skill seminars, which were very helpful in getting new ideas for my own work. Every year it always was a pleasure to join the Grako Retreat. The DFG also supported me throughout my parental leave, for which I am very thankful.

Working in a joyful environment made work much easier sometimes. I was lucky to work with people with whom I could always laugh but also could have discussions about work and life. In our working group I would like to thank Peter Düwell, Stephe Hoffmann, Jonathan Ellermeier, Mareike Stieg, Ebba Beller, Alexander Steger, H el ene Bourhis, Hannah Lohr, Hannes H olz, Anja Funk, Igor Lazic, Sabrina Kirchleitner and last but not least Daniel Be  for giving me support and for having a great time in the lab.

The Division of Clinical Pharmacology is an inspiring environment where I got lots of support from other working groups. AG Endres and Kobold: special thanks to Natascha K pper and Susanne Wenk who always listened to my concerns and helped me a lot coping with everyday problems. AG Rothenfusser: very special thanks to Simone Willms who consistently had an ear or two for me and who became a good friend of mine. AG Anz: special thanks to Sascha Haubner for showing me “tricks” for immunohistochemistry. Naturally, I would like to thank all the other former and present lab members for sharing their knowledge and friendship.

PD Dr. Jens Siveke from 2. Medizinische Klinik und Poliklinik, Klinikum rechts der Isar (Technical University of Munich), provided the pancreatic cancer cell lines from GEMM tumors, such as the T110299 cell line, and gave me access to tissue blocks from GEMM tumors for immunohistochemistry studies.

I would like to thank PD Dr. med. Doris Mayr from the Department of Pathology of the LMU Munich for support in histology and preparation of tumor slices for immunohistochemistry.

Very special thanks go to my family, Nicolas and Noah. Thank you for all your support, encouragement, trust and love all the time!!!

Eidesstattliche Versicherung

Adunka, Tina

Ich erkläre hiermit an Eides statt, dass ich die vorliegende Dissertation mit dem Thema

Characterization of murine pancreatic carcinoma models regarding immunosuppressive mechanisms and therapy with bifunctional siRNA targeting galectin-1

selbstständig verfasst, mich außer der angegebenen keiner weiteren Hilfsmittel bedient und alle Erkenntnisse, die aus dem Schrifttum ganz oder annähernd übernommen sind, als solche kenntlich gemacht und nach ihrer Herkunft unter Bezeichnung der Fundstelleneinzeln nachgewiesen habe.

Ich erkläre des Weiteren, dass die hier vorgelegte Dissertation nicht in gleicher oder in ähnlicher Form bei einer anderen Stelle zur Erlangung eines akademischen Grades eingereicht wurde.

Ort, Datum

Unterschrift Doktorandin/Doktorand